SINTEF Energy Research

SINTEF Energy Research

Address: 7034 Trondheim NORWAY
Reception: Sem Sælands vei 11
Telephone: +47 73 59 72 00
Telefax: +47 73 59 72 50

http://www.energy.sintef.no

E. No.: NO 939 350 675

TECHNICAL REPORT

SUBJECT/TASK (title)

Characterisation of MSW for Combustion Systems

CONTRIBUTOR(S)

Lars Sørum

CLIENT(S)

IEA Task 23

TR NO.	DATE	CLIENT'S REF.	PROJECT NO.
TRA5395	2001-02-22	Niranjan Patel	17X196

ELECTRONIC FILE CODE	RESPONSIBLE (NAME, SIGN.)	CLASSIFICATION
	Lars Sørum	Open

ISBN NO.	REPORT TYPE	RESEARCH DIRECTOR (NAME, SIGN.)	COPIES	PAGES
82-594-2029-5		Inge R. Gran		99

DIVISION	LOCATION	LOCAL TELEFAX
Thermal Energy	Kolbjørn Hejes vei 1A	+47 73 59 28 89

RESULT (summary)

MSW consists of several different fractions such as paper/cardboard, plastics, wet organic wastes, glass, metals, etc. The complexity of MSW in terms of composition, together with the increasing awareness of the environmental hazards of waste disposal and lack of landfill sites, have in the last decades promoted an increased number of alternative waste treatment systems. Material recovery and re-use, combustion with energy recovery, composting and landfilling are the most common parts of today's waste management system. Factors influencing the choice of MSW management systems are waste amounts and composition, environmental and economical aspects and infrastructure (i.e. type of housing, access to landfill sites, possible energy buyers, etc.). The choice of waste management system will influence the composition of MSW subjected to energy recovery. The increased separation of components from the waste stream and complex waste management systems gives new possibilities for classification of waste as a fuel with a certain quality and composition. Knowing the composition and combustion characteristics of the respective components will make it easier for operators and manufacturers of combustion plant to assess the consequences of burning different wastes. Some of the most important environmental aspects of MSW combustion have been investigated in detail in this work, with emphasis on two important parameters:

- Changes in composition (related to waste management)
- Fuel complexity (i.e. many different components with different combustion properties)

KEYWORDS

SELECTED BY AUTHOR(S)		
	Municipal solid Waste (MSW)	Fast kommunalt avfall
	Combustion	Forbrenning

TABLE OF CONTENTS

Page

1 SUMMARY 4

2 CHARACTERISATION OF MSW COMPONENTS FOR COMBUSTION SYSTEMS 6
2.1 Introduction 6
2.2 Objectives 6

3 THERMAL CHARACTERISATION OF MSW 7
3.1 Objectives 8
3.2 Chemical composition of MSW 8
3.2.1 Paper and cardboard fraction 10
3.2.1.1 Chemical composition and structure 10
3.2.1.2 The process of papermaking – the production of paper pulp 14
3.2.1.3 Paper and cardboard used in this study 15
3.2.2 Plastic fraction 16
3.2.2.1 Chemical composition and structure 17
3.2.3 Multi-material fraction 18
3.2.4 Wood and cotton 18
3.2.5 Chemical bonds in polymers 18
3.3 Experimental methods and equipment 19
3.3.1 Proximate analysis and higher heating value (HHV) 19
3.3.2 Thermogravimetric (TGA) kinetic study 20
3.4 Kinetic analysis 23
3.4.1 Literature survey on chemical kinetics from pyrolysis of MSW 24
3.5 Results and discussion 27
3.5.1 Proximate analysis and HHV 27
3.5.2 Evaluation of TGA experiments 29
3.5.3 Cellulosic fraction of MSW 29
3.5.3.1 Kinetic evaluation of spruce and birch 32
3.5.3.2 Kinetic evaluation of Cotton from sweater and pure unbleached cotton linters 33
3.5.3.3 Kinetic evaluation of newspaper and cardboard 35
3.5.3.4 Kinetic evaluation of recycled paper and glossy paper 38
3.5.3.5 Comparison of cellulosic substances 39
3.5.4 Plastic fraction 41
3.5.4.1 Kinetic evaluation of HDPE 43
3.5.4.2 Kinetic evaluation of LDPE and coloured plastic bag 44
3.5.4.3 Kinetic evaluation of PS and PP 46
3.5.4.4 Kinetic evaluation of PPVC and UPVC 47
3.5.4.5 Comparison of plastics 49
3.5.5 Multi-material fraction 51
3.5.5.1 Juice carton and milk carton 51
3.5.6 Mixtures 54

3.6 Sources of errors 55
3.7 Conclusions 58
3.7.1 Higher heating value determination and proximate analysis 58
3.7.2 TGA experiments and kinetic study 59
3.8 References 61

4 FORMATION OF NO FROM COMBUSTION OF VOLATILES FROM MUNICIPAL SOLID WASTE COMPONENTS AND THEIR MIXTURES. 65
4.1 Abstract 65
4.2 Introduction 66
4.3 Experimental methods 67
4.4 Experimental results 73
4.4.1 Single Components 73
4.4.2 Mixtures 78
4.5 Modelling 82
4.5.1 Methods 82
4.5.2 Simulations of paper 84
4.5.3 Simulations on plastic 91
4.6 Conclusions 94
4.7 References 96

5 FURTHER WORK 99

1 SUMMARY

A brief summary and main conclusions of the two different parts of this report are given below.

Part I

Pyrolysis Characteristics and Kinetics of Municipal Solid Wastes

Pyrolysis characteristics and kinetics of several different components, representing the dry cellulosic fraction and plastics of MSW, has been investigated. The aim of this study was to obtain detailed information on the pyrolytic degradation characteristics and chemical kinetics of the most important components in MSW, which can be useful in the modelling, design, and operation of thermal conversion processes for MSW (i.e. pyrolysis, gasification and combustion systems). The pyrolytic degradation characteristics of these components have been studied by thermogravimetry (TGA). In addition, proximate- and ultimate analysis and determination of the higher heating value (HHV) are included. The variations in fuel properties of the paper/cardboard and plastic components were relatively large. The ash content for the different paper/cardboard components, varied from 1-28 wt%, with corresponding HHV values of 19.3-10.4 MJ/kg and fixed carbon content of 10.5-4.7 wt%. The plastics PS, PP, LDPE and HDPE were 100% volatile and HHV were between 42-47 MJ/kg. PVC, on the other hand, has a similar content of hydrocarbons and consequently a similar HHV as the cellulosic fraction (22.8 MJ/kg). The major difference between PVC and the cellulosic fraction with regards to the ultimate composition was that PVC had a chlorine content of 48 wt% and only 6 wt% of oxygen. Paper and cardboard have a similar pyrolytic degradation behaviour as wood, occurring at 200-500^{o}C. The DTG temperature peak was located at approximately 360^{o}C. The degradation of PS, PP, LDPE and HDPE occurred at 350-500^{o}C, while PVC had a completely different degradation behaviour, volatilising between 200^{o}C and 525^{o}C in two major steps. The cellulosic fraction of MSW was modelled as a set of three reactions describing the degradation of hemicellulose, cellulose and lignin, with average activation energies of 111, 244 and 43 kJ/mole, respectively. PS, PP, LDPE and HDPE were all modelled as a single reaction describing the thermal degradation of the hydrocarbon polymer with activation energies of 312, 337, 341 and 445 kJ/mole, respectively. The degradation of PVC was modelled with three reactions describing the release of benzene during dehydrochlorination, dehydrochlorination and degradation of remaining hydrocarbons with activation energies of 388, 110 and 150 kJ/mole, respectively. Possible interactions between different paper and plastic components in mixtures were also investigated. The only significant interaction between the different components was between the cellulosic fraction and PVC. In a mixture, the dehydrochlorination of PVC increases the reactivity of cellulosic matter.

Part II

Formation of NO from Combustion of Volatiles from Municipal Solid Wastes

An experimental and theoretical study on the formation of NO from combustion of volatiles from municipal solid wastes has been performed. Experiments on single components and their mixtures were conducted in a small-scale fixed bed reactor. In addition, numerical simulations using the opposed flow diffusion flame program OPPDIF were performed to obtain a further understanding of the experimental results. Conversion factors for fuel-N to NO were determined for single components of newspaper, cardboard, glossy paper, low-density polyethylene (LDPE) and poly(vinylchloride) (PVC) and their mixtures, using gases with oxygen concentrations of 12, 21 and 40 vol.%. For single components experiments at 100 vol.% oxygen were also performed. The conversion factors for paper and cardboard varied from 0.26 to 0.99. The experiments and simulations both show that NO was mainly formed from the fuel-nitrogen for the paper and cardboard. The conversion factor for LDPE and PVC varied from 0.71 to 10.09 and 0.04 to 0.37, respectively. Conversion factors higher than 1.0 in the case of LDPE clearly show that NO was formed by thermal and/or prompt mechanisms. For the plastics LDPE and PVC the experiments show that NO mainly originates from the thermal and possibly the prompt NO mechanisms. Increased formation of NO was observed for newspaper, cardboard, glossy paper, PVC and LDPE, when increasing the oxygen concentration in the oxidiser from 12 to 40 vol.%. Increasing the temperature of the oxidiser from 973 to 1123 K led to more NO from newspaper and LDPE. Simulations with OPPDIF confirmed these trends.

For mixtures, a comparison between calculated conversion factors (based on a weighted sum of the conversion factors for single components) and the experimentally determined conversion factor for pellets of the mixture were performed. For mixtures of paper and cardboard a significant difference in conversion factor for the sum of single components and mixture experiments could only be found at 40 vol.% of oxygen. For mixtures of paper/cardboard and plastics, however, significant differences in the conversion factor were observed at all oxygen concentrations when comparing experiments on a mixture of paper and plastics with the weighted sum of the single components. The explanation was found in the different combustion properties for paper/cardboard and plastic, which in this case make the formation of thermal NO from LDPE more favourable for the single component than in mixtures with other components. The simulations with OPPDIF confirmed the trends observed in the experimental study and allowed an assessment of the contribution of the different mechanisms of NO formation.

2 CHARACTERISATION OF MSW COMPONENTS FOR COMBUSTION SYSTEMS

2.1 Introduction

The need for characterisation of MSW is demonstrated through the diversity of components constituting MSW and a large number of different treatment systems. Characterisation of MSW components can serve as a foundation, when decisions on waste management are made and should be included in a total life cycle evaluation of a product. Characterisation of the components of input MSW is also important in design and operation of incinerators. What will be the consequences of source separation for combustion plants? Do we separate fractions of combustible waste in MSW for material recovery that might be more suitable for energy recovery? What will be the consequences of different mixture ratios of paper and plastics in RDF combustion systems?

In order to answer these questions we need to know more about the characteristics of the different components in the combustible fraction of MSW and RDF. We also need to know more about their behaviour as single components and if there are any interactions in mixtures of different components.

This project will focus on thermal characterisation of different combustible components in MSW. Different types of paper and cardboard, plastics and multi-material components such as beverage cartons will be investigated. Included in a thermal characterisation will be determination of higher heating value, proximate analysis and a detailed investigation of the chemical kinetics during pyrolysis. A detailed characterisation of NO emission during combustion and NOx formation mechanisms for single components and mixtures will also be performed.

In order to answer the above-mentioned questions, a lot of work has to be done. Not only investigation of the characteristics of the different components in combustion systems should be performed. A comparison of the different treatment methods with focus on main components should be performed. The above mentioned study will hopefully bring us a step forward to a more comprehensive and detailed analysis of proper treatment systems for the different components of MSW.

2.2 Objectives

The objectives of this project are:

- Review work on thermal characterisation of MSW/RDF components.
- To investigate and report characteristic behaviour of different types of paper, plastics and multi-material components such as beverage cartons during pyrolysis. Proximate analysis and determination of higher heating value will also be included.
- To investigate and report a detailed characterisation of NO emission during combustion of single particles.
- To produce a status report detailing the findings of the study

3 THERMAL CHARACTERISATION OF MSW

Characterisation of municipal solid waste (MSW) has been conducted for several years. MSW quantities[1,2], composition[1,3,4], proximate[5], ultimate[6], trace element analysis[4,7,8] and chemical kinetic analysis[9] have all been reported more or less detailed. The need for characterisation of MSW is demonstrated through the diversity of components constituting MSW. Paper, plastics, wet organic waste (wood, grass and food wastes) are the main components of the combustible fraction of MSW. Figure 1 shows the difference in composition in MSW in some selected countries in Europe and USA.

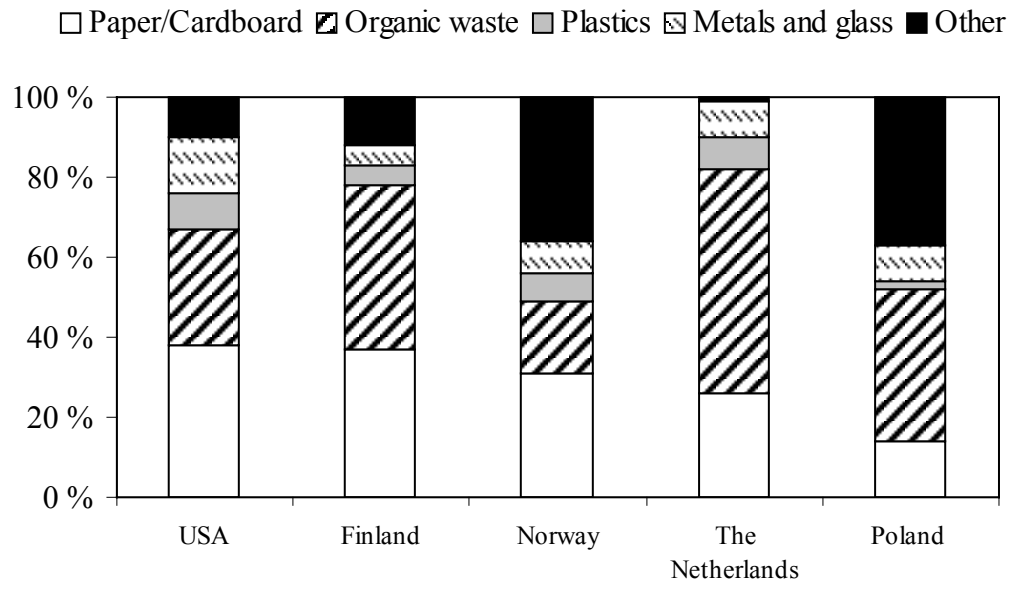

Figure 1. Comparison of composition of MSW in some selected countries[10,11,12,13].

Knowing that each country may have different compositions of MSW (Figure 1) and waste management policy, it is obvious that the external conditions for selecting the proper energy recovery solution can be quite different. Around the world, the yearly per capita generation of MSW varies. Poland has the lowest generation with 260 kg/capita, whereas Norway, The Netherlands and Finland have 470, 520 and 624 kg/capita respectively[10,14]. USA has the highest generation with 800 kg/cap[14]. These enormous amounts of MSW have internationally increased the interest for and fraction of MSW being subjected to reuse, recycling or combustion with energy recovery on the expense of landfilling. Many countries have banned landfilling of wet organic waste. This alone will influence the composition of MSW going to mass burn incinerators as it normally constitute approximately 20 to 30% of the total MSW composition[11,12]. In addition to this, changing consumer patterns and new products will alter the composition of MSW. Characterisation of MSW components can serve as a foundation, when decisions on waste management are made and should be included in a total life cycle evaluation of a product. Characterisation of the components of MSW is important in design and operation of incinerators.

3.1 Objectives

Pyrolysis can be a separate process in itself or be regarded as a part of the combustion process. The present work on thermal degradation and pyrolysis kinetics has the following objectives:

- To obtain information about the thermal degradation of MSW components and mixtures under pyrolysis conditions
- Determine the kinetic parameters of the reactions involved in the thermal degradation of each component
- Obtain knowledge on the link between thermal degradation reactions and chemical composition

3.2 Chemical composition of MSW

The MSW combustible fraction mainly consists of cellulosic matter (paper, wood, wet organic fraction) and different plastics. The cellulosic matter can be divided into three different substances, namely hemicellulose, cellulose and lignin, which all have a different thermal decomposition characteristics. The plastic fraction constitutes of several different types with varying composition. The most common plastic types are the pure hydrocarbon plastics such as HDPE (high density polyethylene), LDPE (low density polyethylene), PS (polystyrene) and PP (polypropylene) and the chlorine containing PVC (polyvinylchloride). General information on the production, chemical structure and composition of paper and plastic have been collected from a selection of books and reports[16,17,18,19,20,21,22].

Table 1. Ultimate analysis of MSW and MSW fractions[6,23]. Included is also calculated values of higher and effective heating values.

	Composition [wt%]	**C [wt%]**	**O [wt%]**	**H [wt%]**	**N [wt%]**	**S [wt%]**	**Cl [wt%]**	**Ash [wt%]**	**Moisture [wt%]**	**HHV [MJ/kg]**	**H_{eff} [MJ/kg]**
MSW	**100**	**37.53**	**26.85**	**4.98**	**0.96**	**0.24**	**0.79**	**28.6**	**24.8**	**15.6**	**10.2**
Paper/Cardboard	33.1	43.11	40.26	5.89	0.20	0.24	0.30	10	10	17.6	14.3
Plastics	6.5	72.89	10.63	10.11	1.10	0.39	3.88	1	10	36.3	28.2
Metal	3.7	-	-	-	-	-	-	100	0	0	0
Glass	6.4	-	-	-	-	-	-	100	0	0	0
Organic waste	24.4	49.00	36.41	6.33	2.4	0.23	0.63	5	70	20.7	3.9
Other combustibles	12.6	52.14	31.34	6.57	2.0	0.66	2.29	5	30	22.6	13.3
Remaining fraction	13.3	-	-	-	-	-	-	100	0	0	0

3.2.1 Paper and cardboard fraction

The paper fraction in MSW consists of several different types of paper and will thus behave differently during thermal degradation. In this study, three different types of paper and one type of cardboard have been investigated. Newspaper, recycled paper (made of 100% recycled paper) and one type of glossy magazine paper were used. The cardboard used was brown cardboard from a cardboard box. Paper as we know it today is always made of fibrous raw material. The most important source of fibre is wood. The raw material for paper production can be any type of tree, both hardwood and softwood. More than 90% of the world's total fibre production originates from wood. In some parts of the world, other cellulosic matter such as bagasse and bamboo is also used for the production of paper.

3.2.1.1 Chemical composition and structure

Paper consists of mostly the same components as wood namely cellulose, hemicellulose and lignin. However, the share of the three components can be quite different dependent on the type of paper. Fibres from different raw materials have different physical properties such as length, width and thickness. The chemical composition can also be different. Table 2 shows the chemical composition of three typical Scandinavian wood types. Birch is a hardwood, while spruce and pine are both softwoods. The values for cellulose, hemicellulose and lignin are on an extractive-free basis.

Table 2. Chemical compositions of Scandinavian birch, spruce and pine[15].

	Birch	**Spruce**	**Pine**
Cellulose [wt%]	40	44	43
Hemicellulose [wt%]	39	27	27
Lignin [wt%]	21	29	30
Extractives [wt%]	3	2	5

Cellulose. The woods largest single component is cellulose. Cellulose is a clearly definable substance which, in fact, exists in isolation, and in an almost pure form, in the fine hairs attached to the seeds of cotton. Chemically cellulose is a linear polymer of β-D-glucopyranose units linked by 1,4 glycosidic bonds (figure 2). Normally the length consists of 7000 units, but the molecular weight dispersion is very large. It has been shown that cellulose from cotton has a degree of polymerisation (DP) of up to 10000. Because of its fibrous structure and strong hydrogen bonding, cellulose has a high tensile strength and is insoluble in most solvents.

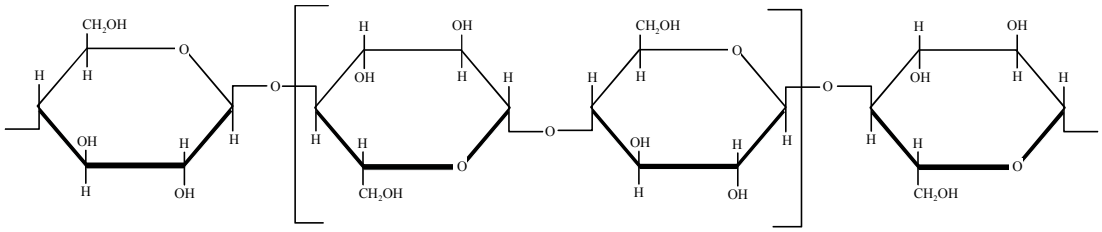

Figure 2. Chemical structure of cellulose

Hemicellulose. Closely associated with cellulose in plant cell walls, particularly those of lignified tissues, is a group of chemically ill defined polysaccharides of low molecular weight to which, the name *hemicellulos*e was given almost a century ago. The loose definition of this group stems from the fact that individual molecules contain more than one kind of sugar residue. These residues are present in variable proportions and will only elucidate the polysaccharide structure in a statistical term. However, although knowledge of the exact chemical structure remains incomplete, the intrinsic component residues of pentose and hexose sugars, together with those of some uronic acids, are well established. Only a few are involved in the hemicellulose of land plants, principally those of D-xylose, D-mannose, D-glucose, D-galactose, L-arabinose, 4-*O*-methyl-D-glucoronic acid, D-galacturonic acid and D-glucuronic acid (Figure 3). The hemicellulose are much more soluble and susecptible to chemical degradation than cellulose. Wood hemicellulose is soluble in water or in aqueous alkali, by which they can be isolated from delignified tissues.

Lignin. Lignin is a complex, systematically polymerised, highly aromatic substance with a three-dimensional, highly branched chain. It never occurs alone in nature, but it is present, as an encrustant, in all woody tissues. The structure of lignin is in large parts determined, but since a quantitatively preparation of lignin has not successfully been separated from the wood, the whole structure is not known. The chemistry of lignin is important in most pulping reactions, since lignin is the less desirable of the three main wood components. Therefore it has to be removed or bleached to an extent varying with the grade of pulp desired. Figure 4 shows a schematic proposal for lignin structure.

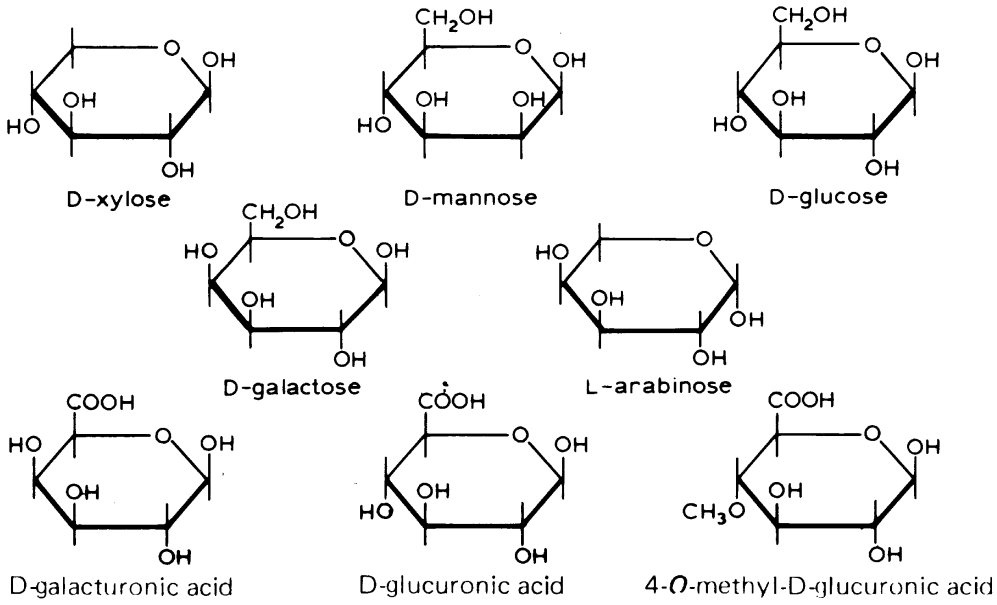

Figure 3. Principal sugar residues of wood hemicellulose.

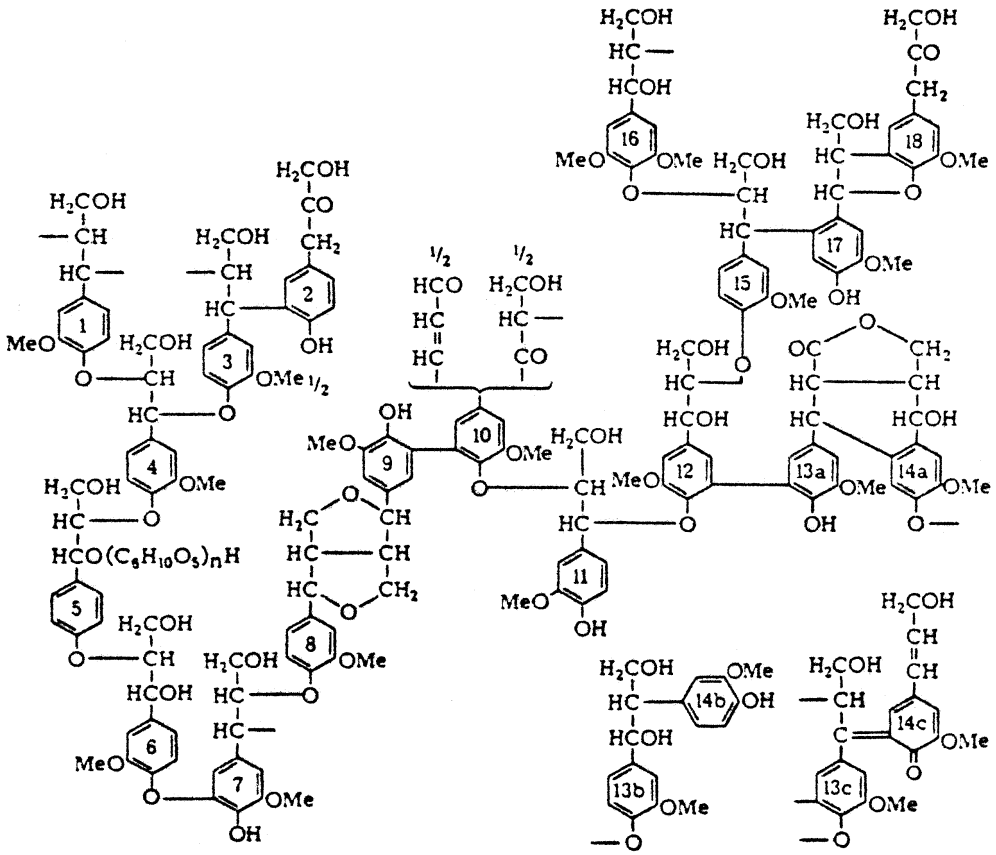

Figure 4. Schematic proposal for lignin structure.

Extractives. The extraneous components of wood include aliphatic, aromatic and alicyclic compounds, hydrocarbons, alcohols, ketons and various acids, esters, phenolic compounds, resins, terpens to mention some. These components are easily extracted from the wood using organic solvents or water.

Inorganic components. In addition to the cellulose, hemicellulose and lignin there are also additives in paper. The main inorganic additives in paper originate from the coating process and can be divided into three different groups: pigment, binder and chemical additives. The pigments contribute with the largest share in the coating process (80-95%), while binder constitutes 5-20% and chemical additives only 1-2%. Without doubt, clay is the most used pigment in the coating process. Table 3 shows a number of different pigments used in paper processing with their chemical composition.

Table 3. Pigment in paper

Pigment	
Clay (kaolin)	$Al_2O_32SiO_22H_2O$
Calcium carbonate	$CaCO_3$
Titan oxide	TiO_2
Satin white	$3CaOAl_2O_33CaSO_43H_2O$
Barium sulphate	BaSO4
Talc	$3MgO4SiO_2H_2O$
Aluminium hydroxide	$Al(OH)_3$

A study of the chemical kinetics of coated printing and writing paper also included an ultimate analysis of this type of paper. The coated printing and writing paper contained 10-15% of calcium carbonate filler and the paper was produced from bleached kraft processed pulp. Table 4, shows the ultimate analysis of the coated paper sample.

Table 4. Ultimate analysis of coated paper sample[24].

Component	
C [wt%]	30.5
H [wt%]	4.6
O [wt%]	37.7
N [wt%]	2.9
S [wt%]	1.5
Cl [wt%]	1.5
Si [ppmw]	112 800
Ca [ppmw]	72 300
Al [ppmw]	48 200
Mg [ppmw]	6 780
Fe [ppmw]	4 160
Cr [ppmw]	30
Mn [ppmw]	29
Zn [ppmw]	< 10
Cd [ppmw]	< 10
Pb [ppmw]	< 10

The main function of the binder is, in dry condition, to bind the pigment on the surface of the paper and hold single pigment particles together. There are two different types of binder: natural and synthetic. In the first group, animal glue and gelatins, casein, soyaprotein, carboxylmethylcellulose and several cellulose derivatives are used. The synthetic binders are made out of dispersion of mixed polymers with a variation in degree of polymerisation. To this group, which goes under the name latex, one will find mixed polymers of styrene-butadiene, butadiene-methyl-metacrylat, acrylic acid ester, butadiene-acrylonitrile and plyvinylacetate. In addition, polyvinylalcohol, which is soluble in water, belongs to this group.

The purpose of the chemical additives is in general to: improve the dispersion of pigment, change the viscosity of the coating melt, reduce the foaming tendency of the coating melt, change colour, harden the coating layer, prevent bacterial attack on the coating melt and serve as a lubricant during the coating process. Chemical additives can both be inorganic and organic, but will not be discussed further here.

3.2.1.2 The process of papermaking – the production of paper pulp

In general one can divide paper production into two different categories, namely mechanical and chemical pulp. Mechanical energy is used for defibration to fibre and fibre fragments for the production of mechanical pulp. When producing mechanical pulp the pulp yield as a percentage of the wood used is typically 96-100%. When producing chemical pulp, chemical energy is used for the removal or softening of the binding substance between fibres so they end up as free single fibres without or with a small amount of mechanical energy (blowing, pumping). The most commonly used boiling processes to make chemical pulp are the sulphite, soda and sulphate (kraft) processes. The most important chemicals used in the Kraft boiling process are NaOH

and Na_2S. Approximately 80% of produced chemical pulp are made by the kraft process. During the kraft process one will have a gradual reduction of the amount of lignin and hemicellulose. In other words, the cellulose becomes more dominant. Increased boiling time decreases the content of hemicellulose and lignin and a minor part of the cellulose. Production of kraft pulp from spruce at a pulp yield of 46%, reduced the hemicellulose share from 29% to 9%. Chemical pulp has a typical pulp yield between 30-60%. In between these two categories one also have what is called half-chemical pulp, which typically has a pulp yield of 50-85%. Half-chemical pulp is made by increasing the chemical treatment from nothing, which is the case for mechanical pulp, in order to decrease the need for mechanical treatment to separate the fibres. Na_2SO_3 alone or Na_2SO_3 and Na_2CO_3 are usually used in the boiling process. Chemically produced pulp is often not white enough to satisfy the requirements of many paper products used today. Removal of the coloured substances, which are considered to be lignin in particular, but it can also be extractives and transformed carbohydrates, is usually done by the use of chlorine and alkali treatment. Chemical pulp with a yield of 55%, can have a lignin content varying from 0.5 % up to 12%. After the bleaching process the lignin content will typically be between 0.2 - 1.0%.

3.2.1.3 Paper and cardboard used in this study

The paper and cardboard samples used in this study are typical for the paper fraction of MSW. There are no available data on the exact composition, but this will be discussed based on general knowledge of the different types of paper and cardboard. Exact composition of each paper and cardboard type including additives is not so easy to obtain due to the companies production secrets. Figure 5 shows the typical paper composition and yield for two types of paper and cardboard.

Newspaper. Mechanical pulp is often used in newspapers or other types of paper with a relatively short life. Up to 5-10% of chemical pulp is often added to the mechanical pulp when producing newspaper, in order to get a better quality and to make the processing easier. In some cases up to 30% of de-inked recycled newspaper pulp can be used for the production of newspaper.

Glossy paper. Glossy paper, coated paper or magazine paper as it often is called is produced in several qualities. Three different qualities could be mentioned. Class I: 60% sulphate mass and 40% mechanical mass, Class II: 50% sulphate mass and 50% mechanical mass, Class III: 30% sulphite mass and 70% mechanical mass. In addition, glossy paper can have up to 30% of additives.

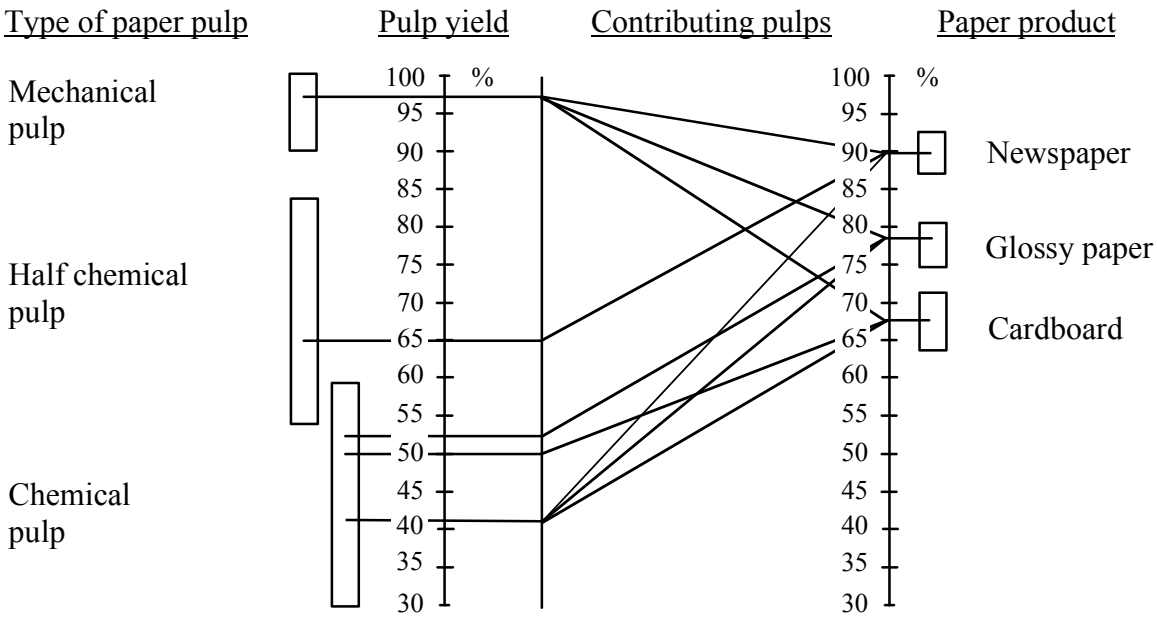

Figure 5. Contributing pulps for different types of paper and cardboard[17].

Recycled paper. Paper made of 100% recycled paper is very hard to characterise. This type of paper can be made of any number of different qualities. It is however characterised by a relative high content of ash.

Cardboard. The type of cardboard used in this study is made of two different types of pulp. Unbleached sulphate pulp are typically used in the flat layer of unbleached cardboard, while unbleached half chemical pulp is used in the corrugated cardboard (the layer in between the two flat layers in cardboard).

3.2.2 Plastic fraction

Today the plastics industry is heavily integrated with the oil industry. Oil is the major raw material for plastic production today. This is very different from the situation 40-50 years ago, when coal and cellulosic material such as waste oak husks, sugar cane, soya beans and natural rubber were the major raw materials.

Six different types of plastic are investigated in this study. HDPE, LDPE, PS, PP, PPVC (plasticised polyvinylchloride) and UPVC (unplasticised polyvinylchloride). Above a certain temperature, all these plastics are capable of flow; in other words, it is essentially plastic, whereas below this temperature it is to all intents and purposes a solid. This is what characterises a thermoplastic.

3.2.2.1 Chemical composition and structure

In order to understand the thermal decomposition of the different plastics, it is important to understand their chemical structure. All plastics materials consists of a mass of very large molecules. In the case of a few naturally occurring materials, such as bitumen, shellac, and amber, the compositions are heterogeneous and complex but in all other cases the plastics materials belong to a chemical family referred to as high polymers. For most practical purposes, a *polymer* may be defined as a large molecule built up by repetition of small, simple chemical units or *monomers*. Figure 6 shows the repeating units or monomers of the different plastics in this study.

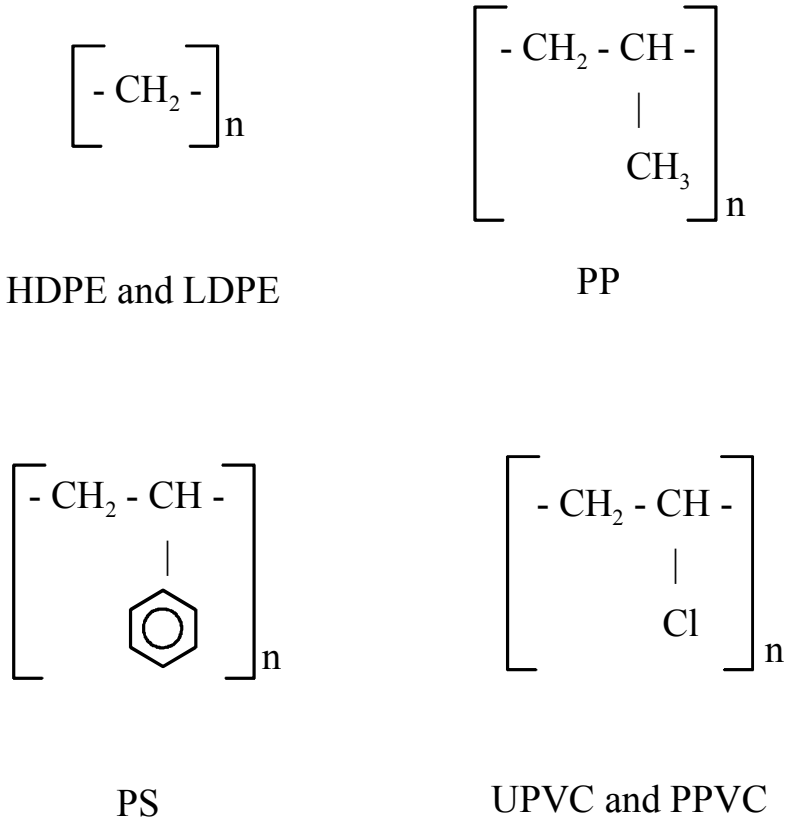

Figure 6. Repeating units for the six different plastics.

HDPE and LDPE. For both HDPE and LDPE the polymer structure is essentially a long chain of aliphatic hydrocarbons. For general technological purposes, the difference in density between HDPE and LDPE is due to the chain branching.

PP. PP has a slightly different structure than LDPE and HDPE with a methyl group (CH_3) in the repeating unit, but is also an aliphatic hydrocarbon type. There is also a difference in melting temperature between PP and regular polyethylene (PE). PP has a melting temperature, which is approximately 50^{o}C higher than PE.

PS. PS is made from the styrene monomer and the repeating unit contains a benzene ring. The presence of the benzene ring results in PS having greater reactivity than PE.

PPVC and UPVC. For PPVC and UPVC the methyl group of PP has been substituted with chlorine (Cl). Commercial PVC polymers are largely amorphous, slightly branched molecules with the monomer residues arranged in head-to-tail sequence. The major difference between PVC and the other plastic is the high content of chlorine (approximately 50 w%). PPVC is built up of 100 parts PVC K-number 70, 48 parts of DEHP plasticiser (di-2-ethylhexyl phthalate), 2 parts of Ba/Zn stabiliser and 5 parts of lubricant/secondary plasticiser. UPVC on the other hand is built up of 100 parts PVC K-number 57, 1.5 parts of Ba/Zn stabiliser, 8 parts of modified acrylat elastomer, 1 part of lubricant/secondary plasticiser and 1.5 parts of acrylat copolymer.

3.2.3 Multi-material fraction

In this study, two types of beverage cartons have been chosen to represent the multi-material fraction. The beverage cartons represent a major share of the multi-material fraction of MSW. Two main types of beverage cartons are used worldwide: those made of paperboard and polyethylene and those made of paperboard, polyethylene and aluminium.

Milk carton. The milk carton consists of paperboard and plastic. The cardboard in these types of cartons is typically made of unbleached, half bleached or bleached chemical pulp. The cardboard is waxed or has a layer of polyethylene both on the inside and outside. The paperboard usually constitutes 90% and the polyethylene 10%.

Juice cartons. The juice carton consists of paperboard, plastic and aluminium. The paperboard and plastic is of the same quality as that of the milk carton. The structure of this type of cartons is polyethylene at the outside, then paperboard, polyethylene, aluminium foil and polyethylene on the inside. The paperboard typically constitutes 75% of the weight, while polyethylene and aluminium foil constitute 20% and 5%, respectively.

3.2.4 Wood and cotton

Two different types of wood were included in this study. One hardwood (birch) and one softwood (spruce). These wood types are typical raw material used in the production of paper, but they are also typical for the wood fraction of MSW. One sample of cotton was taken from a cotton sweater.

Birch and spruce. Birch was taken as a sample of hardwood and spruce was taken as a sample of softwood. Birch has less lignin, but a higher content of hemicellulose than spruce, as can be seen from Table 2.

3.2.5 Chemical bonds in polymers

Several types of chemical bonds are present between atoms and molecules in polymer materials. The single chain molecule is kept together by strong valency bonds

(primary bonds). Much weaker secondary bonding ties the different molecules together. The most important secondary bonds are: dipole forces, induction forces, dispersion forces and the hydrogen bond. Dissociation energies for some selected primary bonds are shown in Table 5.

Table 5. Dissociation energies for some selected primary bonds.

Bond	Dissociation energy [kJ/mole]
C-C	347
C=C	611
C-H	414
C-O	360
C=O	749
C-N	306
C=N	892
C-Cl	339
C-F	431
O-H	465
O-O	147
Si-Si	178
S-S	268

3.3 Experimental methods and equipment

Experimental equipment and applied methods used in this study will be explained in this section.

3.3.1 Proximate analysis and higher heating value (HHV)

Experiments determining moisture, ash, higher heating value, fixed carbon and volatiles have been performed. Since MSW consist of a large number of different components (i.e. different types of paper, different types of plastic, wet organic waste, etc.), it would be almost impossible to have a standard test procedure for each component in MSW. However, there exist several standard procedures for RDF (Refuse Derived Fuel) which could be used for a proximate analysis of MSW components. RDF typically consists of paper and plastic (typical composition 70% paper, 20% plastic, rest 10%). Standard test procedures for RDF is the best available standardised method to use when performing a proximate analysis of MSW fractions. However, standard methods for proximate analysis must be used with caution due to the difference in fuel quality for each fraction and even within each fraction.

Moisture determination. The ASTM E 790 - 87 procedure, "Residual Moisture in a Refuse-Derived Fuel Analysis Sample" was employed for these experiments. Longer drying time (4 hours) and larger samples (up to 12 g) were used, because the dried sample was used for ash and higher heating value determination.

Ash analysis. The ASTM E 830 - 87 procedure, "Ash in the Analysis Sample of Refuse-Derived Fuel", was used to determine the ash content. In order to close the mass balance it was necessary to perform the ash analysis at a higher temperature (950^{o}C) for two of the paper samples. The reason for this was that a significant amount of volatile ash components was released between 575^{o}C and 950^{o}C. For the ASTM standard, 575^{o}C were used, while 950^{o}C was the temperature used to determine the volatile matter. These samples are marked in the table of results (Table 8). Due to lack of right equipment and the properties of some samples, the samples were not milled into small particles (< 0.5 mm) but cut into thin particles (<10 mm). However, the effect of milling the samples into particles less than 0.5 mm was examined for one type of paper for the ash analysis. The deviation between the milled sample and the sample cut into small particles was less than 3%.

Higher heating value. The ASTM D 3286 - 73 procedure, " Gross Calorific Value of Solid Fuel by the Isothermal-jacket Bomb Calorimeter" was used to determine the higher heating value.

Volatile matter. The ASTM E 897 - 88 procedure, "Volatile Matter in the Analysis Sample of Refuse-Derived Fuel" was used to determine volatile matter. The oven used for determining the volatile matter was not a standardised oven, which is described in the ASTM standard, but a muffle oven. As for the ash determination, the samples was not milled into small particles, but cut into thin particles. The deviation between the milled sample and the sample cut into small particles was tested and found to be 0.3%.

Fixed carbon. Fixed carbon was determined by subtracting ash and volatile matter from the initial sample mass.

3.3.2 Thermogravimetric (TGA) kinetic study

The motivation for the TGA experiments was to try to establish a relationship between chemical kinetics and the chemical composition of MSW components. In addition, the knowledge of the thermal decomposition for the different MSW components, including the char forming tendencies, is of interest.

Materials. The materials used in this study were clean samples of different typical solid waste fractions. The different waste fractions consist of different components. The paper and plastic fractions of MSW for instance consists of several different paper and plastic types, therefore different paper or plastic types within a given fraction has been tested. All plastics were pure, none or light coloured, samples. The samples were carefully cut into thin and very small particles in order to avoid heat and mass transfer within the sample during the experiment.

Methods and equipment. Figure 7 shows a schematic diagram of the SDT 2960 Simultaneous TGA-DTA from TA Instruments. The system is based on a dual beam horizontal design in which each ceramic beam (arm) functions as one half of a DTA

thermocouple pair, as well as part of a horizontal null-type balance. One arm accommodates the sample and measures its property changes. The other arm accommodates the reference (typically an appropriate amount of inert material such as aluminium oxide) and is used to generate the DTA (ΔT) measurement, as well as to correct the TGA measurement for temperature effects like beam growth.

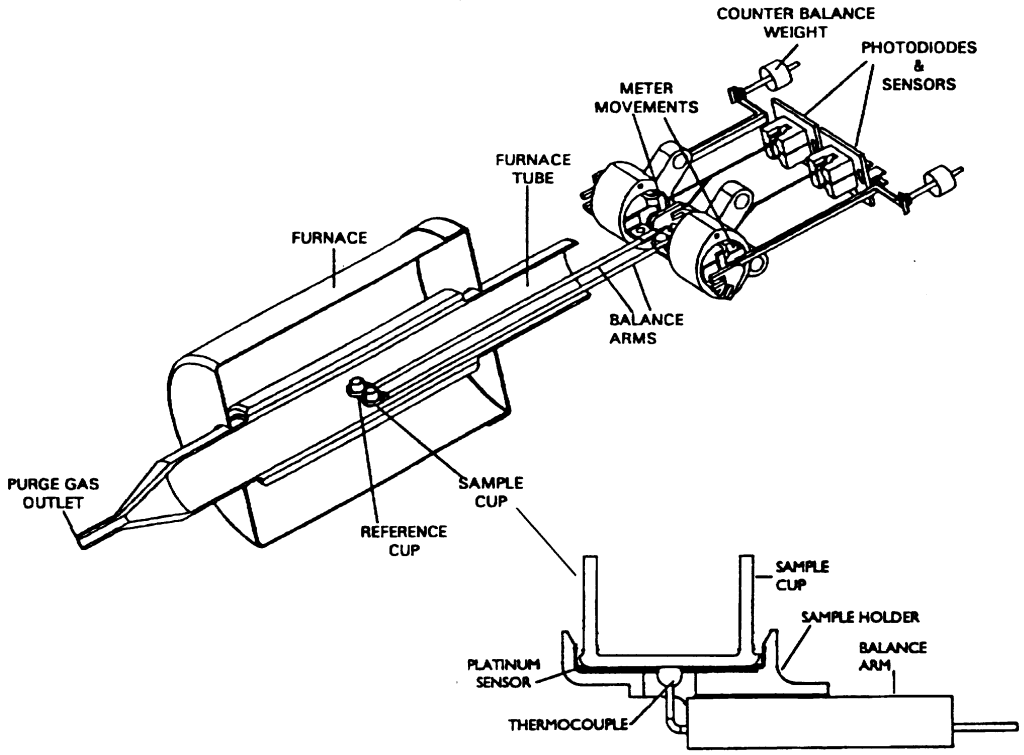

Figure 7. Schematic figure of the SDT 2960 Simultaneous TGA-DTA from TA Instruments.

The TGA weight change is measured by a taut-band meter movement located at the rear of each of the ceramic arms. An optically activated servo loop maintains the balance arm in the horizontal reference (null) position by regulating the amount of current flowing through the transducer coil. An infrared LED light source and a pair of photosensitive diodes detect movement of the arm. A flag at the end of the balance arm controls the amount of light reaching each photo sensor. As weight is lost or gained, the beam becomes unbalanced, causing unequal light to strike the photodiodes. A restoring current is generated to eliminate this imbalance and retain the null position. The amount of restoring current is a direct measure of the weight change.

The DTA (ΔT) measurement is made by a pair of matched platinum/platinum-rhodium thermocouples, which are contained inside the ceramic arms and welded to platinum sensors located in the bottom of the sample and reference holders. The thermocouple in contact with the sample is also used to monitor the sample temperature. The sample and reference cup used in these experiments is made of platinum, which is easy to clean and do not react with most materials.

A bifilar-wound furnace provides uniform controlled heating up to 1500°C. The SDT 2960 have a sample capacity up to 200 mg and a balance sensitivity of 0.1μg. The heating rate can be set from 0.1 to 100°C/min for experiments from ambient to 1000°C and 0.1 to 25°C/min for experiments from ambient to 1500°C.

High purity nitrogen (Hydro Ultra 5.0, 99,999% purity) was used for the experiments at a flow rate of 150 ml/min. The experiments were conducted as follows. Before each experiment, the balance was tarred with the sample and reference cups. Then the sample cup was taken off and the small sample particles were spread in a uniform layer in the sample cup. The sample cup was then placed back on the balance and the furnace was closed. Nitrogen was purged for 20 minutes, then the sample was heated up to 110°C at a heating rate of 30°C/min in order to dry the sample and be sure of an atmosphere free of oxygen. After a drying period of 30 minutes, the sample was heated up to the desired temperature (500 or 600°C) with the pre-selected heating rate (10°C/min). The sample was held at the desired temperature for 5 minutes and then synthetic air was purged at the same flow rate for 20 minutes in order to burn off the sample to ease the cleaning of the sample cup. The heater was then turned off and air purged to cool the reactor. The procedure for these experiments were created and controlled in a program called "Thermal Solutions", specially designed for controlling the SDT 2960 apparatus on an IBM PS/2 77 486DX2 computer.

Selecting the proper sample size and heating rate is very important. Too large samples may shift the decomposition from control by chemical kinetics to control by heat and mass transfer. Performing experiments with a too high heating rate may introduce thermal lag which causes the temperature measurement to be incorrect[25]. Various experiments with different sample size and heating rates have been conducted in order to choose the proper sample weight and heating rate. Sample sizes of 2, 5 and 10 mg and heating rates of 5, 10 and 40°C/min were tested on a reference material (whatman filter paper). Kinetic analysis of the experiments showed that there was not a large difference in activation energy and frequency factor for the different sample sizes. The activation energy varied from 279-281 kJ/mole for the analysis of the TG curves (weight loss curves) and from 261-266 kJ/mole for the analysis of the DTG curves (rate of weight loss curves). Based on these results a sample size of 5 ± 0.2 mg (except for polystyrene (isoprene) where a sample weight of 2.8 ± 0.2 mg was used due to low density) was chosen. Comparing calculated activation energy and frequency factor for experiments at 5°C/min and 10°C/min with a sample weight of 5 mg showed small variations. Experiments at 40°C/min, however, gave a lower activation energy than at 5°C/min and 10°C/min and was therefore excluded. This lower activation energy might be caused by the effect of thermal lag[25]. A heating rate of 10°C/min was chosen in order to reduce the experimental time.

3.4 Kinetic analysis

Several kinetic models have been used in the literature to describe the pyrolysis of biomass and MSW. In this study, a method previously used on biomass has been applied to MSW components[26].

The reaction rate for thermal decomposition of a homogeneous solid is written as:

$$\frac{d\alpha}{dt} = kf(\alpha) \tag{1}$$

where α is the conversion (reacted fraction), k is the reaction rate constant depending on the pyrolysis temperature according to the Arrhenius expression given in equation (2).

$$k = A\exp\left(\frac{-E}{RT}\right) \tag{2}$$

A is the frequency factor, E is the activation energy, R is the gas constant and T is the temperature. The function $f(\alpha)$ is approximated by:

$$f(\alpha) = (1-\alpha)^n \tag{3}$$

where n is the formal reaction order. The conversion, α, can be expressed by:

$$\alpha = \frac{1-m}{1-m_{char}} \tag{4}$$

where m is the actual sample mass and m_{char} is the char yield normalised by the initial sample mass m_0.

Combining equation (1), (2), (3) and (4) gives:

$$\frac{d\alpha}{dt} = A\exp(-E/RT)(1-\alpha)^n \tag{5}$$

The reaction order (n) is strongly connected to the degree of asymmetry of the DTG curves. If the reaction order is larger than one, the descending part of the DTG curve is less steep than in the case of a pure first-order reaction. If the reaction order is lower than one, the descending part becomes steeper than in the case of a pure first-order reaction. However, in this study a reaction order of one has been used.

MSW components such as paper or plastic (PVC) often consists of more than one chemical substance. Assuming that each substance decomposes independently from each other, the overall conversion and rate of conversion for N reactions can be described by:

$$m = 1 - \sum_i c_i \alpha_i \qquad (6)$$

$$i = 1,2,3....N$$

$$-\frac{dm}{dt} = \sum_i c_i \frac{d\alpha_i}{dt} \qquad (7)$$

The separate conversion (reacted fraction) α_i for each component is given by:

$$\alpha_i = \frac{(m_{0,i} - m_i)}{(m_{0,i} - m_{char,i})} \qquad (8)$$

where $m_{0,i}$, m_i and $m_{char,i}$ are the initial sample mass, the actual sample mass and the final char yield (normalised with m_0) of component i, respectively. The components are all assumed to decompose independently according to:

$$\frac{d\alpha_i}{dt} = A_i \exp(-E_i / RT)(1 - \alpha_i) \qquad (9)$$

Here, the reaction order is assumed equal to one (n=1) for all reactions. Coefficient c_i express the contribution of the partial processes to the overall mass loss, m_0-m_{char}:

$$c_i = m_{0,i} - m_{char,i} \qquad (10)$$

In this study, both integral and differential data have been used to evaluate the kinetic parameters. The specific method has previously been used on biomass in order to determine the kinetic parameters of hemicellulose, cellulose and lignin/char. The kinetic evaluation of the experiments is fully described elsewhere[26].

3.4.1 Literature survey on chemical kinetics from pyrolysis of MSW

Determination of kinetic parameters for some selected MSW components have already been done by other researchers. Although the purpose of these studies was not thermal characterisation of MSW components, some of the work has contributed to a better understanding of the thermal decomposition of MSW[28,29,30,31]. In the last two decades, several TGA studies of selected MSW components have been conducted. These studies were performed in order to characterise waste components for practical use and modelling purposes [9,32,33,34,35,36]. Studies on chemical kinetics of single MSW

components such as polyethylene, PVC, polystyrene, polyamide, newspaper and coated writing paper has been done with varying equipment and analysis methods[37,38,39,40,41,42]. Research on chemical kinetics of mixtures of MSW components in order to simulate either MSW or RDF pyrolysis have also been done [43,44,45,46,47,48].

Rather than discussing the different methods and results in detail, Table 6 give a summary of the most important results. As can be seen from Table 6, there is a large difference in methods and results for the different components. These results, however, will be discussed together with the new results obtained in this study. Characterisation of different biomass and MSW components by thermogravimetry have also been performed, however, only the TGA curves and no kinetic analysis was presented in this study[49]. All of the above mentioned work has contributed to a better understanding of pyrolysis of MSW. In spite of the fact that a lot has been done in this area, there is still a need for a detailed thermal characterisation of MSW components. Using a uniform analysis method and link the thermal degradation to the chemical composition will give additional knowledge and understanding of the thermal behaviour of MSW.

Table 6. Survey of kinetic data for MSW components.

Component	n	log(A) [log s^{-1}]	E [kJ/mole]	Conditions	Reference
Coated paper 1	1.5	12.9	182.0	TGA, 4 mg, N_2,	24
Coated paper 2	2.0	4.0	105.0	1, 2 and 5°C/min, 200-630°C	
Hemicellulose[a]	1.0	19.4	119	TGA, 5 mg, N_2,	26
Cellulose[a]	1.0	8.2	260	5°C/min, 150-500°C	
PS 1 (0-15%)	0.00	-	192.6	TGA, 100 mg, vacuum,	28
PS 2 (15-95%)	1.00	-	251.2	5°C/min, 250-500°C	
PE 1 (0-3%)	0.00	-	200.9	Freeman and Carroll method	
PE 2 (3-15%)	-	-	255.3		
PE 3(15-35%)	-	-	-		
PE 4 (35-95%)	1.18	-	280.5		
PP	0.88	16.0	242.8	DTA, N_2, 10°C/min	30
PS	0.50	10.7	172.0	TGA, 4 mg, N_2,	40
LDPE	0.50	11.1	194.2	1.1-5.8°C/min, 230-530°C	
PVC1[b]	1.54	17.6	190.0	TGA, 2-20 mg, He,	42
PVC2[b]	1.80	18.4	260.0	1-50°C/min, 20-550°C	
Newspaper 1[c]	1.00	4.6	126.0	TGA, 100 mg, N_2,	45
Newspaper 2[c]	1.00	-5.1	8.1	50°C/min, 200-900°C	
PP	1.00	11.6	264.6	Coates and Redfern method	
HDPE	1.00	15.4	326.1		
HDPE	0.74	14.0	233.2	TGA, 4 mg, N_2,	46
LDPE	0.63	12.1	206.4	1-5.5°C/min,	
PP	0.90	10.8	183.8	200-530°C	
PS	0.50	10.7	172.0		
PVC 1[d]	1.50	12.2	163.7		
PVC 2[d]	0.00	15.2	190.0		
PVC 3[d]	1.50	16.7	267.1		
PVC 4[d]	1.50	12.7	217.7		
PE	0.30	15.0	248.0	TGA, <10 mg, N_2, 10-20°C/min, 150-800°C	47

Table 7. Survey of kinetic data for MSW components. Continued.

Component	n	log(A) [log s^{-1}]	E [kJ/mole]	Conditions	Reference
Cellulose (whatm. no. 1)	1.00	14.2	205.1	TGA, 70 mg, N_2, 5°C/min, 200-550°C	48
Newsprint	1.00	6.2	110.1		
Kraft paper	1.00	11.5	169.1		
PE	1.00	9.8	174.6		
PS	1.00	9.0	159.1		
Avicel cellulose	1.00	18.0	238.0	TGA, average of 21 exp., 2-80°C/min	51
Cellulosic paper	1.8	17.3	220.0	TGA, 4-5 mg, N_2, 1-5°C/min, 200-550°C	52
Cellulose	1.0	12.1	173.7	TGA, 100 mg, N_2,vacuum 5-9°C/min, 200-600°C	53

[a] Mean values taken from four different types of wood
[b] PVC is divided into two different decomposition areas, 10 mg sample
[c] Newspaper has been divided into two different decomposition areas
[d] PVC is divided into four different decomposition areas

3.5 Results and discussion

In the following section, results from the proximate analysis, HHV determination and the TGA evaluation, are presented as given in reference[54].

3.5.1 Proximate analysis and HHV

Results of proximate, moisture and HHV experiments are given in table 8. The proximate analysis for the different paper components shows a large variation in ash content. A clear linear relationship between ash content and HHV was found for the paper/cardboard fraction as shown in equation (11):

$$HHV\left[MJ/kg\right] = 19.704 - 0.3233 \cdot Ash\left[w\%\right] \qquad (11)$$

The largest deviation from the values obtained for the HHV determination for this empirical formulae was approximately 3%. The volatile matter and fixed carbon content for the paper/cardboard fraction can also be described by linear relationships as a function of ash content as described in equation (12) and (13):

$$Volatile\,matter\left[w\%\right] = 90.198 - 0.8106 \cdot Ash\left[w\%\right] \qquad (12)$$

$$Fixed\,carbon\left[w\%\right] = 9.802 - 0.1894 \cdot Ash\left[w\%\right] \qquad (13)$$

The largest deviation from the experimental values for these empirical formulas were 1.5% and 19% for the volatile matter and fixed carbon respectively. The moisture content decreases with increasing ash content, however no linear relationship was found. It should be noted that the moisture content determined in these samples are pure non-contaminated samples and that the moisture content is a function of the humidity of the air when sufficient time for equilibrium is provided. The linear relationships shown for the paper/cardboard fraction can be explained by the fact that they all originate from the same substance, namely wood, with minor differences in chemical composition on an ash free basis.

Table 8. Proximate analysis and higher heating value of MSW components.

Sample No.	Component	Moisture (%)	Ash	Volatile matter	Fixed Carbon	HHV [MJ/kg]
1	Newspaper	8.1	1.0	88.5	10.5	19.3
2	Cardboard	6.2	8.4	84.7	6.9	16.9
3	100% Recycled paper	5.4	20.2[a] (22.4)[b]	73.6	6.2	13.6
4	Glossy paper	3.7	28.0[a] (42.7)[b]	67.3	4.7	10.4
5	HDPE	0.0	0.0	100.0	0.0	46.4
6	LDPE	0.1	0.0	100.0	0.0	46.6
7	Coloured plastic bag	0.4	1.5	98.5	0.0	45.8
8	PP	0.1	0.0	100.0	0.0	46.4
9	PS	0.7	0.0	99.8	0.2	42.1
10	UPVC	0.1	0.4	94.8	4.8	22.8
11	PPVC	0.3	0.4	95.1	4.5	26.6
12	Spruce	6.9	0.2	89.6	10.2	19.3
13	Birch	6.5	0.3	91.8	7.9	19.1
14	Cotton (from sweater)	4.7	0.1	98.0	1.9	16.8
15	Milk carton	5.1	3.2	90.4	6.4	21.0
16	Juice carton	4.0	7.9	86.0	6.1	24.4

[a] Measured at 950°C.

[b] Measured at 575°C.

For the plastics and the other components of this investigation it is harder to provide any meaningful relationship between proximate parameters since the chemical composition, on an ash free basis, varies largely.

However, for most of the plastics (excluding PPVC and UPVC), a similar behaviour is observed with 100% volatiles and a HHV of approximately 46 MJ/kg with the exception of PS, which have a slightly lower HHV. PPVC and UPVC show a quite different behaviour than the other plastics due to the high content of chlorine. The heating value is lowered by approximately 50% and they have a char-forming tendency with almost 5% fixed carbon.

The two different types of wood and cotton show similar behaviour although cotton has a higher volatile fraction and a lower share of fixed carbon.

It is interesting to see that the multi-material components, juice- and milk cartons behave as a sum of the individual materials. The presence of LDPE in milk carton increases the HHV and volatile matter, while ash content and fixed carbon are reduced compared to cardboard, which is the most comparable in this case. For the juice carton, the presence of aluminium increases the HHV (HHV of aluminium is approximately 30 MJ/kg) and ash fraction, but decreases the volatile matter and fixed carbon.

3.5.2 Evaluation of TGA experiments

The results from this study will be discussed in different sections, one for the cellulosic fraction, one for the plastic fraction and one for the multi-material fraction. All TG curves include ash. The ash content should be subtracted in order to obtain the true char fraction.

3.5.3 Cellulosic fraction of MSW

Several considerations must be made when discussing the results from the experiments and calculations on chemical kinetics for the cellulosic fraction. Since the decomposition has been modelled as a set of independent parallel reactions, it is important to understand how these chemically different components, which constitute paper, decompose during pyrolysis. When trying to link the kinetic behaviour of the cellulosic fraction to the chemical composition, it is also necessary to be aware of differences in decomposition due to catalytic effects or chemical and physical composition and structure. This work will not have an extensive study on the catalytic effects of the inorganic substances from the decomposition of the cellulosic fraction since this have been done by other researchers[26,51,55]. However, washing of newspaper and glossy paper in order to remove ash species was tried, but it was not possible to observe any effect of this washing process. Other studies have shown that washing out ash species may alter the chemical composition of the sample by reducing the hemicellulose to cellulose ratio[51].

Studies have shown that there exists a difference in char fraction and decomposition temperature for cellulose, hemicellulose and lignin for different types of biomass. It is important, however to notice that extracted cellulose, hemicellulose and lignin most likely will behave differently from cellulose, hemicellulose and lignin chemically bound together in wood or paper[26].

Experiments on two different types of wood, namely spruce (softwood) an birch (hardwood) have been performed to illuminate the difference in raw material for paper production and to characterise wood as an component of MSW. Wood can also serve as an example of mechanical pulp since the composition is not altered to any large extent. Cotton, both as cotton linters and as waste cotton from the textile fraction, has been examined as a sample of pure cellulose. The most commonly used paper pulps have also been tested for comparison with wood and paper.

Figure 8 shows TG and DTG curves for three different types of paper, cardboard, and spruce. One interesting observation is the similarity in decomposition between

newspaper and spruce. However, this is surprising, since newspaper mainly consists of mechanical pulp with low ash content. Even the char fraction is equal taking into account that newspaper had approximately 1 % higher ash content than spruce. Subtracting the ash from the remaining residue at 500^{o}C gives similar char fractions for all types of paper. The DTG curves showed a pronounced shoulder prior to the cellulose peak for newspaper and spruce and to a lesser extent recycled paper. This shoulder is believed to be the decomposition of hemicellulose. Cardboard and glossy paper, however, had no pronounced shoulder describing the hemicellulose decomposition even when knowing that both samples contained hemicellulose. Newspaper, with a typical pulp yield of 90%, would, have a hemicellulose content of 26% and a lignin content of 28%. Glossy paper with a typical pulp yield of 75-80 % would have a hemicellulose content of approximately 19% and a lignin content of 26%. Cardboard with a typical pulp yield of 65 – 70 % would have a hemicellulose content of 19% and a lignin content of 18%. The explanation of the lack of shoulder on the DTG curves for hemicellulose for cardboard and glossy paper can be the lower content of hemicellulose and catalytic effects, which can drag the decomposition of cellulose into a lower temperature area. The peak of the highest rate of mass loss for the DTG curves, which supposedly is cellulose, are for cardboard, glossy paper and recycled paper located at a somewhat lower temperature than for newspaper and spruce.

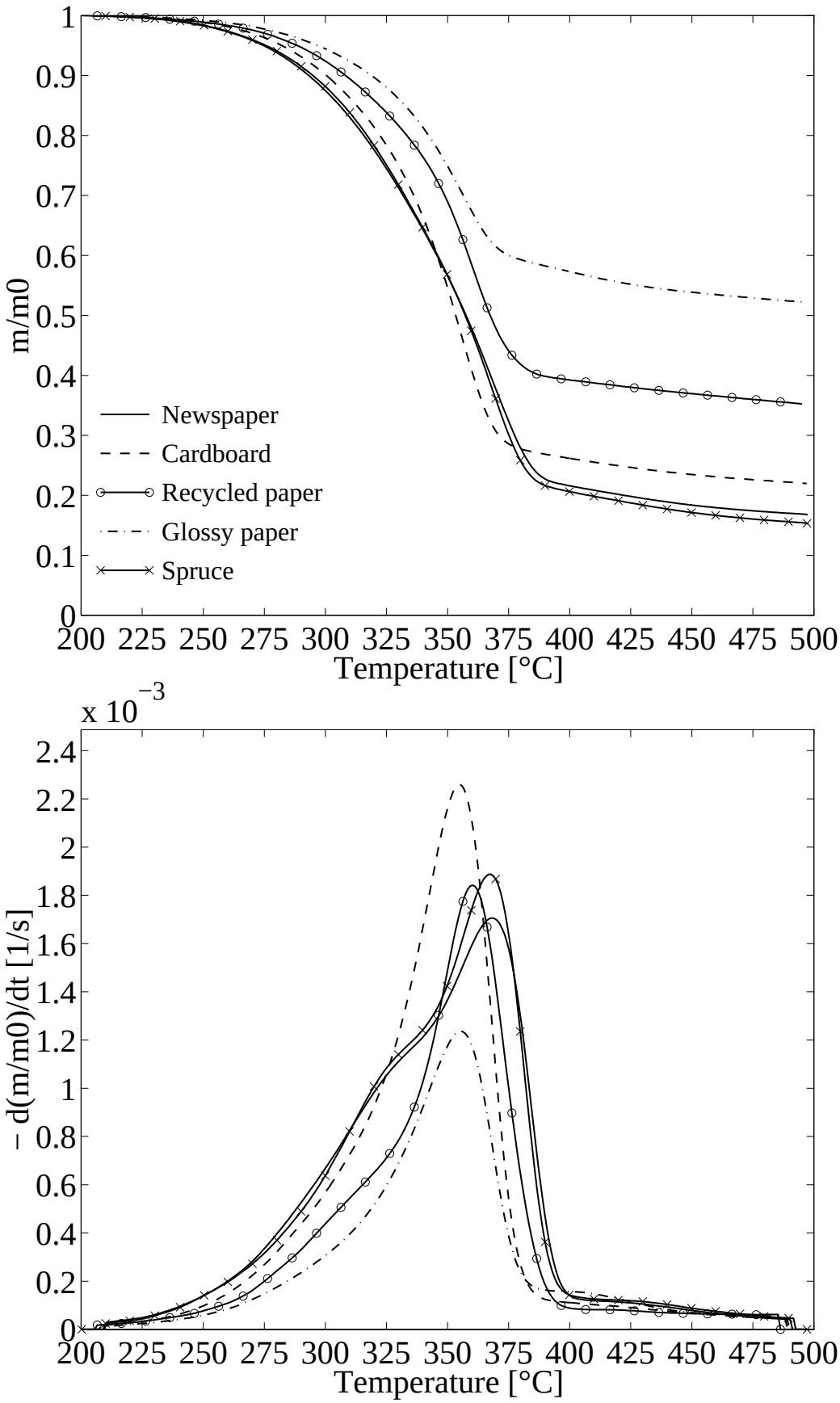

Figure 8. Comparison of TG and DTG curves for three types of paper and cardboard and spruce.

3.5.3.1 Kinetic evaluation of spruce and birch

Figure 9 compares the calculated values and experimental data of weight loss and rate of weight loss for spruce and birch. The two wood species have a similar starting point of devolatilisation at 200°C. At 325°C spruce has a weight loss of 27%, while birch has 35%. As can be observed the degradation of hemicellulose is more pronounced in birch than spruce. This is also expected since birch has a higher hemicellulose content according to Table 2. The remaining residue is quite similar, with 15% for spruce and 13% for birch. In Table 9, the kinetic data obtained from a non-linear least square evaluation of the DTG curves of spruce and birch are presented. Comparing the activation energies for the different reactions show quite similar values. Spruce is modelled with three reactions while birch is modelled with four reactions. The calculated activation energy for reaction 1, is approximately 40 kJ/mole for both spruce and birch. Reaction 1 is considered to be degradation of char from hemicellulose and cellulose and degradation of lignin. This relatively low activation energy together with the low frequency factors indicates that this reaction occur over a broad temperature range and at a low reaction rate. Comparison of reaction 2 and 3 for spruce and birch also show similar values for the activation energy, frequency factors and temperature at the maximum reaction rate according to Table 9. An activation energy of approximately 260 kJ/mole is calculated for reaction 2 for both spruce and birch, which is within the range of activation energies for cellulose found by other researchers[26,51]. The temperature at the maximum reaction rate for reaction 2 is approximately 368°C for both spruce and birch. For reaction 3, which is thought to be the decomposition of hemicellulose, activation energy of approximately 110 kJ/mole is calculated for both spruce and birch. The temperature at the maximum reaction rate for reaction 3 for spruce and birch is approximately 325°C. The fourth reaction for birch, which also can be considered as a part of the hemicellulose decomposition, has activation energy of 162 kJ/mole.

Table 9. Calculated kinetic data for spruce and birch.

Evaluated curve	Reaction 4	Reaction 3	Reaction 2	Reaction 1
	E_4 [kJ/mole] $\log A_4$ [log s^{-1}] c_4 [%] $(T_{peak,4})^{calc}$ [°C]	E_3 [kJ/mole] $\log A_3$ [log s^{-1}] c_3 [%] $(T_{peak,3})^{calc}$ [°C]	E_2 [kJ/mole] $\log A_2$ [log s^{-1}] c_2 [%] $(T_{peak,2})^{calc}$ [°C]	E_1 [kJ/mole] $\log A_1$ [log s^{-1}] c_1 [%] $(T_{peak,1})^{calc}$ [°C]
DTG	-	109.8	255.2	41.3
Spruce	-	7.35	18.85	0.62
	-	33.9	34.2	16.9
	-	326.9	368.7	377.7
DTG	162.3	106.0	262.9	42.9
Birch	13.13	7.08	19.55	0.77
	8.8	33.3	32.6	12.2
	287.6	322.8	367.6	375.5

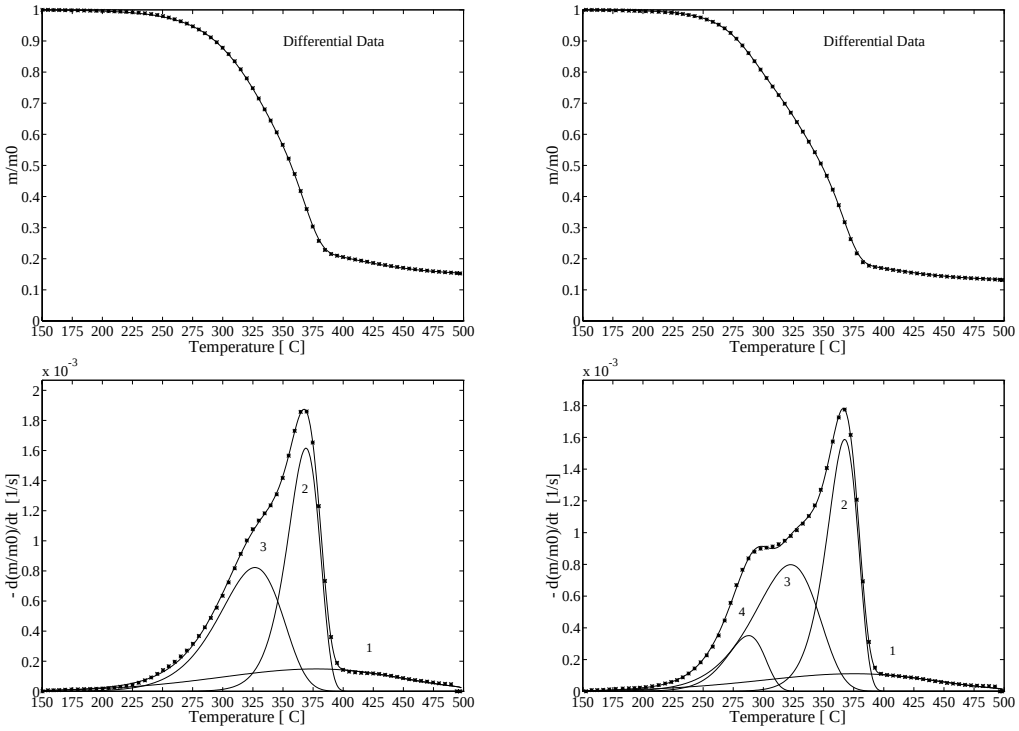

Figure 9. TG and DTG curves for spruce and birch. Spruce to the left.

3.5.3.2 Kinetic evaluation of Cotton from sweater and pure unbleached cotton linters

Cotton has been included in this study as a sample of the most pure form of cellulose found in nature. Pure unbleached cotton linters and cotton taken from a white sweater were examined. Both cottons in this study can be modelled as a single reaction. A difference of approximately 30 kJ/mole in activation energy and 6^{o}C in peak temperature is found for the two cottons (Table 10). Both the activation energy and the peak temperature are in the same range as for spruce and birch cellulose. The remaining residue for cotton linters is approximately 11%, while cotton from the sweater has 6%.

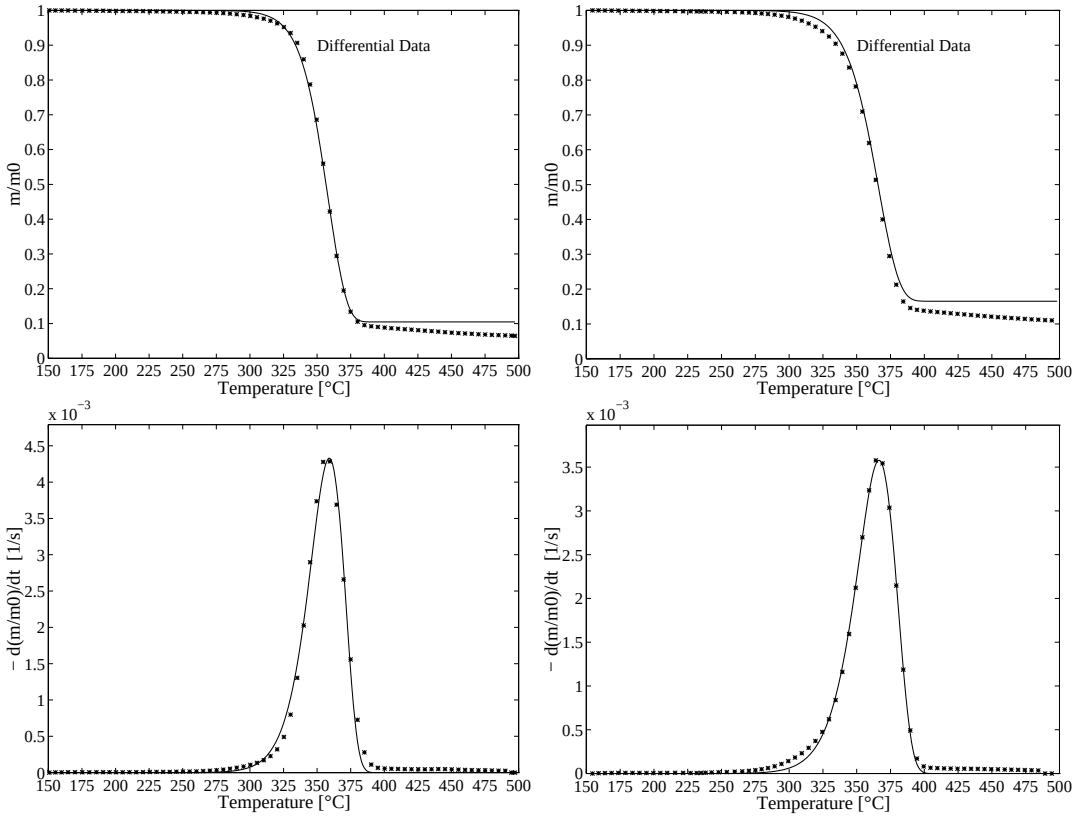

Figure 10. Comparison of TG and DTG curves for cotton from sweater and pure cotton linters. Cotton from sweater to the left.

Table 10. Kinetic data for cotton from sweater and pure unbleached cotton linters.

Evaluated curve	Reaction 1
	E_1 [kJ/mole]
	$\log A_1$ [log s^{-1}]
	c_1 [%]
	$(T_{peak,1})^{calc}$ [°C]
DTG	257.5
Cotton from sweater	19.39
	89.6
	359.5
DTG	229.3
Cotton linters	16.78
	83.5
	366.1

3.5.3.3 Kinetic evaluation of newspaper and cardboard

The TG and DTG diagrams for newspaper and cardboard are given in Figure 11 and Figure 12. Both TG and DTG curves have been evaluated. As Table 11 shows, the differences between these two methods of evaluation for newspaper are minor with respect to the peak temperatures of the three reactions and the activation energy of reaction 1 and 3. However, the difference in calculated activation energy for reaction 2 is somewhat larger. All calculations on paper in this study based on the integral method have a tendency to give higher activation energy for reaction 2 (cellulose) than the differential method. For the other reactions, however, the differences are random and not so evident. Comparison of the activation energy for cellulose with other studies show that the calculations based on the DTG curve gives the most realistic results. Activation energy of 246 kJ/mole and a peak temperature of 371^{o}C, is in the same range as for birch, spruce and cotton. A remaining residue of 16% is in the same range as found for birch and spruce, the ash content taken into consideration. A Comparison between newspaper and spruce, as shown in Figure 8, show similar values for the location of peak temperatures and calculated activation energies. The increase from 0.2% ash (spruce) to 1.0% ash (newspaper) seems to have negligible influence. Reaction 1 and 3 also show similar values in activation energy and peak temperatures as for birch and spruce.

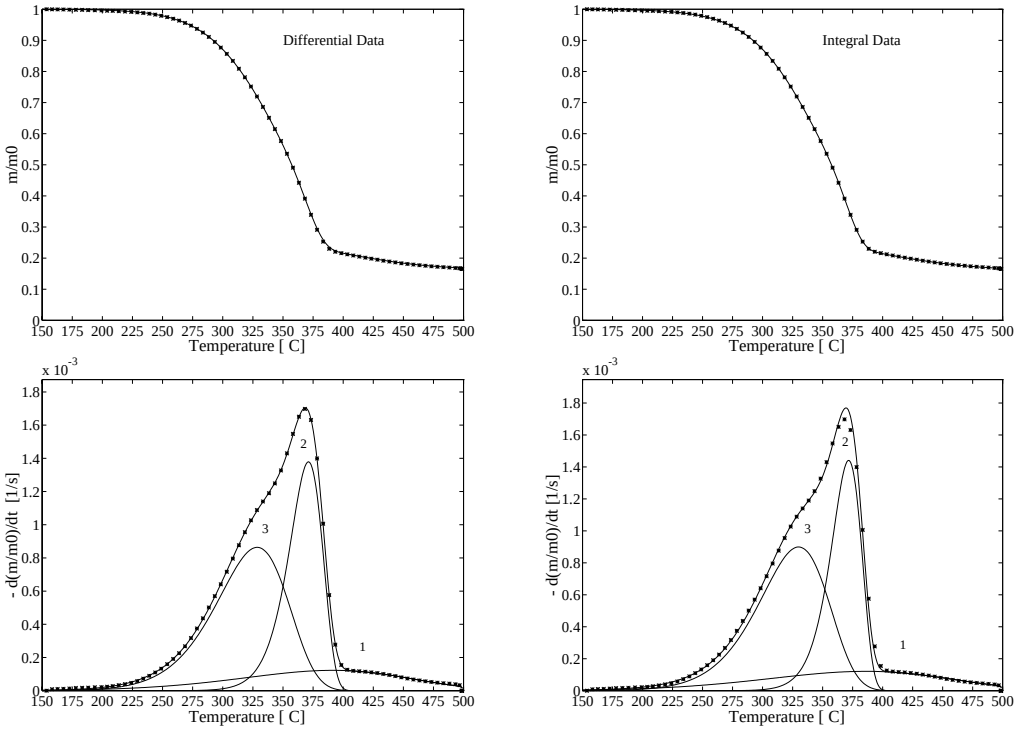

Figure 11. Comparison of TG and DTG curves for newspaper.

Table 11. Kinetic data obtained from TG and DTG evaluation of newspaper.

Evaluated curve	Reaction 3	Reaction 2	Reaction 1
	E_3 [kJ/mole] $\log A_3$ [log s^{-1}] c_3 [%] $(T_{peak,3})^{calc}$ [^oC]	E_2 [kJ/mole] $\log A_2$ [log s^{-1}] c_2 [%] $(T_{peak,2})^{calc}$ [^oC]	E_1 [kJ/mole] $\log A_1$ [log s^{-1}] c_1 [%] $(T_{peak,1})^{calc}$ [^oC]
TG	99.6 6.37 40.9 330.4	270.6 20.04 29.0 371.3	42.2 0.63 13.9 386.4
DTG	96.7 6.12 40.2 328.4	246.1 18.03 30.4 371.3	47.4 1.06 13.0 391.4

Looking at the kinetic parameters for cardboard given in Table 12, the differences between the TG and the DTG analysis are relatively large. The integral method has in this case over-estimated the hemicellulose (reaction 3) fraction of cardboard. This causes an unreasonable high activation energy for cellulose (reaction 2). Relatively large differences in peak temperatures are also observed for the two different methods. There are two reasons why the kinetic data from the differential method in this case is believed to give the most accurate description of the thermal behaviour during pyrolysis. The first reason is that the calculated fraction of hemicellulose is too high using the integral method. The hemicellulose content of cardboard is typically around 20%. The lignin content is typically around 20%, giving a cellulose content of approximately 60%. The calculated c-values are not directly comparable to the real content of hemicellulose, cellulose and lignin, since the char fraction of each individual component is not known. However, an estimated c-value for hemicellulose, which is higher than the c-value for cellulose, seems, in this case, not likely. The other objection against the derived kinetic parameters from the integral method in this case, is the high activation energy for cellulose. The TG method give an activation energy of 297 kJ/mole, while the DTG method give an activation energy of 231 kJ/mole. Comparing these values with the values obtained for cotton linters (229 kJ/mole) and spruce and birch (255 and 263 kJ/mole) and values found by other researchers on cellulose (238 kJ/mole)[51], the activation energy from the TG evaluations seem too high. Subtracting the ash content from the remaining residue gives a char fraction of approximately 13%, which is comparable with newspaper, spruce and birch.

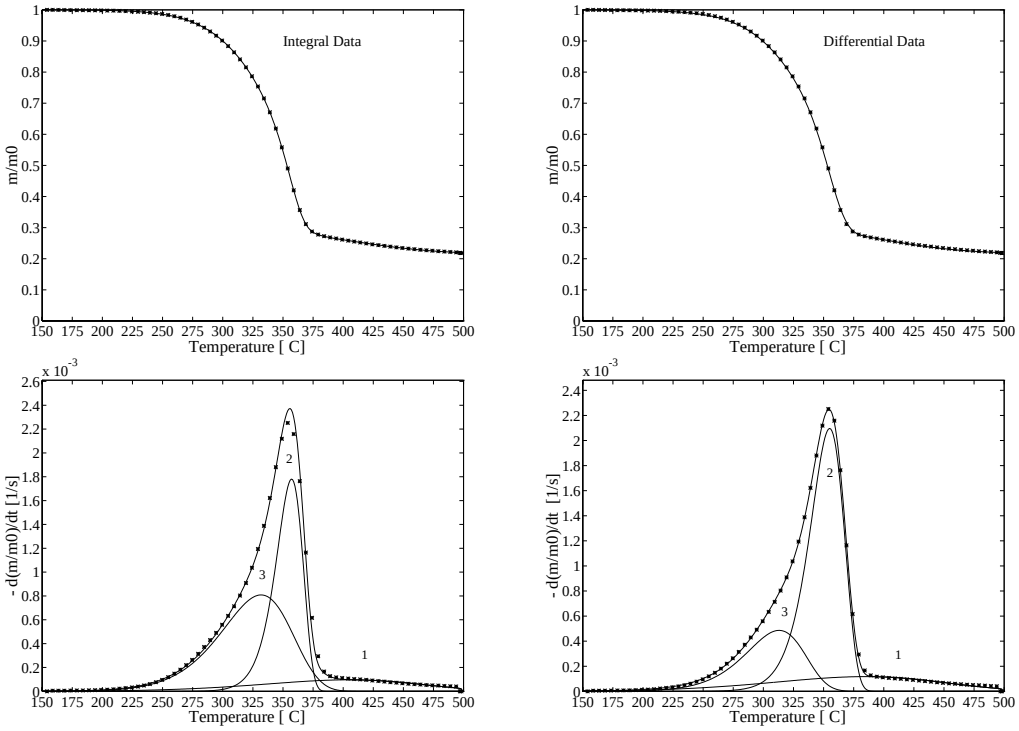

Figure 12. Comparison of TG and DTG curves for cardboard.

Table 12. Kinetic data obtained from TG and DTG evaluation of cardboard.

Evaluated curve	Reaction 3	Reaction 2	Reaction 1
	E_3 [kJ/mole] $\log A_3$ [log s^{-1}] c_3 [%] $(T_{peak,3})^{calc}$ [^oC]	E_2 [kJ/mole] $\log A_2$ [log s^{-1}] c_2 [%] $(T_{peak,2})^{calc}$ [^oC]	E_1 [kJ/mole] $\log A_1$ [log s^{-1}] c_1 [%] $(T_{peak,1})^{calc}$ [^oC]
TG	99.3 6.31 37.2 332.2	296.9 22.79 31.5 357.0	53.2 1.46 9.6 405.2
DTG	112.3 7.82 18.8 313.4	230.6 17.25 47.1 355.0	46.0 0.99 12.5 384.2

3.5.3.4 Kinetic evaluation of recycled paper and glossy paper

Recycled paper is hard to characterise, since it can be made from any number of different types of paper. However, the experiments, showed that a pronounced shoulder could be observed prior to the cellulose peak in the DTG diagrams. As Table 13 shows, the peak temperatures and the obtained activation energies are comparable to those found for other cellulosic materials. Observing the TG curve for glossy paper and the DTG curve for recycled paper and remaining residues at 500°C, it is interesting to see that they are in the same range when subtracting the ash. Glossy paper is modelled with four reactions in order to take into account the observed shoulder (reaction 2) at approximately 400°C. This shoulder is believed to be devolatilisation of additives. The integral method is used for glossy paper due to over-estimation of the devolatilisation of additives when using the differential method. An activation energy of 275 kJ/mole seem high and the reason for this relatively high activation energy can be that the merged DTG curves makes the estimation of the share of hemicellulose and cellulose difficult. The same phenomena were described for cardboard. The activation energies for the other reactions in glossy paper are in the same range as for the other types of wood and paper.

Table 13. Kinetic parameters for recycled and glossy paper. Recycled paper evaluated from DTG curve and glossy paper evaluated from TG curve.

Evaluated curve	Reaction 4	Reaction 3	Reaction 2	Reaction 1
	E_4 [kJ/mole] $\log A_4$ [log s^{-1}] c_4 [%] $(T_{peak,4})^{calc}$ [°C]	E_3 [kJ/mole] $\log A_3$ [log s^{-1}] c_3 [%] $(T_{peak,3})^{calc}$ [°C]	E_2 [kJ/mole] $\log A_2$ [log s^{-1}] c_2 [%] $(T_{peak,2})^{calc}$ [°C]	E_1 [kJ/mole] $\log A_1$ [log s^{-1}] c_1 [%] $(T_{peak,1})^{calc}$ [°C]
DTG	-	136.2	214.0	36.2
Recycled paper	-	10.11	15.67	0.14
	-	11.0	41.4	12.9
	-	309.4	360.2	379.4
TG	99.4	274.7	160.9	44.4
Glossy paper	6.33	20.90	10.34	0.65
	18.3	18.3	2.8	9.4
	330.3	357.1	400.2	415.3

3.5.3.5 Comparison of cellulosic substances

In order to understand the differences between paper and the substance of which it is made of, namely wood, it will be of interest to compare the calculated activation energy, frequency factors and peak temperatures for the different reactions. Table 14, give a summary of the results obtained in this study. Excluded from the calculation of average values are the TG results for cardboard and the DTG results for glossy paper. Two types of cotton and wood constitute their respective fractions. Comparing the calculated activation energy and peak temperature from the DTG analysis for paper and wood show similar results. It can also be observed that the standard deviation is low within each fraction. Reaction 1 for wood had an average activation energy and peak temperature of 42 kJ/mole and 377°C, respectively. Whereas the corresponding values for paper were 43 kJ/mole and 385°C. The activation energy and peak temperature of reaction 2, also known as the decomposition of cellulose, are in the same range, not only for paper and wood, but also for cotton. The activation energy for the three different cellulosic substances for reaction 2 are ranging from 243-259 kJ/mole and the peak temperature is ranging from 362-368°C. The activation energy is in the range of activation energies found for cellulose in a recent review article on cellulose pyrolysis kinetics[51]. For reaction 3 (hemicellulose), the values obtained for paper and wood are similar. Few data has been published on the decomposition of hemicellulose and it is therefore hard to compare the obtained values with others. However, activation energies ranging from 119-170 kJ/mole and frequency factors from $1.6 \cdot 10^8$ to $1.0 \cdot 10^{12}$ s^{-1} has been reported for wood and straw[26,55].

Table 14. Average values for activation energy, frequency factor, fraction and peak temperatures for reaction 1 (lignin), 2 (cellulose) and 3 (hemicellulose) for different types of cellulosic materials (TG and DTG analysis).

	Reaction 1		**Reaction 2**		**Reaction 3**	
	E_{TG} $logA_{TG}$ c_{TG} $(T_{peak,TG})^{calc}$	E_{DTG} [kJ/mole] $logA_{DTG}$ [log s^{-1}] c_{DTG} [%] $(T_{peak,DTG})^{calc}$ [°C]	E_{TG} $logA_{TG}$ c_{TG} $(T_{peak,TG})^{calc}$	E_{DTG} [kJ/mole] $logA_{DTG}$ [log s^{-1}] c_{DTG} [%] $(T_{peak,DTG})^{calc}$ [°C]	E_{TG} $logA_{TG}$ c_{TG} $(T_{peak,TG})^{calc}$	E_{DTG} [kJ/mole] $logA_{DTG}$ [log s^{-1}] c_{DTG} [%] $(T_{peak,DTG})^{calc}$ [°C]
Cotton	- - - -	- - - -	236.5 (35.0) 17.5 (3.1) 90.1 (3.3) 363.3 (4.0)	243.4 (19.9) 18.1 (1.8) 86.6 (4.3) 362.8 (4.7)	- - - -	- - - -
Wood	41.3 (3.5) 0.6 (0.2) 13.8 (1.5) 380.2 (13.7)	42.1 (1.1) 0.7 (0.1) 14.6 (3.3) 376.6 (1.6)	308.8 (5.9) 23.3 (0.4) 27.9 (2.0) 369.6 (1.6)	259.1 (5.4) 19.2 (0.5) 33.4 (1.1) 368.2 (0.8)	104.7 (5.4) 6.8 (0.6) 39.6 (6.2) 330.3 (4.9)	107.9 (2.7) 7.2 (0.2) 33.6 (0.4) 324.9 (2.9)
Paper	40.2 (5.5) 0.4 (0.5) 11.7 (2.3) 387.4 (8.6)	43.2 (6.1) 0.7 (0.5) 12.8 (0.3) 385.0 (6.0)	257.7 (26.0) 19.3 (2.2) 29.5 (11.5) 363.2 (7.3)	246.1 (16.1) 17.0 (1.2) 39.6 (8.5) 362.2 (8.3)	109.3 (17.0) 7.4 (1.8) 24.1 (14.8) 339.0 (14.9)	115.1 (19.9) 8.0 (2.0) 23.3 (15.1) 317.1 (10.0)

(..) standard deviation

Another useful way of comparing and evaluate the obtained results is to present them in an Arrhenius plot. Assuming a first order reaction for equation (5), rearranging and taking the natural logarithm of this equation gives the following expression:

$$\ln(k) = \ln(A) - \frac{E}{RT} \tag{14}$$

Equation (14) is used to plot the temperature dependence of the reaction rate constant. Plotting ln(k) against the inverse of temperature (1/T) (Arrhenius plot) give an opportunity to compare the reaction rate at different temperatures for reactions both of a similar and different nature. It is also possible to determine the dominating reaction at a given temperature by looking at an Arrhenius plot. Figure 13 show an Arrhenius plot of the three reactions, which constitute the thermal decomposition of newspaper during pyrolysis. This figure shows clearly the dominating reactions as a function of temperature.

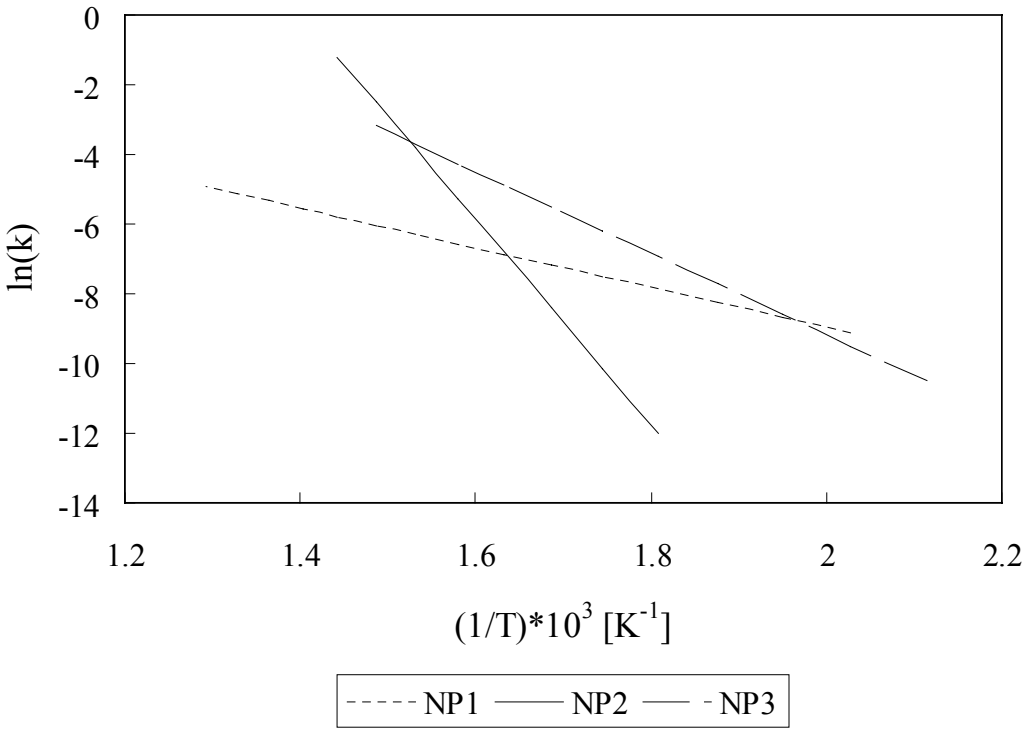

Figure 13. Arrhenius plot of the three pyrolysis reactions for newspaper (NP).

3.5.4 Plastic fraction

As Figure 14 shows, the thermal decomposition of typical plastic in MSW: HDPE, LDPE, PP and PS during pyrolysis seem to fit a single reaction. There is no remaining residue for these plastics as is confirmed by the proximate analysis. UPVC, however behaves quite different from the other plastics and is therefore modelled with more than one reaction. It is also interesting to observe that UPVC, unlike the other plastics, have a remaining residue of approximately 10% at 600^{o}C. The temperature area, in which the different plastics decompose, is quite broad. As Figure 14 shows, the decomposition occurs from 200 to 500^{o}C.

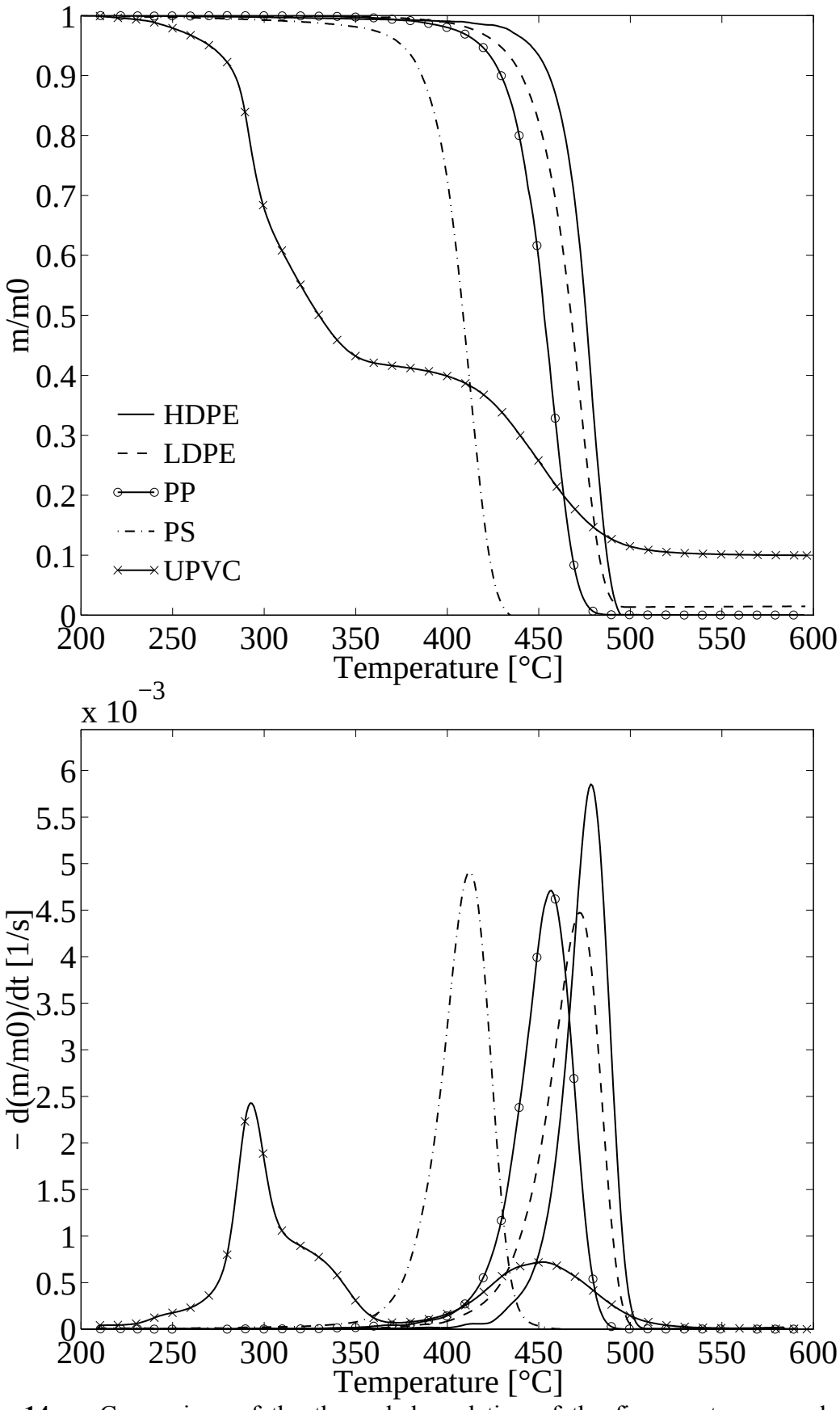

Figure 14. Comparison of the thermal degradation of the five most commonly found plastics in MSW.

3.5.4.1 Kinetic evaluation of HDPE

The decomposition of HDPE is described by a single reaction. The kinetic parameters, which are evaluated both with integral and differential methods, are given in Table 15. A minor difference in activation energy is observed. The highest activation energy is found for the integral method. The activation energy, as found by the differential method, is 445 kJ/mole. As can observed from the TG and DTG curves, the weight loss occurs over a narrow temperature range (~ 425-500^{o}C) at relatively high temperatures. The observed peak temperature is 479^{o}C. The narrow temperature range and the high peak temperature, tell us that the activation energy necessarily must be high. Other researchers have found the activation energy for HDPE, ranging from 233.2 (reaction order 0.74) to 326.1 kJ/mole (reaction order 1.0), according to Table 6. So what is the right activation energy for HDPE? As this study and the study of others show, the activation energy is obviously influenced by the method used to calculate the activation energy based on the experimental data. It can also be influenced by experimental equipment and procedures[25]. From Table 5 we could find the dissociation energy of the C-C bond to be 347 kJ/mole and the C-H bond to be 414 kJ/mole. In addition it is interesting to know that the dissociation energy of the double bond C=C is 611 kJ/mole. All of these bonds are present in HDPE and will thus be helpful in understanding the true activation energy of HDPE. Based on the knowledge of the dissociation energy of the bonds constituting HDPE and knowing that weaker secondary bonds such as dipole forces, induction forces, dispersion forces and the hydrogen bond have little influence on the activation energy, an activation of 445 kJ/mole might seem high, but reasonable.

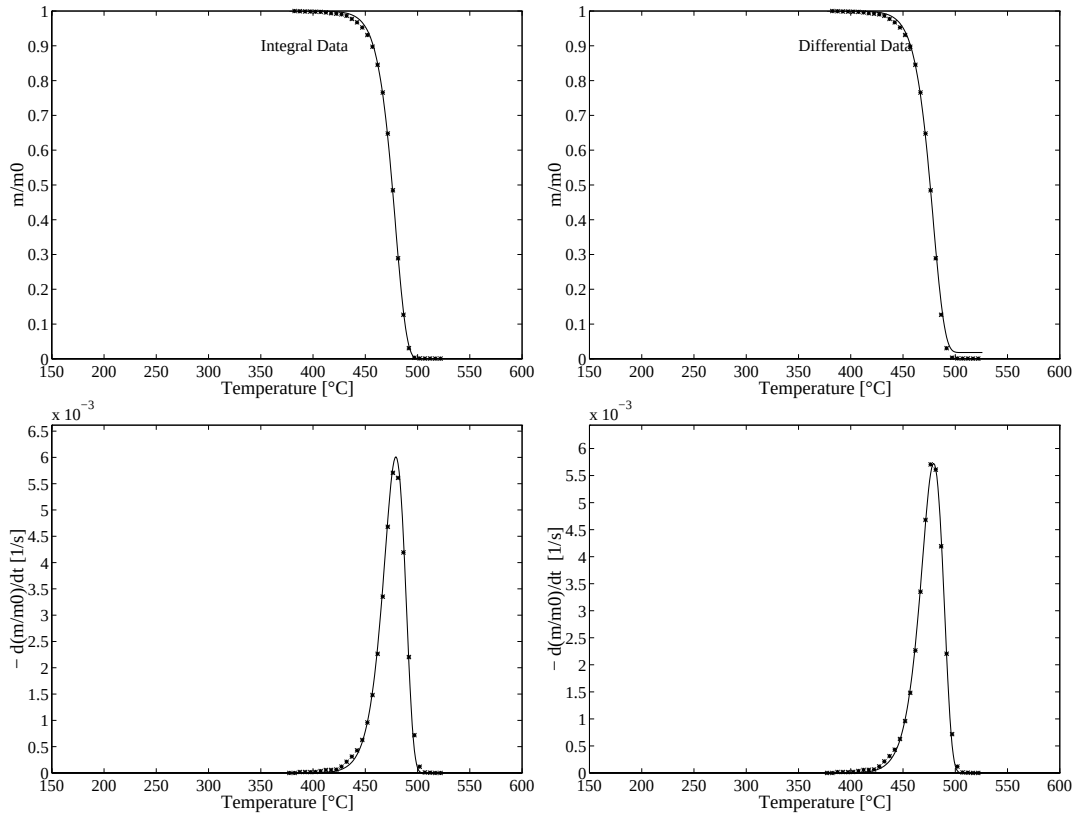

Figure 15. TG and DTG curves for HDPE.

Table 15. Kinetic parameters for HDPE. Kinetic evaluation from TG and DTG curves.

Evaluated curve	Reaction 1
	E_1 [kJ/mole]
	$\log A_1$ [log s^{-1}]
	c_1 [%]
	$(T_{peak,1})^{calc}$ [^oC]
TG	459.1
	30.09
	100.1
	479.4
DTG	445.1
	29.1
	98.2
	479.4

3.5.4.2 Kinetic evaluation of LDPE and coloured plastic bag

Experiments on pure LDPE granulate and coloured plastics bag were performed in order to gain knowledge on the influence of inorganic species. As Table 16 shows, the differences between pure LDPE and the coloured plastic bag is not evident. The peak temperatures and the calculated activation energies are practically equal. The influence of inorganic species is, in this case, not visible. The activation energy of approximately 340 kJ/mole, is relatively high compared to values found by other researchers given in Table 6. Other researchers have reported values from 175 - 280 kJ/mole for decomposition of part of or all of LDPE. The difference in activation energy between HDPE and LDPE is explained by the lower and slightly broader temperature range, in which LDPE decomposes. However, effect of branching may also have an effect. The explanation of the difference between HDPE and LDPE can be that the chain branching causes a somewhat different distribution of the chemical bonds present. Other researchers have concluded that the determining reaction during pyrolysis is the breaking down of the C-C bonds, not only for LDPE but also for HDPE, PP and PS[46].

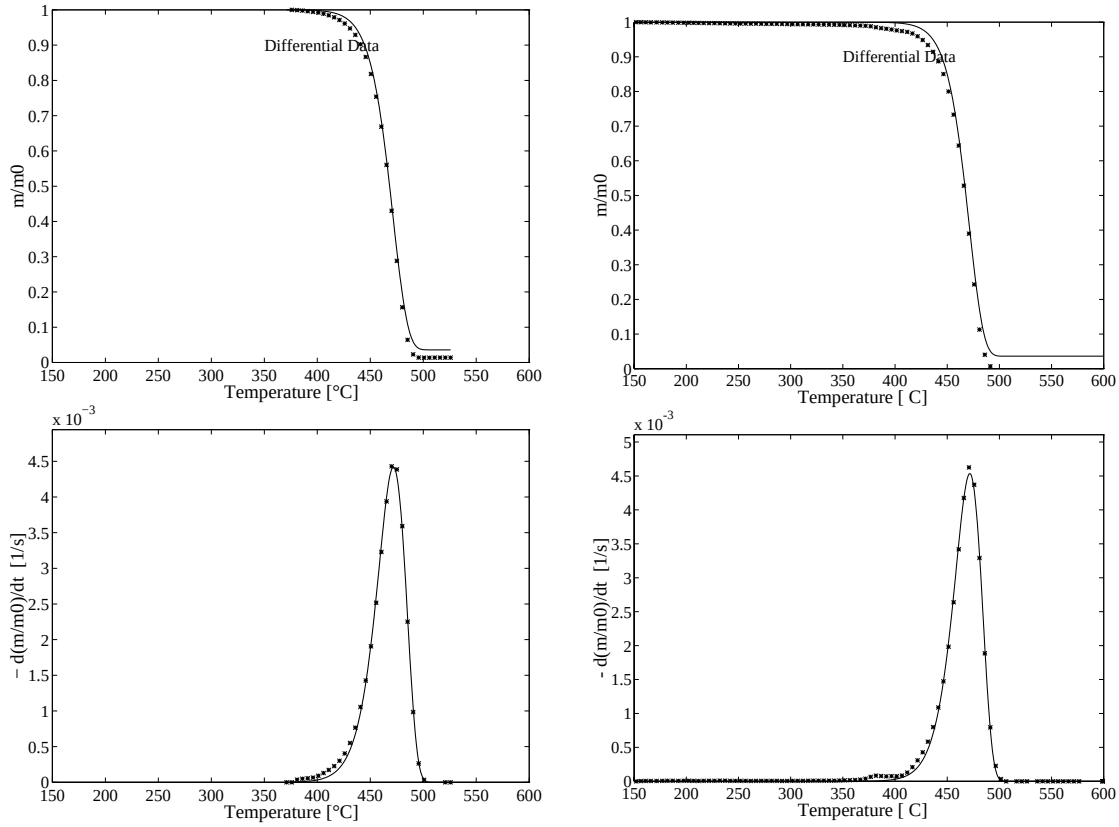

Figure 16. TG and DTG curves for pure LDPE and coloured plastic bag. Pure LDPE to the left.

Table 16. Kinetic parameters for LDPE and coloured plastic bag. Kinetic evaluation from DTG curves.

Evaluated curve	Reaction 1
	E_1 [kJ/mole]
	$\log A_1$ [log s^{-1}]
	c_1 [%]
	$(T_{peak,1})^{calc}$ [°C]
DTG	340.8
LDPE	21.98
	96.3
	472.2
DTG	347.8
Coloured plastic bag	22.49
	96.4
	471.9

3.5.4.3 Kinetic evaluation of PS and PP

PS and PP can both be modelled by a single reaction. PS shows a somewhat different behaviour than both HDPE and LDPE, with lower activation energy. This can be explained by the fact that the decomposition takes place at a lower temperature. PS is decomposed in the temperature range 350 - 450°C with a temperature peak at 413°C. Comparing the chemical structure of PS to LDPE and HDPE, it is interesting to see that bond energies of main chains or weak links are quite different. The presence of the aromatic unit or benzene ring (C_6H_6) in PS causes the branching to be of a phenyl type, as opposed to LDPE and HDPE which have a methyl group (CH_3) as branch[40]. The presence of benzene may lower the bond energy for some of the bonds present in PS compared to LDPE and HDPE where the break down of the C-C bond is dominating[21]. Hence, the reactivity of PS is greater than the reactivity of LDPE and HDPE. PP, however, behaves similar to LDPE and HDPE with an activation energy of approximately 337 kJ/mole and a peak temperature of 456.9°C. The temperature range for the decomposition is 370 - 480°C. The somewhat broader temperature range for decomposition and lower decomposition temperature explains the lower activation energy compared to HDPE. Comparing PP with LDPE show that the slightly lower decomposition temperature and broader temperature range should give a slightly lower activation energy. The presence of the methyl group CH_3 in the repeating monomer can alter the properties of the polymer in a number of ways. However, these changes may be most visible for other use of PP than in thermal degradation systems. The tertiary carbon atom provides a site for oxidation so that the polymer is less stable than polyethylene to the influence of oxygen. In addition, thermal and high-energy treatment leads to chain scission rather than cross-linking[21]. Reported activation energies for PP are ranging from 184 to 265 kJ/mole according to Table 6. However, it is important to notice that these activation energies have been obtained by using different methods than in this study with a reaction order not equal to one.

Table 17. Kinetic parameters for PS and PP. Kinetic evaluation of DTG curves.

Evaluated curve	Reaction 1
	E_1 [kJ/mole]
	$\log A_1$ [log s^{-1}]
	c_1 [%]
	$(T_{peak,1})^{calc}$ [°C]
DTG	311.5
PS	21.84
	98.1
	413.0
DTG	336.7
PP	22.18
	98.4
	456.9

3.5.4.4 Kinetic evaluation of PPVC and UPVC

PPVC and UPVC separate from the other plastics by having a complex decomposition pathway. For PPVC and UPVC, four and three different reactions have been identified respectively. In order to start with the simplest of them, UPVC will be discussed first. As described in section 1.2.2.1 UPVC have only minor parts of additives so the degradation of additives is not evident on the DTG curve. However, it is clear from Figure 17 that the decomposition of UPVC can be described by three reactions. Reaction 3 is assumed to be the release of benzene during the dehydrochlorination. Reaction 2 is assumed to be the dehydrochlorination and reaction 1 is assumed to be the release of remaining hydrocarbons. These assumptions will be discussed further. It is known that benzene is formed after the dehydrochlorination has proceeded for a while. The formed conjugate double bonds form benzene by cyclization[57]. This theory is confirmed by a study using TGA and analysis of the evolved gases by mass spectrometry. Benzene was found in the evolved gases together with HCl. The measurements were performed at 250°C[42]. The activation energy found for the release of hydrocarbons forming benzene is calculated to 388 kJ/mole with a peak temperature of 294°C. The assumption concerning the release of benzene after the dehydrochlorination has started is confirmed by looking at the DTG curve. The release of benzene (reaction 3) start at approximately 250°C, while the release of HCl starts at approximately 200°C. Comparing the activation energy for the release of benzene with other studies is not easy. This is due to different methods used for deriving the kinetic parameters from experimental results. However, an activation energy up to 327 kJ/mole has been found at a conversion of approximately 20%[39]. Another study claimed that the decomposition path of PVC was different at different sample weight. The release of benzene was not observed using a sample weight of 2 mg, while a increase in sample weight to 10 mg gave an evident peak indicating the release of benzene[42]. This finding is examined in this study but the peak describing the release of benzene is evident using both 2 and 5 mg samples. The findings in this study are also confirmed by another study checking samples between 2 to 20 mg[46]. Another theory explaining the presence of two reaction during the first decomposition step is proposed by other researchers. The theory is that the activation energy of the head to tail (H-T) configuration CCl_2-C-H_2-CCl_2-CH_2- is lower than the activation energy of the head to head (H-H) configuration -CCl_2- CH_2-CH_2-CCl_2-. If PVC consists of both H-T and H-H configuration, this will explain the two observed reactions in the first step of pyrolysis of PVC[46].

The dehydrochlorination of UPVC takes place in the temperature range of 200 - 370°C. The activation energy calculated for the release of HCl is 110 kJ/mole and the peak temperature is 316°C. A study of the elemental composition of the residue from pyrolysis of PVC at 375°C confirms the dehydrochlorination reaction. The content of chlorine was not detectable in the residue at this temperature[39] which also was indicated by the study of evolved gases from the first devolatilisation step identifying HCl as a component[42]. The bond energy for the breaking of the C-Cl bond is 339 kJ/mole, but neither this study nor other studies have been able to report activation energies close to the breaking of the primary C-Cl bond. Activation energies for the dehydrochlorination step range from 140 to 190 kJ/mole[42,46]. The reason for the deviation between the activation energy needed for breaking of the primary C-Cl bond and the activation energy obtained in this study is not fully understood. However, one

theory is that the initial reaction of pyrolysis of PVC is the elimination of a chlorine atom adjacent to a C=C bond or at a tertiary C-Cl bond which is weaker than the secondary C-Cl site. The "zipper" dehydrochlorination takes place and will form more C=C bonds. This will enable the dehydrochlorination to occur primarily before other reactions[46].

The second step of the decomposition of UPVC is described by reaction 1. The calculated activation energy and peak temperature is 150 kJ/mole and 455^{o}C, respectively. The decomposition takes place between 350 to 525^{o}C. Reaction 1 describes decomposition of the remaining hydrocarbons. The chemical nature of the remaining hydrocarbon is not known and hence it is difficult to explain the activation energy of the second step of decomposition for UPVC on basis of the chemical structure. However, an activation energy of 260 kJ/mole has been reported for the second step[42]. The calculated share of reaction 2 (HCl) (c-value 38%) is fairly consistent with the content of chlorine.

The decomposition of PPVC is somewhat more difficult to explain due to the plasticiser additive DEHP. From the DTG curve in Figure 17 one additional shoulder can be observed compared to UPVC. The rate of conversion for the first step is also higher than for UPVC. In PPVC a plasticiser named DEHP constitute approximately 30% of the composition, whereas the remaining chemical structure and compound is mainly the same as for UPVC. The presence of the DEHP additive makes however the calculation of the activation energy for the first step of conversion difficult. It is obvious that the share of dehydrochlorination (HCl) step is overestimated (56%). The share of HCl should be close to 30%. This overestimation of the HCl share causes the share of conversion of DEHP to be underestimated (7%). The share of conversion for DEHP should also be close to 30%. For reaction 1 and 3 (release of benzene and devolatilisation of remaining hydrocarbons) the activation energies are slightly higher but in the same range as for UPVC. The location of peak temperatures is also in the same range. It is interesting to observe that the decomposition of PPVC starts approximately 50^{o}C lower than UPVC. This assumed to be the decomposition of DEHP.

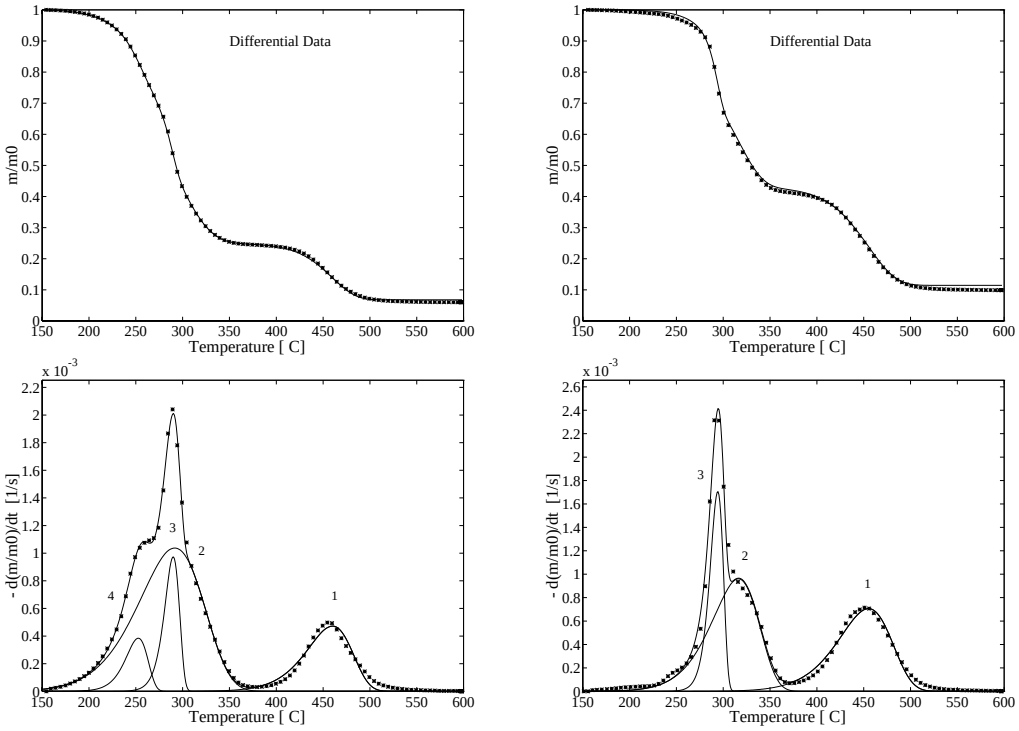

Figure 17. TG and DTG curves for PPVC and UPVC. PPVC to the left.

Table 18. Kinetic parameters for PPVC and UPVC. Kinetic evaluation of DTG curves.

Evaluated curve	Reaction 4	Reaction 3	Reaction 2	Reaction 1
	E_4 [kJ/mole] $\log A_4$ [log s^{-1}] c_4 [%] $(T_{peak,4})^{calc}$ [^oC]	E_3 [kJ/mole] $\log A_3$ [log s^{-1}] c_3 [%] $(T_{peak,3})^{calc}$ [^oC]	E_2 [kJ/mole] $\log A_2$ [log s^{-1}] c_2 [%] $(T_{peak,2})^{calc}$ [^oC]	E_1 [kJ/mole] $\log A_1$ [log s^{-1}] c_1 [%] $(T_{peak,1})^{calc}$ [^oC]
DTG *PPVC*	194.3 17.45 7.2 252.2	336.0 29.51 12.2 290.3	72.0 4.32 55.7 291.3	178.8 10.57 18.1 460.5
DTG *UPVC*	- - - -	388.2 34.13 19.3 294.4	110.4 7.59 37.7 315.8	149.8 8.5 31.6 454.8

3.5.4.5 Comparison of plastics

Arrhenius plots of the temperature dependent reaction rate constant give an opportunity to compare the different plastics in terms of reactivity. Looking at Figure 18, one can observe that HDPE have the highest reaction rate until approximately 500^{o}C. From 500^{o}C to 400^{o}C the reaction rate of LDPE is higher than for HDPE. The slope of the ln(k) plot is similar for LDPE, PP and PS, but the reaction rate is shifted towards lower temperatures. Figure 19 shows the Arrhenius plot of the three different

reactions describing the decomposition of UPVC. In the first step of decomposition reaction 3 is the dominating from approximately 270°C to the end of the reaction at 320°C. A slight overlap for reaction 2 and 3 is observed dominated by reaction 2. Ranking the different plastics by reactivity would give the following list (starting with the thermally most stable plastic): HDPE > LDPE > PP > PS > UPVC > PPVC.

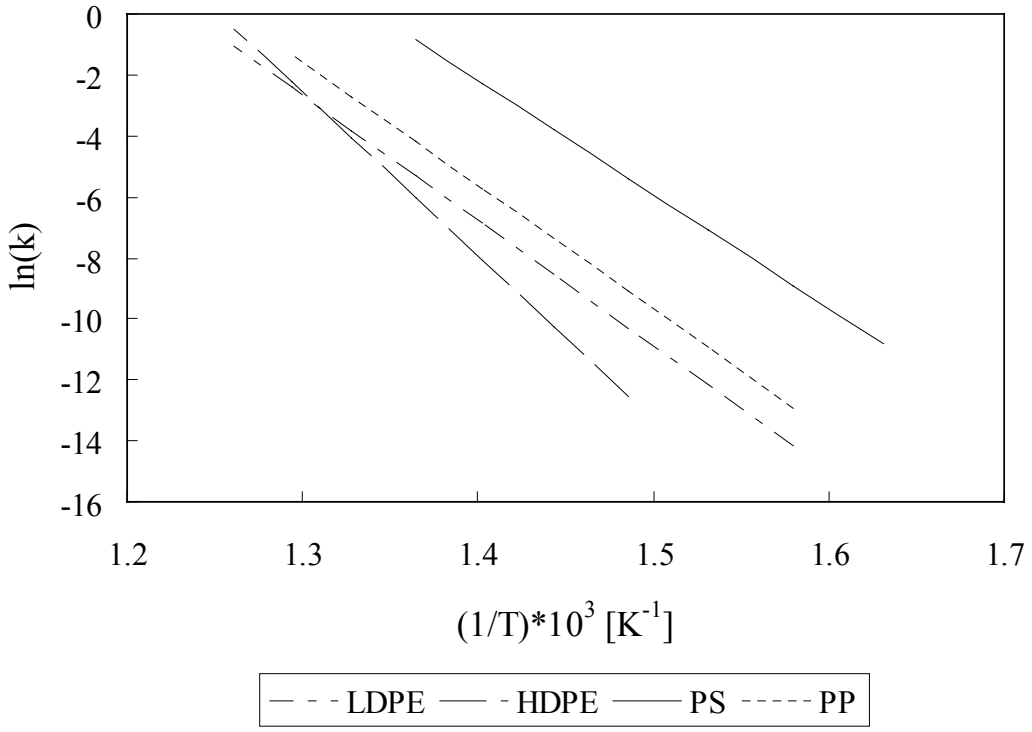

Figure 18. Arrhenius plot of LDPE, HDPE, PS and PP.

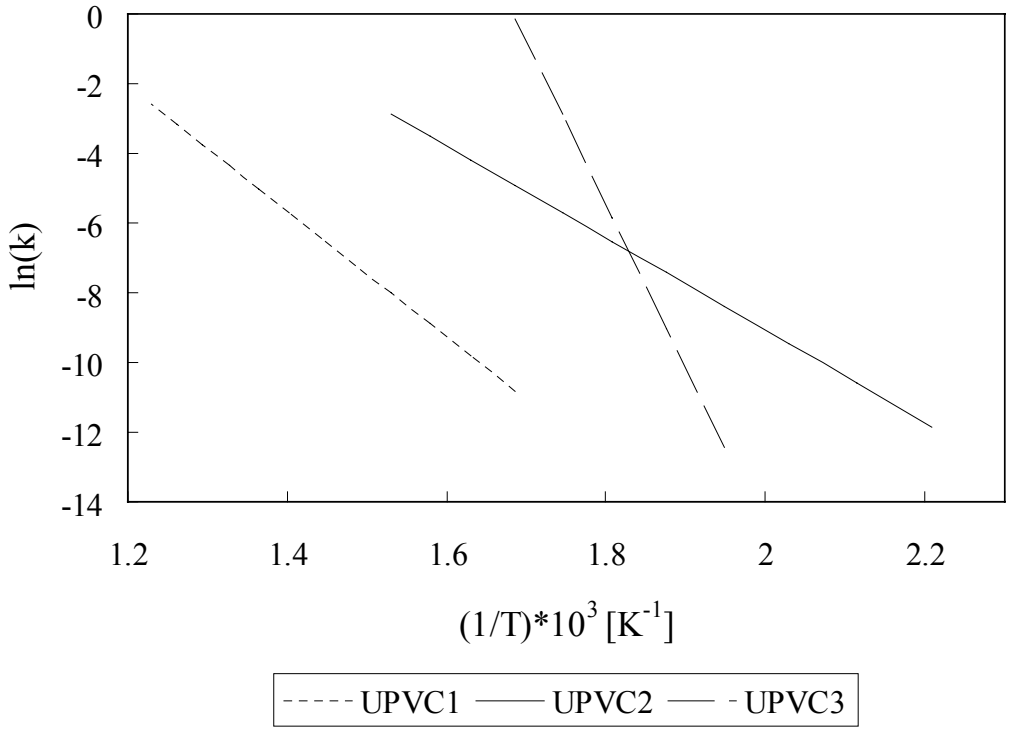

Figure 19. Arrhenius plot of the three reactions constituting UPVC.

3.5.5 Multi-material fraction

In order to check the possibility of determining the activation energy of a physical mixture of paper and plastic, experiments on juice and milk cartons were performed.

3.5.5.1 Juice carton and milk carton

Two different types of beverage cartons were used for the study of the multi-material fraction. The TG and DTG diagrams in Figure 20 show similar behaviour for both juice and milk carton. The only visible difference is the higher fraction of remaining residue for juice carton and the higher paper to plastic ratio for milk carton. The higher share of remaining residue for juice carton is due to the content of aluminium (5%) in juice carton. However, the content of aluminium should to some minor extent be compensated by the higher paper to plastic ratio for milk carton. This is not evident looking at the TG curves. The similarity observed in the TG and DTG diagrams is confirmed by the kinetic analysis. The results from the kinetic analysis given in Table 19 show almost identical values both for the activation energy and peak temperature. A comparison of the activation energy of reaction 2,3 and 4 to the mean values obtained from the analysis of different types of paper in Table 14, show that they are within the range set by the standard deviation. The only exception is reaction 2 for milk carton which is slightly below. It must, however, be noticed that reaction 4

(hemicellulose) is overestimated for both juice- and milk carton. The lack of shoulder for reaction 4 causes this overestimation and will have an effect of the calculation of activation energies. For reaction 1 (LDPE) the activation energy and peak temperature is very close to those obtained in the kinetic analysis of pure LDPE (section 1.5.4.2) only with a slightly lower activation energy and peak temperature. Figure 21 show the reaction rate constant as a function of temperature for the individual reactions of milk carton. This figure demonstrates the behaviour of a multi-material component containing both paper and plastic. The individual behaviour of paper/cardboard and LDPE has been discussed earlier and will not be discussed further here. However, one can observe that there is only one overlapping reaction (reaction MC2), which is the decomposition of lignin/char of the paperboard. LDPE is the dominating reaction above approximately 440°C.

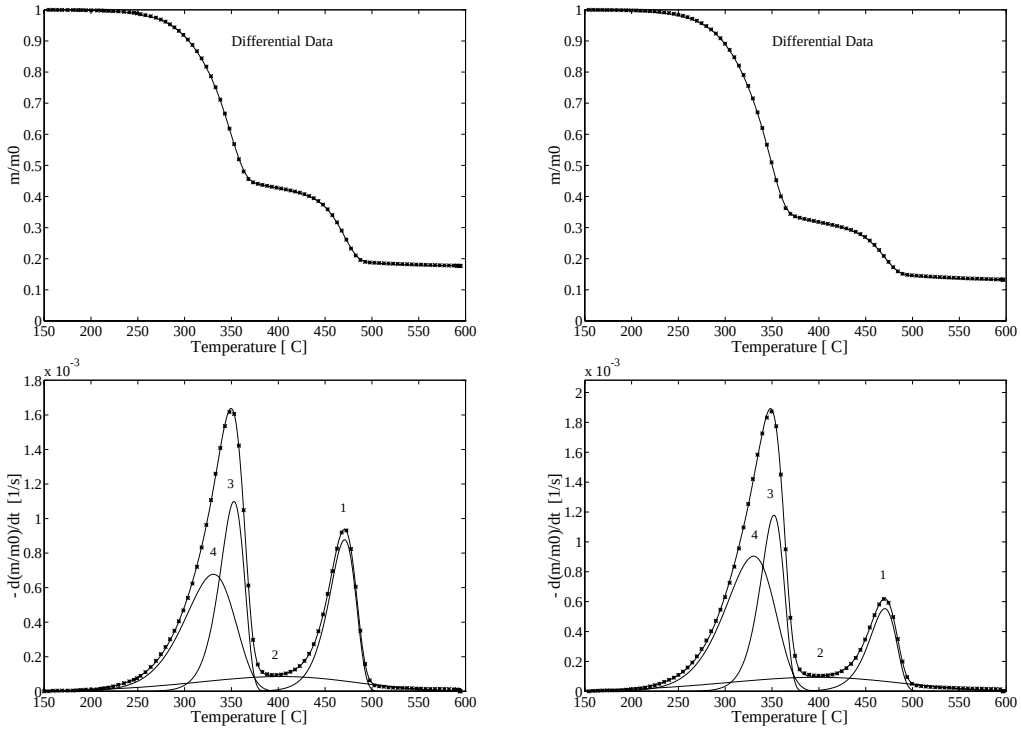

Figure 20. TG and DTG curves for juice and milk cartons. Juice carton to the left.

Table 19. Kinetic parameters for juice and milk carton evaluated with differential method.

Evaluated curve	Reaction 4	Reaction 3	Reaction 2	Reaction 1
	E_4 [kJ/mole] $\log A_4$ [log s^{-1}] c_4 [%] $(T_{peak,4})^{calc}$ [°C]	E_3 [kJ/mole] $\log A_3$ [log s^{-1}] c_3 [%] $(T_{peak,3})^{calc}$ [°C]	E_2 [kJ/mole] $\log A_2$ [log s^{-1}] c_2 [%] $(T_{peak,2})^{calc}$ [°C]	E_1 [kJ/mole] $\log A_1$ [log s^{-1}] c_1 [%] $(T_{peak,1})^{calc}$ [°C]
DTG	109.0	249.0	39.7	321.2
Juice carton	7.21	18.90	0.31	20.62
	28.7	22.7	10.9	19.9
	330.1	352.9	402.1	470.7
DTG	110.1	257.0	35.2	316.2
Milk carton	7.31	19.59	-0.06	20.28
	37.6	23.6	12.9	12.7
	330.6	352.4	397.6	470.4

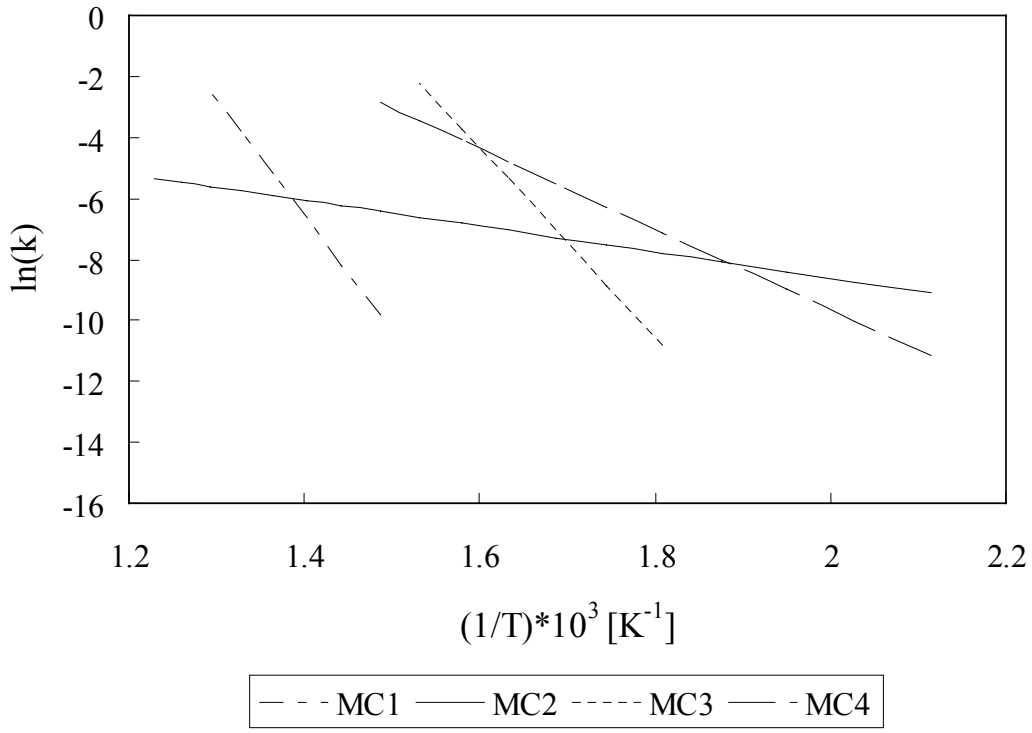

Figure 21. Arrhenius plot of milk carton.

3.5.6 Mixtures

In order to check possible interaction between different components in MSW, a study was performed on mixtures of two components. The sample weight of the mixtures were 10 mg with 50% (5 mg) of each component. In the mixture experiments paper was laid in the bottom of the sample cup and plastics at the top. This ensure the best possible mixing, due to the fact that paper decomposes at a lower temperature and hence will have the possibility to interact with the plastics before it escapes the sample cup. The plastic will also melt prior or in the same temperature range when paper starts to decompose, so laying the plastic in the bottom would not give the paper the possibility to interact with the plastic. For the experiments with mixture of paper and mixture of plastics, the components where not put in different layers, but thoroughly mixed. Newspaper and glossy paper were chosen for this study, representing the paper fraction. Newspaper has a low ash content and glossy paper has a high ash. This choice was made in order to see if there could be any interactions between components in a physical mixture due to catalytic effects caused by the ash. LDPE and UPVC were picked out to represent the plastic fraction. LDPE and UPVC decompose in a completely different pattern and constitute a major share of the plastics found in MSW.

The curves presented in Figure 22 represents the mass fraction (m/m_0) and reaction rate ($d(m/m_0)/dt$) for the mixture of two components and the sum of the individual components. The experiments on mixtures and single components are performed in exactly the same way with the same procedures. The experiments on mixtures were performed with a sample weight of 10 mg, while the experiments on single components were performed with a sample weight of 5 mg. The curve representing the sum of the individual components is derived by first multiplying the data (curve value) for each component by this components contribution in the mixture experiment. In this case a factor of 0.5, corresponding to 50% in the mixture was used for both components. Secondly the contribution from each component is added to derive the sum of the two components. In other words, the curve representing the sum of experiments on single components, is a weighed contribution from each component. Experiments on mixtures of different types of paper and paper and LDPE were performed, however no interaction was found.

Mixing UPVC with newspaper gave evident interactions in the low temperature area. The dehydrochlorination of UPVC seems to increase the reactivity of the cellulosic substance newspaper, even in a physical mixture. At 320^{o}C, the conversion of the sum of the single components is approximately 40%, while the conversion of the mixture is 55% giving a difference of 15%. However, the interactions in the low temperature area have no impact on the decomposition of UPVC and char from newspaper in the higher temperature area as can be observed in Figure 22. Another study investigating the co-pyrolysis of PVC with straw also found evidence of interaction during the dehydrochlorination step. One probable explanation of the interaction between straw and PVC was that the liberated HCl may interact chemically with the cellulose, probably catalysing an acid hydrolysis type of reaction making it less stable[44]. No other theory for the interaction between paper and UPVC will be presented here as it is beyond the scope of this work. The same phenomena as described for the mixture of UPVC and newspaper is observed for the mixture of UPVC and glossy paper. At a

temperature of 320°C, the conversion of the sum of single components is 28%, while the conversion of the mixture is 42%.

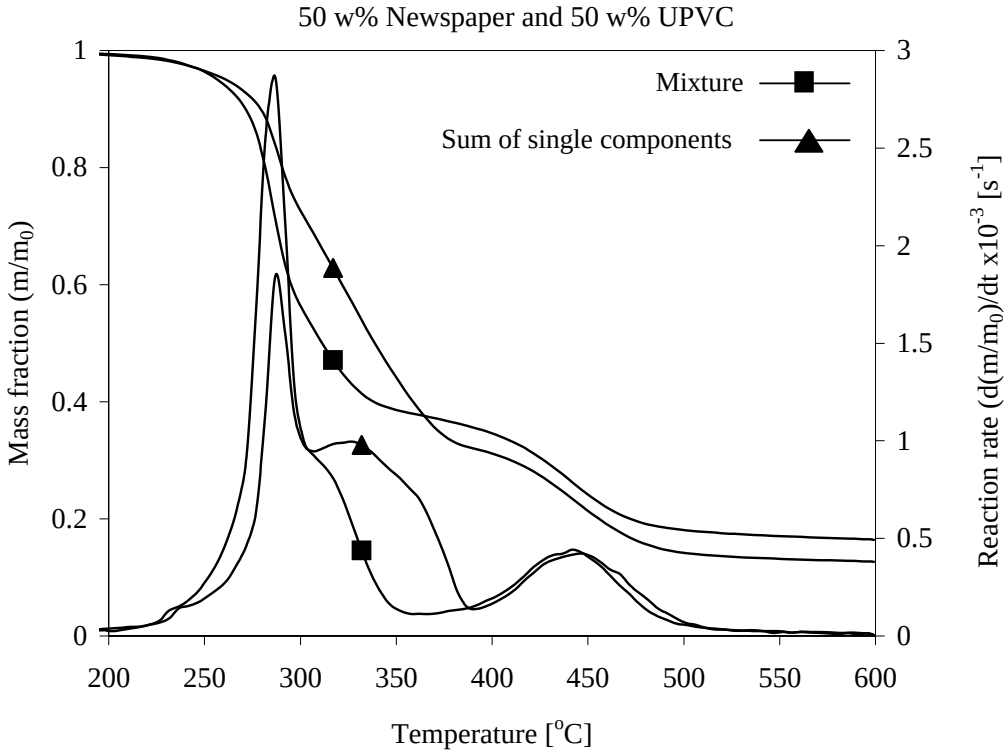

Figure 22. Decomposition of UPVC and newspaper. TG and DTG diagrams of a mixture of 50% UPVC and 50% newspaper and the sum of the single components.

3.6 Sources of errors

For determination of moisture, HHV, volatile matter and ash, standardised methods have been employed. These standardised methods also include an estimate of precision and bias. However, the repeatability for determination of HHV, volatile matter and ash content was checked. The standard deviation of the determination of ash, HHV and volatile matter was 5%, 0.5% and 2.3% respectively. The relatively high standard deviation for determination of ash can be explained by the low content of ash in the test sample (newspaper ~1% ash). The method used for determination of ash set a typical ash content of 20% when evaluating the precision and bias.

The sources of errors for the experiments performed on the TGA apparatus have been thoroughly investigated by other researchers and will not be subject to any comprehensive discussion here[26]. A check of the repeatability of experiments has been performed. Figure 23 show the repeatability of five experiments on whatman filter paper. The sample weight was approximately 5 mg. The results show that the peak temperature and reaction rate is almost identical. The char fraction, however, is subject to a larger deviation. This has also been discussed by others[26]. An evaluation of the standard deviation of calculated kinetic parameters are listed in

Table 20.

Table 20. Evaluation of repeatability of calculated kinetic parameters. TG and DTG analysis.

Sample no.	**TG**		**DTG**	
	E [kJ/mole]	logA [log s^{-1}]	E [kJ/mole]	logA [log s^{-1}]
1	274.7	20.94	257.5	19.52
2	281.4	21.50	265.8	20.22
3	283.1	21.66	267.8	20.40
4	285.0	21.84	268.3	20.45
5	280.1	21.42	265.2	20.19
Average value	280.9	21.50	264.9	20.20
Standard deviation	3.9	0.30	4.3	0.40

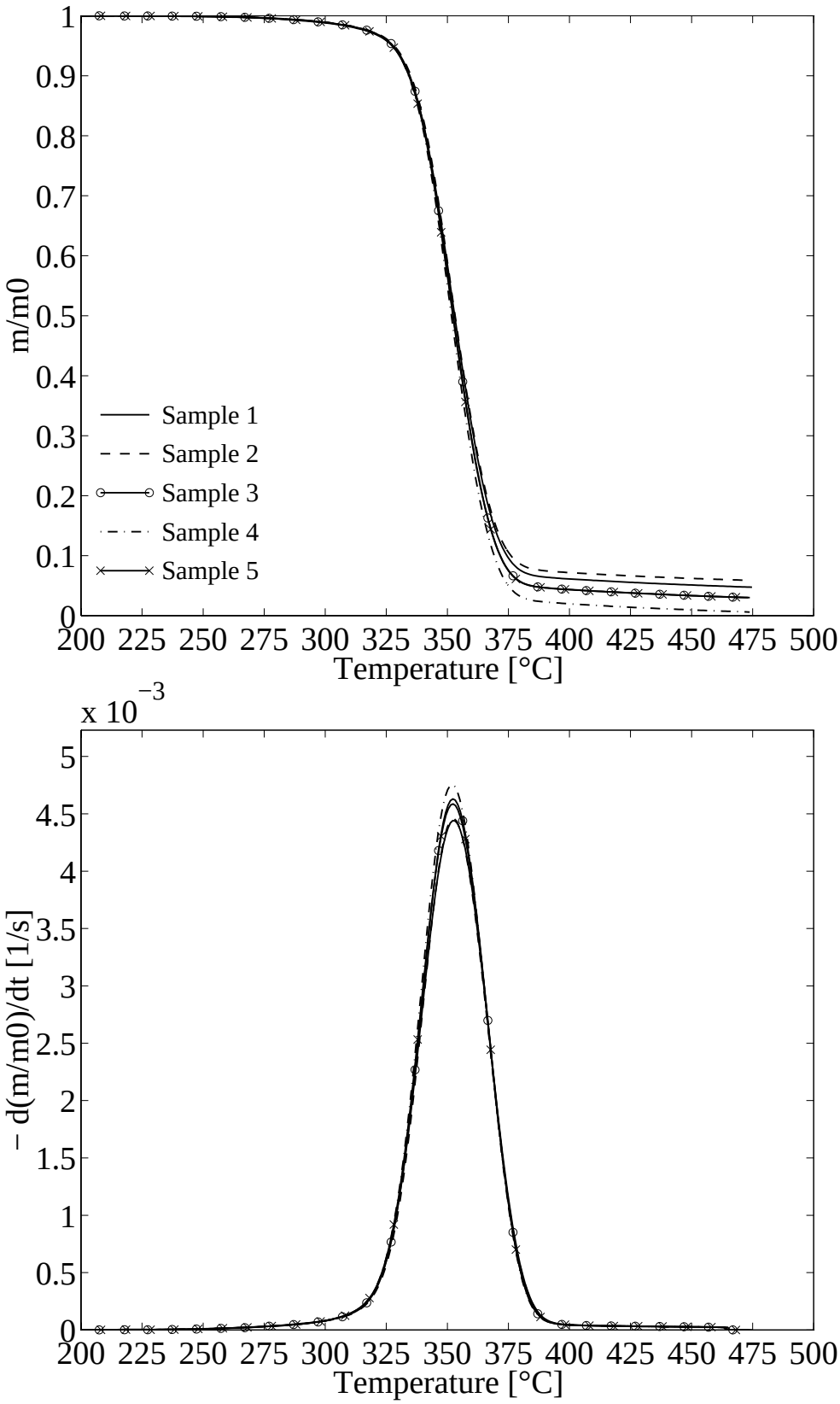

Figure 23. Repeatability tests for whatman filter paper.

3.7 Conclusions

Sixteen different components, representing the major share of the dry combustible fraction of MSW, has been subjected to thermal characterisation. Different types of paper, one type of cardboard, one type of cotton and two types of wood has been examined. Representing the plastic fraction six of the most commonly found plastics in MSW was chosen. Two samples of cartons representing the multi-material fraction were also subject to investigation in this study. The thermal characterisation has included determination of higher heating value and moisture, a proximate analysis and TGA experiments including determination of kinetic parameters. This study has shown that paper and cardboard have a similar thermal decomposition and properties as wood. The major difference is the higher content of ash due to additives in paper. This higher ash content has a minor influence on the thermal degradation during pyrolysis. It has also been shown that HHV and the proximate behaviour can be expressed as a linear function of the ash content. The TGA experiments showed that, the high content of ash in some component does not cause any catalytic effects to other components in a mixture. The plastic components in this study proved to have a high volatile fraction, approximately no ash and a high heating value compared to the cellulosic fraction. With the exception of PPVC and UPVC, the thermal degradation of plastics occurs at a higher temperature over a more narrow temperature range. In combustion systems care should be taken when increasing the plastic to paper ratio. The release of heavy hydrocarbons at higher temperatures from plastics will increase the need for air supply. The melting behaviour of plastic should be taken into consideration when constructing an incinerator. Combustion of a high PVC to paper ratio will release volatiles at a lower temperature, which might influence the construction of the air supply in an incinerator. This knowledge on thermal behaviour of single components in MSW and their behaviour in mixtures can serve as a foundation for decision making in waste management in general and especially for constructors and operators of MSW/RDF incinerators.

3.7.1 Higher heating value determination and proximate analysis

A moisture determination was performed for all samples. The results show a variation between approximately 4 to 8% for the cellulosic and multi-material fraction of MSW, while the plastics had practically no moisture.

Higher heating value. For the three different types of paper and cardboard, the HHV was linear function of the ash content, ranging from approximately 10 to 20 MJ/kg. The two types had practically the same HHV as for newspaper, while cotton had a somewhat lower HHV. The plastics in this study had similar HHV approximately 45 MJ/kg with the exception of the two types of PVC, which had a HHV approximately one half of the other plastics due to the high concentration of chlorine (~50%). For the multi-material samples, it is clear that the heating value equals the sum of each component. Giving a HHV slightly higher than for paper, due to the content of LDPE and aluminium.

Proximate analysis. Caution should be taken when performing proximate analysis of MSW components. The reason for this is that the chemical composition can vary to a great extent between the different components, giving room for misinterpretation of

results. However, a proximate analysis has been performed using standardised methods for RDF. The three different types of paper and cardboard had ash content ranging from 1% to 28%, while the two types of wood and cotton had almost no ash. Practically no ash was found for the plastic samples with only exception of the coloured plastic bag which had approximately 2% ash. This is as expected as the plastic samples in this study was pure and non-coloured. The ash content of the multi-material fraction (juice and milk cartons) was approximately 5%. The volatile matter for the paper/cardboard fraction ranged from 67% to 89% with corresponding fixed carbon ranging from 5% to 11%. The volatile matter of wood was approximately 90% with corresponding amount of fixed carbon around 10%. Cotton had 98% volatiles and 2% fixed carbon. The multi-material fraction had 86% to 90% volatile matter and approximately 6% fixed carbon. All plastics, with the exception of UPVC and PPVC, had virtually 100% volatile matter and no fixed carbon. UPVC and PPVC had approximately 95% volatile matter and 5% fixed carbon.

3.7.2 TGA experiments and kinetic study

A kinetic study of each component has been performed trying to link the chemical composition to the thermal decomposition and obtained data from the kinetic analysis. The following major conclusions can be drawn:

Paper and cardboard can be modelled as a set of three reactions describing the decomposition of hemicellulose, cellulose and combined char/lignin decomposition. The only exception was glossy paper, which had a forth reaction describing the volatile release of additive.

The obtained data from the kinetic analysis were in the same range as obtained for other cellulosic substances such as wood and straw.

- The lack of a pronounced shoulder for the hemicellulose reaction can lead to a overestimation of the hemicellulose to cellulose ratio.

- No effect of washing paper samples in order to remove ash and hence remove the possibility of catalytic reactions was discovered.

- The degradation of paper and cardboard started at approximately 200^{o}C. At 500^{o}C most of the volatile reactions was finished. The highest reaction rate was located at approximately 360^{o}C.

- HDPE, LDPE, PP and PS could all be modelled as a single reaction describing the decomposition of the polymer.

- UPVC and PPVC on the other hand were modelled with three and four reactions, respectively. This is reflected by a more complex chemical composition, compared to the other plastics.

- For PPVC as opposed to UPVC, it was hard to get a good estimation of the dehydrochlorination reaction. This reaction was overestimated leading to an underestimation of the devolatilisation of the additive.

- HDPE, LDPE, PP and PS were all volatilised between 350^{o}C and 500^{o}C.

- UPVC and PPVC had a completely different volatile behaviour, volatilising between 150^{o}C and 525^{o}C.

- For the multi-material fraction, it was possible to identify decomposition of paperboard and LDPE. Kinetic parameters matched well with those found for decomposition of paper/cardboard and pure LDPE. It should be noticed that there was no pronounced shoulder for the decomposition of hemicellulose leading to an overestimation of the hemicellulose to cellulose ratio.

3.8 References

1 Franklin, M. A., Report No. PB88 – 232780, Franklin Associates Ltd., USA, 1988.

2 Falnes, A. and Vinju, E., Report No. C402, Statistics Norway, Norway, 1997.

3 Kauffman, C.R., *in Wastetech '91: Canadian Waste Management Conference*, Toronto, 1991, pp. 1-13.

4 Rigo, H. G. and Chandler, A. J., *in Proceedings of the National Waste Processing Conference*, ASME, 1994, pp. 49-63.

5 Gort, R., Phd thesis ISBN 90-9008751-6, Twente University, The Netherlands, 1995.

6 Tillman, D. A.*, in The Combustion of Solid Fuels & Wastes*, Academic Press, San Diego, USA, 1991.

7 Clarke, M. J., *Waste Age United States*, 1991, **May**, 105.

8 Rosseaux, P., *Biocycle*, 1989, **9**, 81.

9 Garcia, A. N., Marcilla, A., Font, R., *Thermochimica Acta,* 1995, **254**, 277.

10 Willigenburg, A. and Malinen, H., *Warmer Bulletin*, 1995, **47**,16-17.

11 Norwegian Pollution Control Authority, Our Common Environment - Waste, Report TA 664, 1992 (in Norwegian).

12 US Environmental Protection Agency, *Characterisation of Municipal Solid Waste in the United States – 1997 Update*, Report No. EPA 530-R-98-007,1998.

13 Kulik, A. and Witoszek, A., *WPROST*, 1994, **4**, 36-37.

14 Temmink, H., *Biomass and Bioenergy*, 1995, **vol. 9**, 351-363.

15 Wenzl, H.F.J., *in The Chemical Technology of Wood*, Academic Press Inc., 1970.

16 Rydholm, S. A., *in Pulping Processes*, Interscience Publishers, USA, 1965.

17 Olsson, I., *in Papertypes for different use*, No. X-731, Swedens Forrest Industry Union, Markaryd, Sweden, 1986 (in swedish).

18 Hult, N., *in Coating of paper*, No. Y-308, Swedens Forrest Industry Union, Markaryd, Sweden, 1986 (in swedish).

19 Christensen, P. K., *Wood processing chemistry*, Compendium from Institute of Chemical Engineering, Norwegian University of Science and Technology, 1995 (in norwegian).

20 Rance, H. F., *in Handbook of Paper Science – Vol. 1*, Elsevier, The Netherlands, 1980.

21 Brydson, J.A., *in Plastics Materials*, Butterworth-Heinemann Ltd., Oxford, UK, 1995.

22 Agrawal, R.K., Phd thesis no. 8504302 Clarkson University, USA, 1984.

23 Norwegian Pollution Control Authority, Emissions from MSW management, Report 96:16 (in Norwegian), 1996.

24 Wu, C-H., Chang, C-Y., Lin, J-P., and Hwang, J-Y., 1997, *Fuel*, **12**, 1151-1157.

25 Grønli, M.G., Antal Jr., M.J. and Varhegy, G., *to be printed in Ind. Eng. Che*m. *Res*.1998.

26 Grønli. M.G., Phd thesis NTNU 1996:115, The Norwegian University of Science and Technology, 1996.

27 Carrasco, F., *Thermochimica Acta*, 1993, **213**, 115-134.

28 Anderson, D. A. and Freeman, E. S., *Journal of Polymer Science*, 1961, **vol. 54**, 253.

29 Friedman, H. L., *Journal of Polymer Science: Part C*, 1965, **6**, 183.

30 Reich, L., *Journal of Applied Polymer Science*, 1966, **vol. 10**, 465.

31 Dodson, B. and McNeill, I. C, *Journal of Polymer Science: Polymer Chemistry Edition*, 1976, vol 14, 353.

32 Grassie, N., McNeill, I. C. and Cooke, I., *Journal of Applied Polymer Science*, 1968, **vol. 12**, 831.

33 Wilkins, E. S., Wilkins, M. G., *Journal of Environmental Science and Health*, 1985, **A20(2),** 149-175.

34 Tsang, W. and Walker, J. A., *Resources and Conservation*, 1982, **9**, 355-365.

35 Ishii, Y., Ishii, N. and Iida, Y., *Conservation & Recycling*, 1987, **4**, 229-236.

36 Krieger-Brockett, B., *in Proceedings from Nordic Seminar on Biomass Gasification and Combustion*, Norway, 1993.

37 Helt, J. E., Agrawal, R. K. and Myles, K. M., Report No. ANL/CNSV--54 DE87 002352, Argonne National Laboratory, USA, 1986.

38 Volkov, V. S., Khabenko, A. V., Ganzha, V. I., Dolmatov, S. A. and Prilepskaya, T. I., *International Polymer Science and Technology*, 1991, **10**, 36.

39 Wu, C-H, *The Canadian Journal of Chemical Engineering*, 1994, **4**, 644-650.

40 Wu, C-H, Chang, C-Y, Hor, J-L, Shih, S-M and Chen, L-W, *International Symposium on Energy, Environment and Information Management*, Argonne National Laboratory, USA, 1992.

41 Agrawal, R. K., Gandhi, F. and McCluskey, R. J., *Journal of Analytical and Applied Pyrolysis*, 1984, **6**, 325-338.

42 Bockhorn, H., Hornung, A., Hornung, U., Teepe, S. and Weichmann, J., *Combustion Science and Technology*, 1996, **vol. 116-117**, 129-151.

43 Wu, C-H, Chang, C-Y, Lin, J-P and Hwang, J-Y, *Fuel*, 1997, **12**, 1151-1157.

44 McGhee, B., Norton, F., Snape, C. E. and Hall, P. J., *Fuel*, 1995, **1**, 28-31.

45 Fritsky, K. J., Miller, D. L. and Cernansky, N. P., *Journal of Air & Waste Management Association*, 1994, **vol. 44**, 1116-1123.

46 Wu, C-H, Chang, C-Y, Hor, J-L, Shih, S-M, Chen, L-W and Chang, F-W, *Waste Management*, 1993, **vol. 13**, 221-235.

47 Cozzani, V., Petarca, L. and Tognotti, L., 1995, *Fuel*, **6**, 903-912.

48 Agrawal, R. K., *in Compositional Analysis by Thermogravimetry*, ASTM STP 997, C.M. Earnest, Ed., American Society for Testing and Materials, Philadelphia, USA, 259-271, 1988.

49 Gaur, S. and Reed, T. B., Report No. NREL/TP-433-7965, National Renewable Energy Laboratory, USA, 1995.

50 Wu, C-H., *Canadian Journal of Chemical Engineering*, 1994, **4**, 644-650.

51 Antal, M. J. and Varhegyi, G., *Industrial & Engineering Chemistry Research*, 1995, **34**, 703-717.

52 Kashiwagi, T. and Nambu, H., *Combustion and Flame*, 1992, **88**, 345-368.

53 Ward, S.M. and Braslaw, J., *Combustion and Flame*, 1985, **61**, 261-269.

54 Sørum, L, Phd thesis, Norwegian University of Science & Technology, Institute of Thermal Energy and Hydropower, in progress.

55 Varhegyi, G., Szabo, P. and Antal M. J., *in Advances in Thermochemical Biomass Conversion*, Blackie Academic & Professional, GB, 1994.

56 Miller, R. S. and Bellan, J., *Combustion Science and Techn*ology, 1997, **Vol. 126**, 97-137.

57 Faximile from Ånund Ryningen at Hydro Porsgrunn Tehcnical Center-PVC, 02.03.98.

4 FORMATION OF NO FROM COMBUSTION OF VOLATILES FROM MUNICIPAL SOLID WASTE COMPONENTS AND THEIR MIXTURES

Chapter 4 is recently published in the Scientific Journal Combustion & Flame.

Reference:

Sørum, L, Glarborg, P., Jensen, A., Skreiberg, Ø. and Dam-Johansen, K. "Formation of NO from Combustion of Volatiles from Municipal Solid Waste Components and Their Mixtures", Comb. & Flame, 123:195-212, 2001.

4.1 Abstract

An experimental and theoretical study has been performed on the formation of NO in the combustion of volatiles from municipal solid wastes. Experiments on single components and their mixtures were conducted in a small-scale fixed bed reactor. Numerical simulations using the opposed flow diffusion flame program OPPDIF were performed to obtain a further understanding of the experimental results. Conversion factors for fuel-N to NO have been determined for single components of newspaper, cardboard, glossy paper, low-density polyethylene (LDPE) and poly(vinylchloride) (PVC) and their mixtures, using gases with oxygen concentrations of 12, 21 and 40 vol.%. For single components experiments at 100 vol.% oxygen were also performed. The conversion factors for paper and cardboard varied from 0.26 to 0.99. The conversion factor for LDPE and PVC varied from 0.71 to 10.09 and 0.04 to 0.37, respectively. Conversion factors higher than 1.0 in the case of LDPE clearly a show that NO is formed by thermal and/or prompt mechanisms. For mixtures, a comparison between calculated conversion factors (based on a weighted sum of the conversion factors for single components) and the experimentally determined conversion factor for pellets of the mixture were performed. For mixtures of paper and cardboard a significant difference in conversion factor for the sum of single components and mixture experiments could only be found at 40 vol.% of oxygen. For mixtures of paper/cardboard and plastics, however, significant differences in the conversion factor were observed at all oxygen concentrations when comparing experiments on a mixture of paper and plastics with the weighted sum of the single components. The explanation is found in the different combustion properties for paper/cardboard and plastic, which in this case make the formation of thermal NO from LDPE more favourable for the single component than in mixtures with other components. The simulations with OPPDIF confirmed the trends observed in the experimental study and allowed an assessment of the contribution of the different mechanisms of NO formation.

4.2 Introduction

In recent years, waste management has become increasingly complex. Earlier, Municipal Solid Waste (MSW) was sent to landfill sites, which was considered the most economic way of handling MSW. However, in the last two decades awareness of the environmental hazards and a lack of landfill sites, have promoted an increased number of alternative waste treatment systems. Today MSW management systems are complex and a product of several different factors. Factors influencing the choice of MSW management systems are composition of the waste, environmental and economical aspects and also infrastructure (i.e. type of housing, access to landfill sites, etc.) Material recovery and re-use, combustion with energy recovery, composting and landfilling are the most common parts of today's waste management system. There is an international trend towards increasing material re-use and recycling. The increased recycling of materials, such as paper, plastic and beverage cartons may influence the performance of combustion systems. The increased complexity of MSW management systems makes detailed characterisation of MSW components necessary. The trend today is to classify waste into categories depending on composition. Classification of waste as a fuel with a certain quality and composition will make it easier for operators and manufacturers of combustion plant to assess the consequences of burning different wastes. To do this, fundamental knowledge of the combustion properties of the different components and possible interactions in mixtures should serve as a basis for these decisions.

Reducing the emission of nitrogen oxides (NO_x) from burning MSW and Refuse Derived Fuel (RDF) is one of the challenges in this field. NO_x abatement is generally divided into two categories. Primary measures involve treatment prior to or during the combustion process and are not considered to be part of the air pollution control (APC) system. Generally, there are a wide range of primary reduction techniques, such as staged air combustion, reduced excess air (improved mixing), reburning, flue gas recirculation and combustion with pure oxygen. Pickens [1] reported that typical baseline NO_x emission levels for commercial moving grate and stoker incinerators were 350-600 mg/Nm^3 at 7 vol.% oxygen. Emissions of nitric oxides are generally lower with fluidised beds than with grates for two reasons: the combustion temperature is lower and the excess air level is lower (typically 50% lower excess air) [2]. Primary measures can achieve up to 70% reduction. However, secondary measures, which are part of the APC system, are often necessary [3].

A nitrogen-content of 0.45 wt% is typical for MSW [4,5]. For paper and plastics typical nitrogen-contents ranging of 0.11 - 0.8 and 0.3 - 0.85 wt%, respectively, have been reported [4,5]. Chemically paper and cardboard consists of three main constituents, namely hemicellulose, cellulose and lignin [6]. Aho et al. [7] concluded that nitrogen in fuels with a high O/N ratio, such as wood, mainly can be found in pyrrolic forms. Nitrogen, however, might also be found in additives, such as colour, ink and binders. Bowman [8] stated that for fossil fuels the conversion of fuel-N to NO is strongly dependent on the fuel-air ratio and on combustion temperature, and only slightly dependent on the identity of the parent nitrogen compound.

Typically, of the NO_x formed during the combustion of waste, nitric oxide (NO) is the major component, with a much smaller fraction, usually less 5% of the total NO_x, appearing as nitrogen dioxide (NO_2) and an almost insignificant amount of

nitrous oxide (N_2O) [9]. Abbas [9] also stated that 5 - 15 % of the total NO is formed by the thermal NO mechanism, while up to 5% is formed in the prompt mechanism. The remaining NO is formed through conversion of fuel-N to NO (fuel NO).

The objective of this study was to investigate the formation of NO in detail for different components of MSW such as paper, cardboard and plastics and their mixtures. The mechanisms of NO formation have been studied experimentally and with numerical simulations, investigating the influence of oxygen concentration and temperature and mass of sample. The focus has been on determining typical conversion levels and trends for NO formation from different MSW components in a small-scale laboratory furnace and not on absolute emission levels for MSW combustion plants.

4.3 Experimental methods

Five components of MSW were investigated in this study, both as single components and in mixtures. Newspaper (NP), glossy paper (GP) and cardboard (CB) were chosen as representatives of the cellulosic paper/cardboard fraction of MSW. Low-density polyethylene (LDPE) taken from a white coloured plastic bag and poly(vinylchloride) (PVC) taken from a grey coloured piece of a solid plate, were chosen to represent the plastic fraction. Table 1 shows results from a C/H/N/S/Cl analysis of both fresh samples and char formed at 1123 K and a proximate analysis of each component. The proximate analysis was performed according to ASTM standards for RDF. These standards specify 848 K for the determination of ash and 1223 K for measuring volatile matter. However, in order to be sure of closing the mass balance for the proximate analysis, determination of ash was also performed at 1223 K. Only GP experienced a significant weight loss between 848 and 1223 K (ash-content reduced from 44 to 27 wt%). The ultimate analysis of NP, CB and GP shows similar results. The nitrogen-contents of NP, CB and GP were 0.11, 0.11 and 0.14 wt%, respectively. However, it should be noted that the carbon-content of the char for GP was ~ 40% lower than for NP and CB. The proximate analysis shows that the ash-content of GP is 27 wt%, whereas the ash-content in NP and CB is 0.6 and 1.2 wt%, respectively. Comparing GP to NP and CB, less moisture, volatile matter and fixed carbon for GP was observed. PVC and LDPE have a similar low content of nitrogen with 0.04 and 0.05 wt%, respectively. The nitrogen-content in PVC and LDPE can originate from compounding ingredients such as stabiliser, plasticiser, extenders, fillers, pigment, etc. since the original polymers does not contain nitrogen. It is known, for example, that stabiliser for PVC contains nitrogen [10]. Otherwise, the ultimate and proximate analysis of PVC and LDPE shows different characteristics. PVC has ~ 50 wt% of chlorine, whereas LDPE consists of carbon and hydrogen. PVC has a fixed carbon content of almost 15%, while LDPE has 100% volatile matter on an ash free basis.

Pellets of the different components and mixtures of components were prepared. Paper and plastic were cut into small pieces (~ 5x5 mm) and compressed. The components constituting the mixture pellets were mixed thoroughly before compression. The thorough mixing and compression increases the possibility of interactions between the different components. The pellets were ~ 12 mm in diameter with varying heights, depending on the material, ranging typically from 8 - 25 mm.

The combustion experiments were performed in an electrically heated small-scale fixed bed reactor, a schematic drawing of which is shown in Fig. 1. The top section consists of an outer steel tube and an inner alumina tube to prevent reactions catalysed by steel in the freeboard.

The pellets were put in a cylinder (i.d. 13 mm; height 54 mm), which was open at the top, allowing pyrolysis gases and tars to escape and enter the reactor. The solid wall and the height of the cylinder do not allow oxygen to react with the sample inside the cylinder. Hence, this study only investigates the formation of NO from combustion of the volatile material in the fuel (volatile fraction 85 - 100% on a dry ash free basis). Heterogeneous reactions (oxidation of char) have not been examined in this study. An inconel wire fastened the cylinder to the top screw. The cylinder with the sample was lowered into the reactor just above the air distribution plate, which had 127 holes of diameter 0.55 mm. The reactor had seven separately controlled heating elements, two in the bottom section (preheating of oxidiser) and five in the top section. The heating elements were controlled so that the freeboard section was isothermal as close as possible.

Table 1. C/H/O/N/S/Cl (dry ash free) analysis of fresh samples and char formed at 1123 K and proximate analysis (n.d. = not determined).

Sample	C [wt%]	H [wt%]	O[a] [wt%]	N [wt%]	S [wt%]	Cl [wt%]
Fresh samples						
Newspaper	52.1	5.9	41.86	0.11	0.03	n.d.
Cardboard	48.6	6.2	44.96	0.11	0.13	n.d.
Glossy paper	45.6	4.8	49.41	0.14	0.05	n.d.
LDPE	85.7	14.2	0.05	0.05	0.00	n.d.
PVC	41.4	5.3	5.83	0.04	0.03	47.7
Char						
Newspaper	92.3	1.3	6.29	0.11	n.d.	n.d.
Cardboard	85.4	1.2	13.32	0.08	n.d.	n.d.
Glossy paper	56.7	0.6	42.7	<0.05	n.d.	n.d.
PVC	71.4	1.9	1.0	<0.05	n.d.	25.7

	Ash [wt%]	Volatile matter [wt%]	Fixed carbon [wt%]	Moisture [wt%]
Newspaper	0.6	80.5	11.0	7.9
Cardboard	1.2	81.9	10.3	6.6
Glossy paper	27.0	65.1	4.4	3.5
LDPE	2.1	97.6	0.0	0.3
PVC	4.2	81.4	14.4	0.0

[a] O obtained by difference

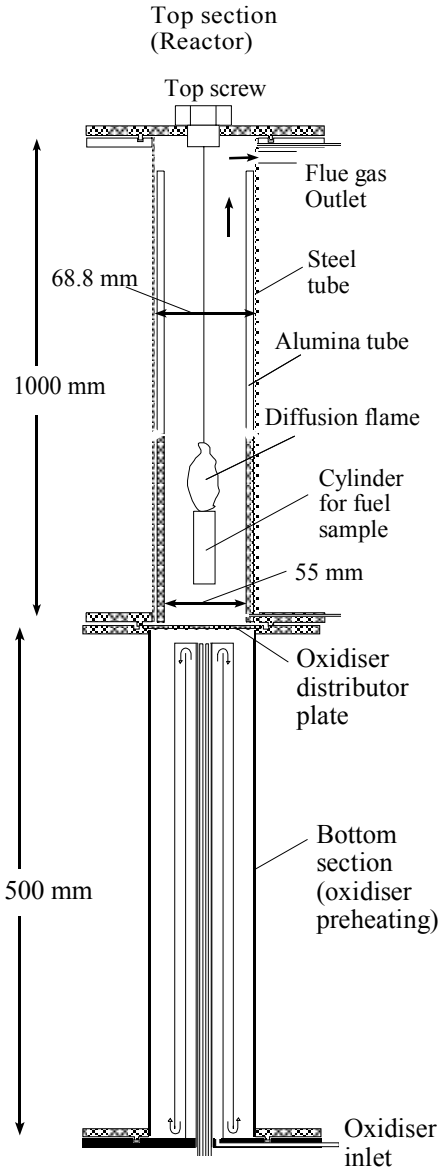

Figure 1. Schematic drawing of reactor.

Figure 2 shows the experimental set-up. High purity N_2 and O_2 were delivered from pressurised bottles connected with a pressure control valve. A mass flow controller controlled the flow-rate of each gas, before the gases were mixed in the mixing vessel. The mixed gas was fed to the bottom of the reactor for preheating. The flue gas was sampled at the top of the reactor, by sending it through a small cyclone to remove particles. A sample line from the cyclone delivered gas to the analysers. The pump and mass flow controllers ensured a constant flow to the analysers. A particle filter and a condenser were connected to the sample line prior to the pump to remove fine particles and water from the flue gas. The analysers were connected in series. Oxygen was measured with a paramagnetic (Hartmann & Braun Magnos 3) analyser,

CO_2 and CO were measured with infrared (Hartmann & Braun analysers URAS 4 and URAS 3G) analysers, respectively. Nitric oxide was measured by the non-dispersive ultraviolet absorption technique (Hartmann & Braun Radas 2 analyser). Sulphur dioxide was also measured by an ultraviolet absorption analyser (NGA 2000 MLT). The concentrations of O_2, CO_2, CO, NO_x and SO_2 were continuously recorded by a data acquisition system every half-second. The typical uncertainty in all these measurements was a maximum deviation of 1% of the range of each analyser.

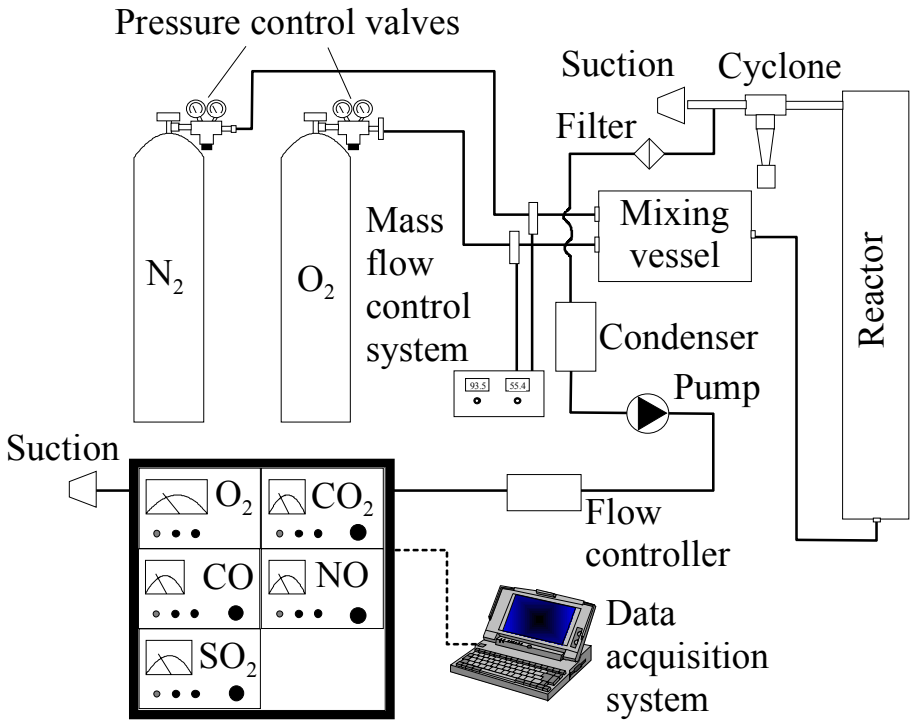

Figure 2. Experimental set-up.

Table 2 shows the experimental matrix for this investigation. Samples heavier than 0.12 g (0.2 g in the mixture with paper/cardboard and PVC) for LDPE were not used, since the reactor was not big enough to handle the sudden release of hydrocarbon volatiles from this fuel. Samples above 0.12 g gave problems from a lack of oxygen causing incomplete combustion, resulting in high values of CO. Increasing the flow of oxidiser did not promote complete oxidation, because this also reduced the residence time. The variations in compositions for the different mixtures of paper, cardboard and plastics in Table 2 reflect the typical composition of MSW and RDF [11,12 ,14]. However, compositions outside this range were also studied.

Table 2. Experimental matrix.

Component	Sample mass [g]	Temperature range [K]	O_2 concentration in oxidiser [vol.%]
Single components			
Newspaper	0.2 - 2.0[a]	973-1123[b]	12, 21, 40, 100[d]
Cardboard	2.0	1123	12, 21, 40, 100
Glossy paper	2.0	1123	12, 21, 40, 100
LDPE	0.05 – 0.2[a]	973-1123[c]	12, 21, 40, 100[e]
PVC	2.0	1123	12, 21, 40, 100
Mixture of paper/cardboard 20-80% Newspaper 10-70% Cardboard 10-70% Glossy paper	2.0	1123	12, 21, 40
Mixture of plastics 33-67% LDPE 33-67% PVC	0.2	1123	12, 21, 40
Mixture of paper/cardboard and plastics 15-60% Newspaper 10-55% Cardboard 10-55% Glossy paper 10% LDPE 10-55% PVC	2.0	1123	12, 21, 40

[a] Variation of sample weight performed at 1123 K and 21 vol% O_2.
[b] Variation of temperature performed with a sample weight of 2.0 g.
[c] Variation of temperature performed with a sample weight of 0.12 g.
[d] Variation of O_2 concentration performed with a sample weight of 2.0 g and temperature of 1123 K.
[e] Variation of O_2 concentration performed with a sample weight of 0.12 g and temperature of 850°C.

The measurements from the combustion experiments were analysed and the conversion factor for volatile fuel-nitrogen to NO was calculated for each experiment, from integrating the transient [NO] over time. Equation (1) describes how the conversion factor for the volatile nitrogen was calculated.

$$NO/fuel\text{-}N = V/(m_0 \cdot X_N/M_N) \cdot \sum [NO] \cdot \Delta t \qquad (1)$$

In Eq. 1, V [Nm^3/s] is the constant gas flow rate, m_0 [g] is the initial volatile mass of the sample on dry basis, X_N [-] is the initial mass fraction of volatile nitrogen in the sample, M_N [g/mol] is the atomic weight of nitrogen, [NO] [mol/Nm^3] is the transient NO concentration and ?t [s] is the time interval for recording of data. The conversion

of fuel-N to NO can be considered as a two-step process. The first step (in this case pyrolysis in the cylinder) will convert volatile nitrogen to intermediate products, such as HCN and NH_3. The second step is the conversion of the intermediate products to NO. Some of the volatile nitrogen will also be converted to N_2 in both steps; however, Eq. 1 calculates the total conversion of volatile nitrogen to NO.

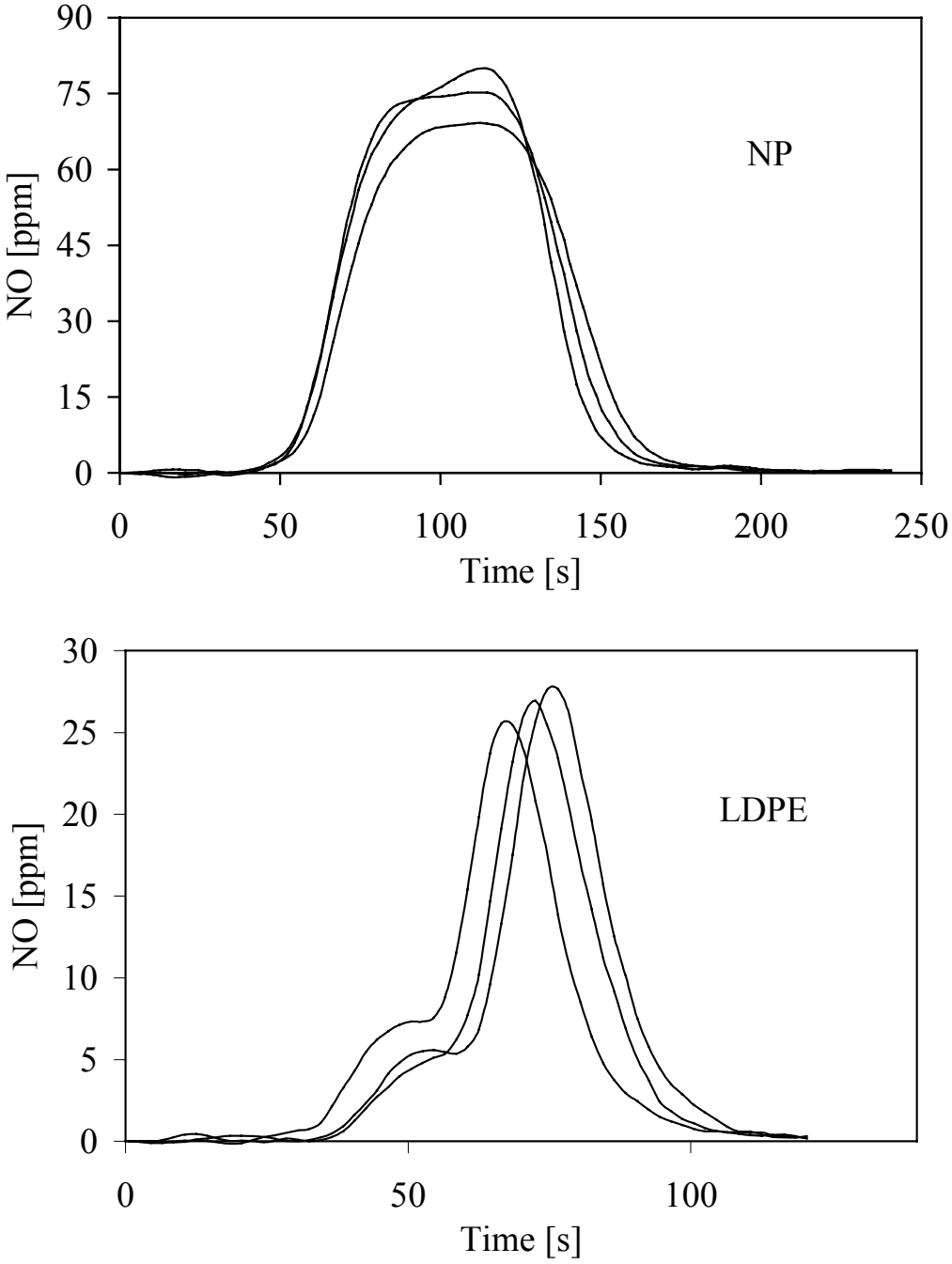

Figure 3. Repeatability tests of NO emission level for NP and LDPE. Sample mass m_{NP} = 2.0 g and m_{LDPE} = 0.12 g, Reactor temperature T = 1123 K, O_2 concentration = 21 vol%.

The repeatability of the experiments was checked, both for single components and for mixtures. Three experiments in succession, under identical experimental conditions, were performed. Figure 3 shows the emission level of NO as a function of time for three experiments on NP and LDPE. The emission levels were quite well repeated for both NP and LDPE. The conversion factor was calculated for each of these experiments and a standard deviation in the conversion factor of 3.6 and 3.7 % was found for NP and LDPE, respectively. Standard deviations of 2.5 and 1.9 % were found for a chosen composition of mixture of paper/cardboard and a mixture of paper/cardboard and plastics, respectively.

4.4 Experimental results

Experiments have been performed on single particles of NP, CB, GP, LDPE and PVC. In addition, experiments with mixtures of only paper/cardboard, mixtures of plastics and mixtures of paper/cardboard and plastics have been performed.

4.4.1 Single Components

Figure 4 shows [NO] from the five different components in this study. NP and CB have similar [NO] profiles. The overall profiles for GP, LDPE and PVC, however, are significantly lower. The differences between the components can be explained by differences in fuel properties; elemental composition, devolatilisation behaviour and in the case of LDPE, the samples mass is also of great importance (0.12 g versus 2.0 for the other fuels). For PVC and LDPE small but significant amounts of NO was observed at all oxygen concentrations prior to the major formation of NO. After a detailed study of the data, minor oxygen consumption was also observed. A small blue and yellow flame was observed before the major combustion took place. The minor formation of NO for PVC and LDPE may therefore partly be explained by a minor release of volatiles creating a small flame before the main combustion took place. However, other factors such as a release of a larger amount of volatile nitrogen and higher flame temperature in the first stage of devolatilisation compared to the second stage can explain the observed NO formation.

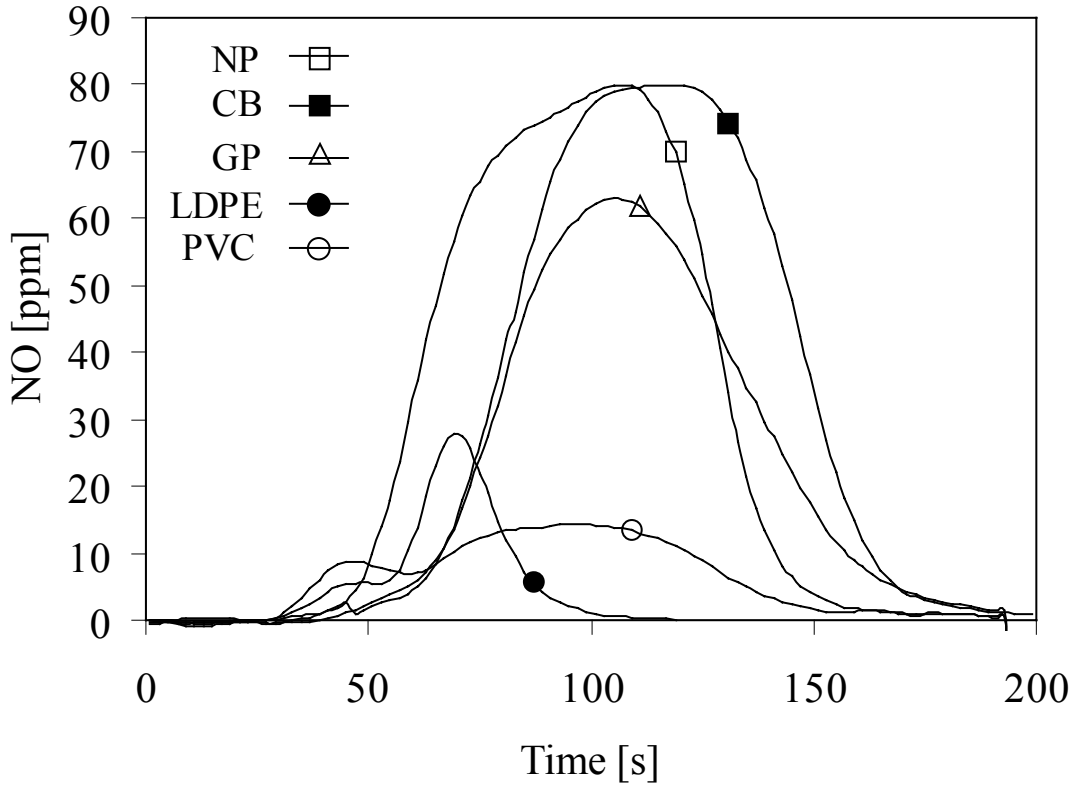

Figure 4. Transient emission levels of NO for the different components in this study. Sample weight equals 2.0 g with the exception of LDPE (sample weight = 0.12 g). Reactor temperature = 1123 K and O_2 concentration = 21 vol%.

Figure 5 shows [CO_2] and [O_2] for experiments on 0.12 g of LDPE and 2.0 g of NP; NP has a burnout time of ~ 2 minutes, while the burnout time for LDPE is ~ 30 seconds. The observed difference in burnout time is explained by different devolatilisation rates and masses of sample. The peak oxygen consumption for LDPE is slightly higher than for NP. The oxygen consumption is controlled by the devolatilisation rate and pyrolysis gas composition. The stoichiometric oxygen requirements calculated from their elemental compositions for LDPE (consisting of hydrogen and carbon) and NP (with a high yield of oxygen) are 209 and 83 mole/kg_{fuel}, respectively. These values are similar to the calculated oxygen consumption for experiments on LDPE and NP at base case conditions (21 vol.% oxygen and 1123 K), being 238 and 78 mole/kg_{fuel}. Taking the weight of the volatile fraction of the samples into consideration, the total number of moles of oxygen needed for complete combustion of LDPE and NP are 0.029 and 0.133, respectively. Given similar release rate of volatiles, the burnout time would be ~ 14 times higher for NP than for LDPE, while the actual burnout time ratio is ~ 4. Although the release rate is significantly lower, the peak oxygen consumption is higher for LDPE than for NP. Hence, a lower release rate of volatiles and higher oxygen requirement for LDPE, explains the different oxygen consumption curves.

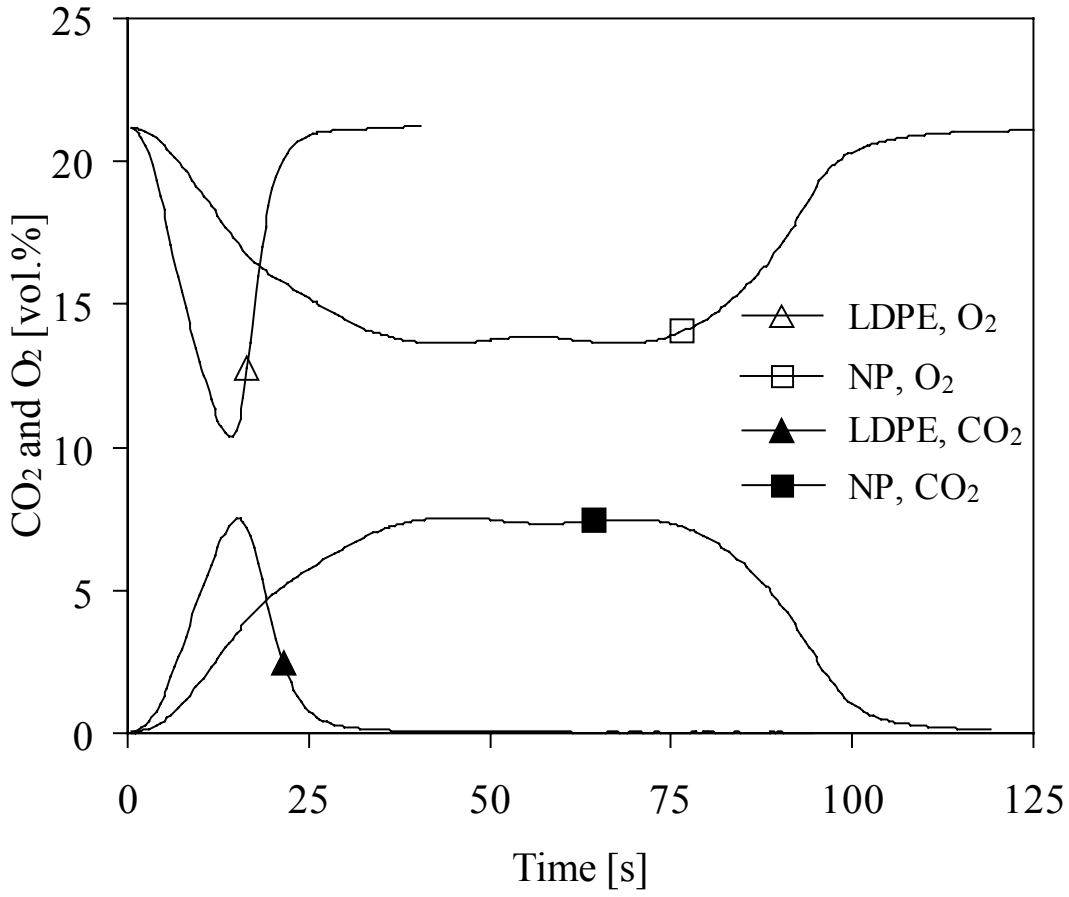

Figure 5. CO_2 and O_2 levels for experiments on LDPE and Newspaper. Reactor temperature is 1123 K and O_2 concentration is 21 vol%. m_{LDPE} = 0.12 g and m_{NP} = 2.0 g.

Table 3 shows the calculated conversion factors for single components as a function of oxygen concentration. Only minor differences in the conversion factors were observed from 12 to 21 vol.% O_2. Therefore, it was decided to run experiments with oxygen concentrations above 21 vol.% O_2, which should result in a more intense flame with a higher temperature, thereby forming thermal NO. Three experiments were conducted for each oxygen concentration, except for 100% O_2, where one experiment was performed on each sample. Average values for the conversion factor and standard deviation are shown in Table 3.

Table 3. Average conversion factor (NO/fuel-N) for single components of 2.0 g as a function of oxygen concentration in oxidiser at a reactor temperature of 1123 K.

O_2 [vol.%]	Newspaper	Cardboard	Glossy paper	LDPE[a]	PVC
	$\overline{(NO/fuel-N)}$ STDEV [%]	$\overline{(NO/fuel-N)}$ STDEV [%]	$\overline{(NO/fuel-N)}$ STDEV [%]	$\overline{(NO/fuel-N)}$ STDEV [%]	$\overline{(NO/fuel-N)}$ STDEV [%]
12	0.49 1.3	0.48 2.4	0.27 1.6	1.60 9.8	0.21 6
21	0.54 3.7	0.53 0.9	0.26 1.8	1.96 3.7	0.23 10.2
40	0.99 2.4	0.86 2.6	0.32 4	10.09 7.2	0.37 6.9
100[c]	0.50	0.42	0.23	0.71 (0.38)[b]	0.04

[a] Sample size 0.12 g
[b] Sample size 2.0 g
[c] Only one experiment

The fraction of volatile nitrogen is determined by subtracting the remaining nitrogen-content in the char as determined from the proximate and ultimate analysis. However, the conditions for devolatilisation of nitrogen may vary for different fuels and conditions. In order to validate the use of a proximate and ultimate analysis to determine the fixed content of a certain element, a mass balance for carbon was calculated for each of the experiments (C in fresh sample vs C in char, CO and CO_2). Using the ultimate analysis on fresh samples, char formed at 1123 K and measured CO and CO_2 values closes the mass balances for carbon well (within ± 10 wt%). The results also showed that the major part of the volatile-C is found in CO_2 (>95%). PVC produces the largest fraction of CO from volatile-C (~5% of volatile-C), while corresponding values for other samples are typically 0-3%.

The conversion factors for NP are 0.49, 0.54 and 0.50 at 12, 21 and 100 vol.% oxygen, respectively. The corresponding values for CB are 0.48, 0.53 and 0.42. At 40 vol.% O_2 the conversion factor increases to 0.99 for NP and 0.86 for CB, which is approximately a 80% increase from 21 vol% oxygen for NP and a 60% increase for CB. These results show that the NO formation is more sensitive to combustion temperature caused by a higher oxygen concentration, than to a higher availability of oxygen. In other words, very similar behaviour was observed for NP and CB for all oxygen concentrations. Skreiberg et. al. [13] reported a conversion factor of ~ 0.3 and 0.45 at 11 and 21 vol.% oxygen for a spruce sample of 700 mg at 1073 K in the same reactor as in this study. However, the conversion factor was based on total conversion of the fuel (volatiles and char) and not only on volatiles, as in this study.

Glossy paper, however, behaves differently with conversion factors of 0.27, 0.26 and 0.23 at 12, 21 and 100 vol.% oxygen. When increasing the oxygen

concentration from 21 to 40 vol.% O_2, a small increase in conversion factor from 0.23 to 0.32 was observed. Comparing the conversion factors at 12, 21 and 100 vol% O_2 for GP with NP and CB, the conversion factor for GP is approximately a factor of two lower. The explanation may be that the GP sample contained a more iron than NP and CB [14]. Mori et. al. [15] studied the effect of iron catalysts on the fate of fuel-nitrogen during coal pyrolysis; they concluded that an iron content of 0.2-0.7 wt% promoted both the formation of N_2 and lower yields of HCN, NH_3, N-containing oil, tar and char. However, the very high amount of ash in GP may also contain other catalytic species and have the same effect as iron on the conversion of fuel-nitrogen.

The large conversion factors for LDPE clearly indicate the production of thermal NO and possibly prompt NO too. The conversion factor increased ~ 500% when the oxygen concentration was increased from 21 to 40 vol.%. The prompt NO mechanism is important at fuel-rich conditions [16], so this large increase in the conversion factor can mainly be explained by a larger formation of thermal NO due to a higher combustion temperature with more O_2 present. PVC shows similar behaviour to GP: the conversion factor increased by ~ 60% from 21 to 40 vol.% O_2. However, the conversion factor with 100 % O_2 is close to zero. One of the most important differences between PVC and the other fuels used in this study is the high content of chlorine. The low conversion factor with pure O_2 implies that the formation of NO at lower O_2 concentrations is by the thermal and/or prompt mechanism. However, due to high concentrations of chlorine in PVC, the formation mechanism for NO is more complex and presently not fully understood, even though several studies have investigated the effect of chlorine in combustion processes [17-20].

The oxidation of CO by the hydroxyl radical (OH) is much faster than steps involving O_2 or O [16]. However, the fuels in this study contain sufficient hydrogen to produce hydroxyl radicals, so the oxidation of CO becomes fast and incomplete combustion is avoided. This is confirmed by the low CO emissions observed at all oxygen concentrations for all components.

The influence of the sample's mass was investigated for NP and LDPE. The conversion factor for NP increased from 0.50 to 0.59 when its mass was reduced from 2.0 to 0.2 g with 21 vol.% oxygen. For LDPE the conversion factor increased from 2.05 to 2.73 with a reduction in sample mass from 0.2 to 0.05 g. Care should be taken interpreting these results, since different variables are coupled. Less sample results in lower consumption of oxygen and more excess air. A smaller sample also increases the uncertainty in the calculation of the conversion factor.

For NP and LDPE, the influence of reactor temperature was investigated: a decrease from 1123 to 973 K resulted in a decrease in conversion factor from 0.50 to 0.45 for NP and from 1.96 to 1.89 for LDPE. These experiments were performed with 21 vol.% oxygen and samples of 2.0 g and 0.12 g were used for NP and LDPE, respectively. The differences in fuel-N content for the components in this study are minor; therefore the reduction in conversion when increasing the nitrogen-content, as stated in the literature [21], is considered of minor importance.

4.4.2 Mixtures

The conversion factors for the experiments on mixture pellets were compared to the conversion factors calculated for an imaginary pellet built up from the weighted contributions of each component's conversion factor. The experiments on mixtures and single components were performed in exactly the same way with a mass of 2.0 g, except for experiments on single particles of LDPE, where a sample of 0.12 g was used. The conversion factor for the imaginary pellet is described by:

$$(NO/fuel-N)_{SUM\ OF\ SINGLE\ COMPONENTS} = \sum_j Y_i \cdot (NO/fuel-N)_i \qquad (2)$$

In Eq. 2, Y_i is the mass fraction of component i, $(NO/fuel\text{-}N)_i$ is the conversion factor for component i as found from the single component experiments and j denotes the number of components in the actual mixture.

The experiments on mixtures of paper and cardboard gave some interesting results at 40 vol.% O_2. As shown in Fig. 6, the conversion factor for the mixture at 40 vol.% O_2 was ~ 10-20% lower than the value calculated from the single components. This indicates that the lower conversion factor for the mixture pellet is mainly caused by a lower temperature and hence less contribution from thermal NO. The lower temperature can be explained by differences in the measured transient oxygen consumption for the different fuels and hence the devolatilisation rate. The oxygen consumption for the single components had somewhat different profiles and maximum values. The transient oxygen consumption for the mixture is a function of composition. However, at this high inlet oxygen concentration, a difference in the transient oxygen consumption and hence temperature, might influence the NO emissions significantly, since a large fraction of the NO is formed thermally. For experiments at 12 and 21 vol.% O_2 the differences in the conversion factors for mixtures and the calculated sum of single components were minor, being within the experimental error. For all experiments on mixtures of paper and cardboard, no influence of a special component could be detected, when the fraction of each component was varied.

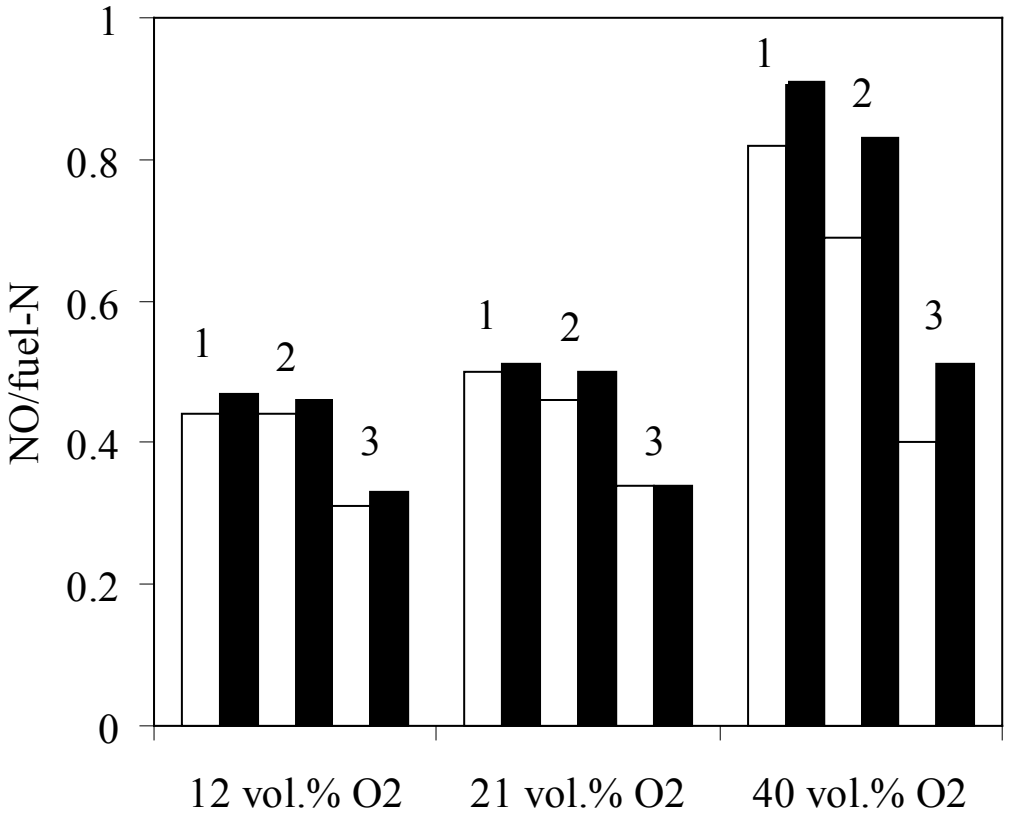

Figure 6. Conversion factor for mixtures of paper as a function of O_2 concentration in inlet gas. White bars denotes experiments on a pellet of the mixture. Black bars denote the conversion calculated factor from single components. 1: NP = 80 wt%, CB = 10 wt%, GP = 10 wt% ; 2: NP = 20 wt%, CB = 70 wt%, GP = 10 wt%; 3: NP = 20 wt%, CB = 10 wt%, GP = 70 wt%.

Interpretation of the experimental results on mixtures of LDPE and PVC were somewhat more difficult, due to the small sample mass leading to a higher degree of uncertainty. The results showed no clear trends with oxygen concentration or mixture ratio, indicating little or no interaction between the two components.

Figure 7 shows the conversion factors for different mixtures of paper and plastic compared with calculated values. All the mixtures of paper and plastics show conversion factors lower than estimated from the single components. The major reason is that the contribution from LDPE in the mixture is not as much as expected. In fact, the conversion factor for LDPE as a single component exceeds unity for all oxygen concentrations, clearly indicating a contribution from thermal or possibly prompt NO. The conditions for formation of thermal NO are not as favourable for the mixture as for the single component. An indication on the difference in flame temperature for the different fuels is the adiabatic flame temperature. The adiabatic flame temperature is the maximum combustion temperature, which will be higher

than those actually attained in the reactor, given that there will be significant radiative heat losses. However, as an indicator of differences between fuels and mixtures of different fuels, and not as a quantitative measure of combustion temperature and hence NO formation, it is useful. Equilibrium calculations with CHEMKIN III [22] were performed with the same oxygen concentrations as for the experiments. For LDPE, the major pyrolysis product is ethene (C_2H_4) [23]. Ethene was used in the equilibrium calculations simulating the combustion of LDPE. For paper the following composition of the pyrolysis gas was used [24]: 0.4 vol.% H_2, 41.1% CO, 46.6% CO_2, 8.3% CH_4 and 3.6% H_2O. For PVC, a pyrolysis gas corresponding to the elemental composition was used: 60 vol.% C_2H_4 and 40 vol.% HCl. Calculations were also made for a mixture of paper and plastics, with a composition corresponding to 80 wt% paper, 10% PVC and 10% LDPE. The mixture had the following gas composition: 0.3 vol.% H_2, 31.6% CO, 35.9% CO_2, 6.4% CH_4, 18% C_2H_4, 5% HCl and 2.8% H_2O. Table 4 shows the calculated adiabatic flame temperatures for the different fuels at the same oxygen concentrations at different fuel/air ratios. The oxygen concentrations are corresponding to those used in the experiments, while λ=3 correspond to the maximum λ observed for NP at base case conditions at maximum oxygen consumption. Initial temperatures of 673 K for paper and mixture of paper and plastics and 773 K for LDPE and PVC were used according to their devolatilisation temperatures as observed from a thermogravimetric analysis of the different components. Increasing λ from 1.5 to 3.0 decreases the adiabatic flame temperatures for paper, LDPE and the mixture with 472, 638 and 571 K, respectively. An adiabatic temperature difference at λ=1.0 increasing from 259 to 621 K when increasing the oxygen concentration from 12 to 100 vol.% is observed when comparing paper and LDPE. PVC has a slightly lower adiabatic flame temperature than LDPE at all oxygen levels. A temperature difference of 163 to 322 K when increasing the oxygen concentration from 12 to 100 vol.% oxygen is observed when comparing the mixture to LDPE. Knowing that the formation of thermal NO increases exponentially with temperature, starting at approximately 1600-1700 K [25], a small temperature change will significantly alter the yield of thermal NO. The relative temperature contribution of LDPE in the flame of the volatile fraction of the mixture is therefore not as large as if one summarises the weighted conversion factors for the single components. This is especially evident for experiments at 40 vol.% O_2, where the conversion factor of LDPE as a single component is very high (see Table 3). No clear trend towards a reduced conversion factor for mixtures with a high content of PVC was observed.

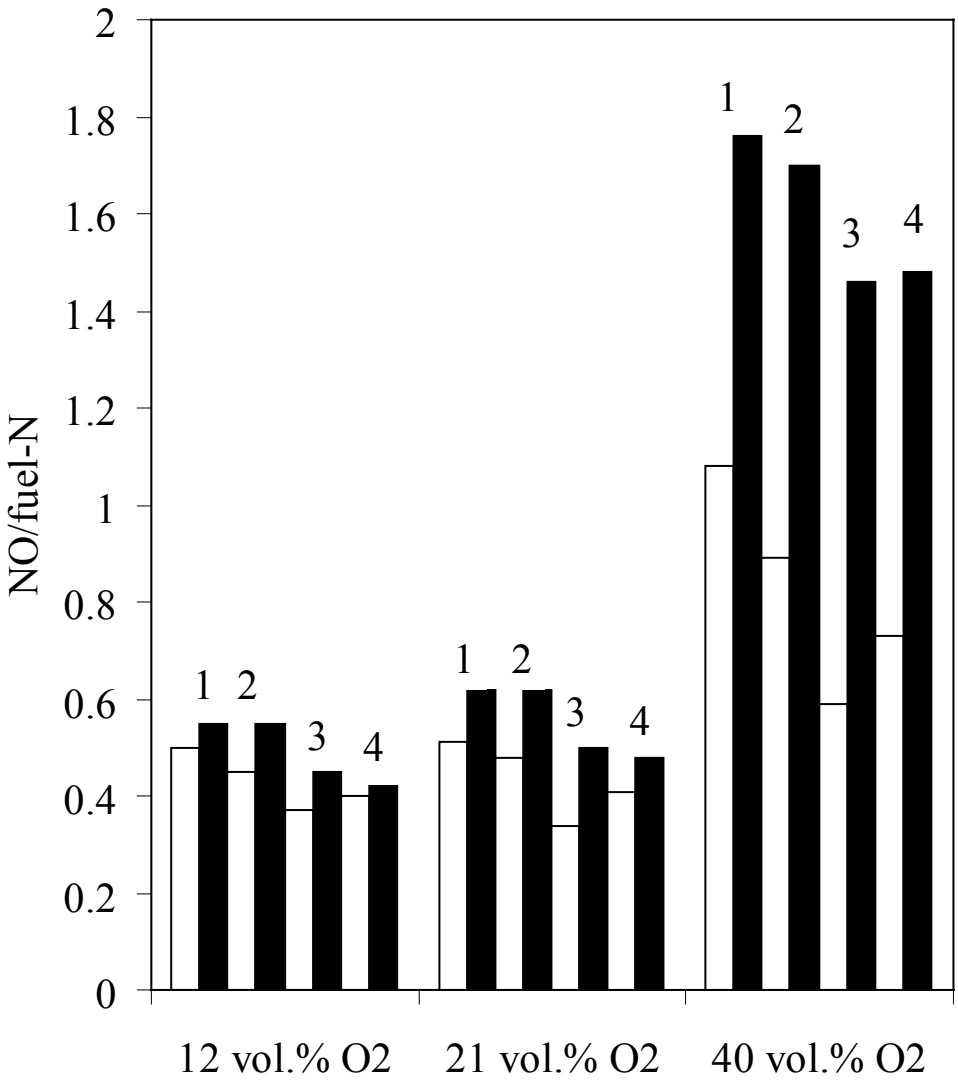

Figure 7. Conversion factors for mixtures of paper and plastic as a function of O_2 concentration in inlet gas. White bars denote experiments on mixtures. Black bars denote the conversion factor calculated from single components. 1: NP = 60 wt%, CB = 10 wt%, GP = 10 wt%, LDPE = 10 wt%, PVC = 10 wt%; 2: NP = 15 wt%, CB = 55 wt%, GP = 10 wt%, LDPE = 10 wt%, PVC = 10 wt%; 3: NP = 15 wt%, CB = 10 wt%, GP = 55 wt%, LDPE = 10 wt%, PVC = 10 wt%; 4: NP = 15 wt%, CB = 10 wt%, GP = 10 wt%, LDPE = 10 wt%, PVC = 55 wt%;.

Table 4. Adiabatic flame temperatures for pyrolysis gas from paper, LDPE, PVC and mixture of paper and plastics at different oxygen concentrations in oxidiser and λ.

Sample	**12 vol.% O_2**	**21 vol.% O_2**	**40 vol.% O_2**	**100 vol.% O_2**
λ=1.0				
Paper	1840	2174	2417	2598
LDPE	2099	2556	2912	3219
PVC	2001	2472	2833	3131
Mixture	1936	2350	2655	2897
λ (at 21 vol.% O_2)	**1.5**	**2.0**	**2.5**	**3.0**
Paper	1955	1749	1597	1483
LDPE	2260	1973	1768	1622
PVC	2155	1867	1667	1524
Mixture	2073	1816	1634	1502

4.5 Modelling

The opposed flow diffusion flame code in Chemkin III [22], OPPDIF [26], was used for a parametric study and for comparison with *trends* observed in the experimental study. OPPDIF is a Fortran code, which computes the steady state solution for axisymmetric diffusion flames between two opposing nozzles. The one-dimensional model predicts the species, temperature and velocity in the core flow between the nozzles (excluding edge effects). Several aspects of opposed-flow or counter-flow diffusion flames, such as flame structure, extinction limits and burning velocities, have been studied numerically and experimentally [27-34]. Mechanisms for NO formation in opposed-flow diffusion flames have also been investigated. The contributions from thermal, prompt [35] and N_2O mechanisms have been identified for different fuels under different conditions [36,37]. Turns [38] has reviewed the formation of NO_x in nonpremixed flames and concluded that research was needed into several aspects of NO formation in both laminar and turbulent jet flames. However, no literature was found on the formation of NO during the combustion of pyrolysis gases from paper or plastics.

4.5.1 Methods

The experimental set-up is a co-flow system, whereas the OPPDIF program describes an opposed-flow system; consequently differences in residence time and flame structure may occur. However, in laminar diffusion flames, the chemistry, independent of flow arrangements (co-flow vs opposed-flow system), is occurring in the flame close to or at stoichiometric conditions. The important parameters in the simulation of an opposed flow diffusion flame include the velocities of the two gas flows and the separation between the two nozzles; these two parameters characterise the residence time. A typical velocity in an experiment with NP was estimated to be ~

20 cm/s for the whole pyrolysis period for the gas flowing out of the cylinder and ~ 40 cm/s for the oxidiser. In this study the distance between the nozzle was kept constant at 2.0 cm, whereas the exit velocities were varied with a constant fuel/oxidiser ratio of 0.5 similar to the experiments. Keeping the velocity gradient (i.e. strain rate) constant, when changing the separation distance and velocities of the fuel and oxidiser can be used as a control parameter. However, due to differences between experimental and simulation conditions, using the strain rate as a parameter in the parametric study would not further explain the experimental results. The temperature of the fuel (pyrolysis gas) is 673 K for simulating the burning of on paper and 773 K plastic (C_2H_4). These temperatures were found from a thermogravimetric analysis (TGA) of the components. The TGA study gave the degree of degradation as a function of temperature, not taking into account the possible influence of heat and mass transfer. The temperature of the oxidiser in the simulations was 1123 K unless indicated otherwise.

The kinetic reaction schemes used for simulations on paper and plastic are slightly reduced subsets of the chemical kinetic model for hydrocarbon/NO interactions proposed by Glarborg et. al. [39]. The reaction mechanism used for paper had 39 species with a total of 239 reversible reactions, while that for plastic (taken as C_2H_4) involved 43 species with a total of 258 reversible reactions. The pyrolysis gas composition for paper/cardboard was estimated from the literature. For paper an average of all gas compositions obtained from a study of the pyrolysis of paper and cardboard, with the exception of two experiments performed at low temperature, was used [24]. The minor amount of hydrocarbons was taken into account as CH_4 in the gas composition. The tar fraction was assumed to crack, yielding a gas of the same composition as the primary gas: 0.4 vol.% H_2, 41.1% CO, 46.6% CO_2, 8.3% CH_4 and 3.6% H_2O. This gas composition was used in all simulations, unless otherwise mentioned. The content of NH_3 and HCN was not measured in the above-mentioned study.

Little information on the release of fuel-nitrogen during the pyrolysis of MSW components or biomass has been found. Ammonia is believed to be the dominant fuel-N product from pyrolysis of low rank fuels (biomass, peat, lignite and low rank coals) [40]. However, for bituminous coals and anthracites HCN is the dominant nitrogenous product of pyrolysis. Others [41] have found for the pyrolysis of different biomasses and coals, that the HCN/NH_3 ratio decreased with increasing O/N ratio for the parent fuel. However, for O/N ratios above 20, the HCN/NH_3 ratio was relatively constant at ~ 0.15. For pine bark, which has an O/N ratio similar to paper, the HCN/NH_3 ratio was found to be 0.1 [41]. The total conversion of fuel-N to NH_3 and HCN during pyrolysis shows large variations. An investigation of the formation of NH_3 and HCN from the pyrolysis of peat, coal and bark at low heating rates showed that all fuels produced more NH_3 than HCN [42]. It was further found that increasing the heating rates resulted in a higher conversion of fuel-N to NH_3 and HCN. The fraction of nitrogen remaining in the char after pyrolysis ranged from 15 wt% for peat to 70 wt% for bark. The heating rate and devolatilisation temperature play important roles in the devolatilisation of fuel-N. Previous studies [43] have shown that char from coal will be enriched in nitrogen at a low degree of devolatilisation, i.e. during heating to a low final temperature or at very short residence times. At higher devolatilisation temperatures, nitrogen is released faster than the volatiles, so the final

nitrogen-content of the char may be lower than that of the parent coal. The same study stated that the amounts of NH_3 and HCN released during pyrolysis depend on a number of factors, most importantly coal type, heating rate, final temperature and residence time.

Based on the information found in the literature, the HCN/NH_3 ratio was set to 1/9 for the simulations on pyrolysis gas from paper. Estimating the conversion of volatile fuel-N to NH_3 and HCN is difficult. Leppälahti [42] stated that for peat, which has a similar volatile fraction of fuel-N as paper, the conversion to NH_3 was between 17-24 wt% and that the conversion to HCN was between 3 to 9 wt% of the initial fuel-N. As observed in the ultimate analysis of char from newspaper (see Table 2), 15% of the nitrogen in paper remains in the char. Furthermore, it is assumed that 50% of the remaining volatile-nitrogen is converted to N_2 either before escaping the pellet or inside the cylinder. Based on the elemental composition of the fuel, the above ratio of HCN/NH_3 of 1/9 and the assumption that 50% of the volatile nitrogen is converted to N_2, the concentrations of NH_3 and HCN in the pyrolysis gas from paper were set to 900 and 100 ppmv, respectively. For all simulations the calculated conversion factor means the conversion of NH_3 and HCN (in the pyrolysis gas) to NO.

For the simulation of LDPE, C_2H_4 was chosen as a fuel corresponding to the content of carbon and hydrogen in the fuel and experimental data obtained from literature [23].

4.5.2 Simulations of paper

The temperature and concentrations of species, as a function of the distance X from the fuel nozzle, for simulations of the pyrolysis gas from paper are shown in Fig. 8. The peak temperature is observed slightly to the fuel side. OPPDIF estimates the flame thickness by assuming that the flame starts where the temperature equals the fuel temperature plus 10% of the maximum temperature increase. The end point of the flame is estimated the same way using the temperature of the oxidiser as starting point. A flame thickness of ~ 6 mm was estimated using this method. Consumption of the species CO, CH_4 and NH_3 is observed in Fig. 8, when the fuel is entering the flame region; formation of HCN and NO is observed in the first section of the flame on the fuel side. The peak formation of NO is observed on the fuel side at a temperature slightly lower than the peak temperature. At the point of peak formation of NO, most of the NH_3 and HCN have been consumed.

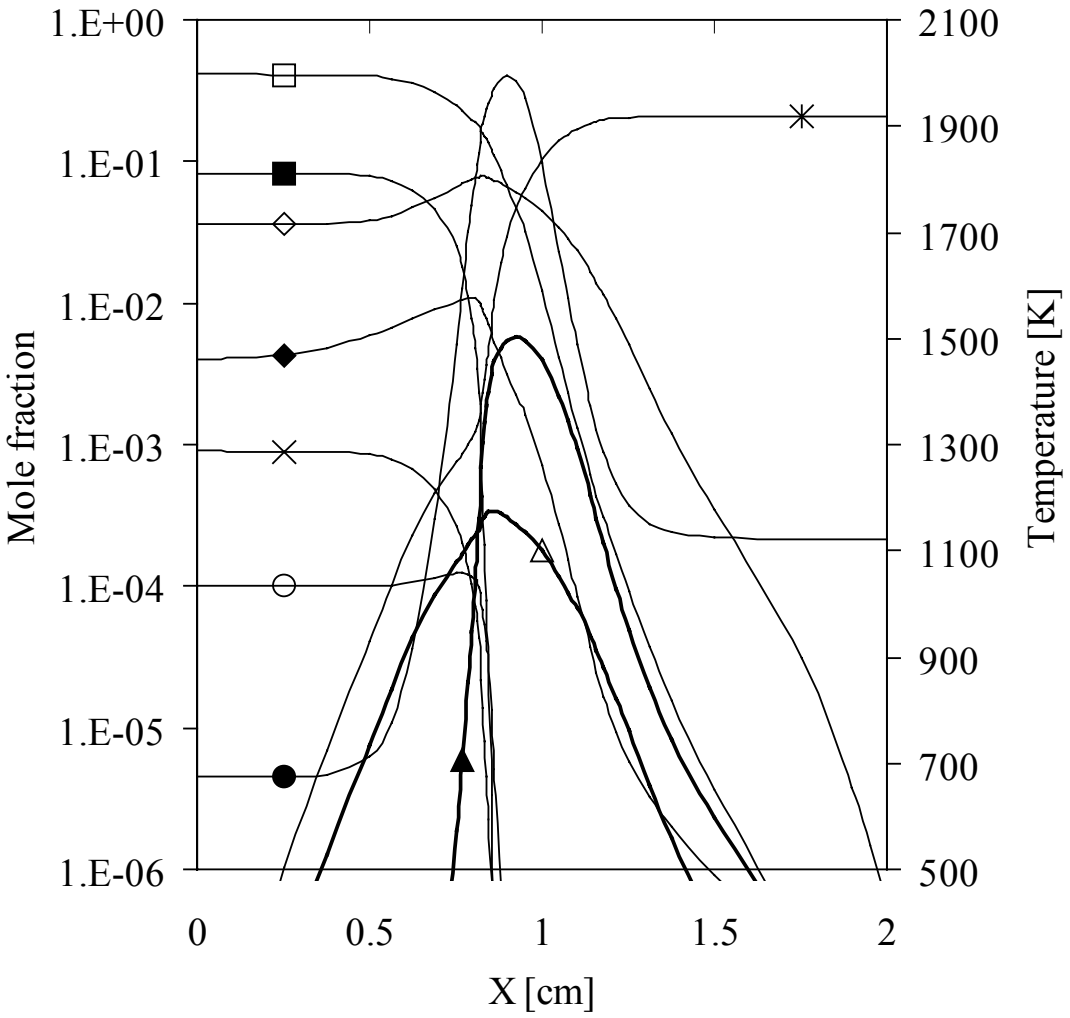

Figure 8. Calculated temperature (?) and concentrations of species as a function of distance from the fuel nozzle for simulation on paper at 21 vol% oxygen and an oxidiser temperature of 1123 K. The concentrations are for CO (?), CH_4 (¦), H_2O (?), H_2 (?), NH_3 (x), HCN (?), NO (?), OH (?) and O_2 (*).

Figure 9 shows the contributions of fuel, prompt and thermal NO_x mechanisms to the conversion factor for paper at different oxygen concentrations in the oxidiser. The initiating reactions for the thermal and prompt NO_x mechanisms were removed from the reaction scheme for the respective calculations. A peak temperature of 2260 K was observed for simulations at 40 vol.% oxygen, whereas the peak temperature at 21 vol.% oxygen was 2000 K. This increase in temperature is the main reason for the high contribution from thermal NO_x at 40 vol.% oxygen. An increased oxygen concentration results in a larger conversion factor when only considering fuel-nitrogen for the simulations on paper. The conversion factor for experiments with pure oxygen, however, was more similar to the values obtained at 12 and 21 vol.% oxygen. The minor formation of prompt NO observed in Fig. 9 can be explained by

the observed formation of HCN in Fig. 8. The rest of the amount of NO derives mainly from the fuel-nitrogen species, NH_3 and HCN, and a minor amount of thermal NO.

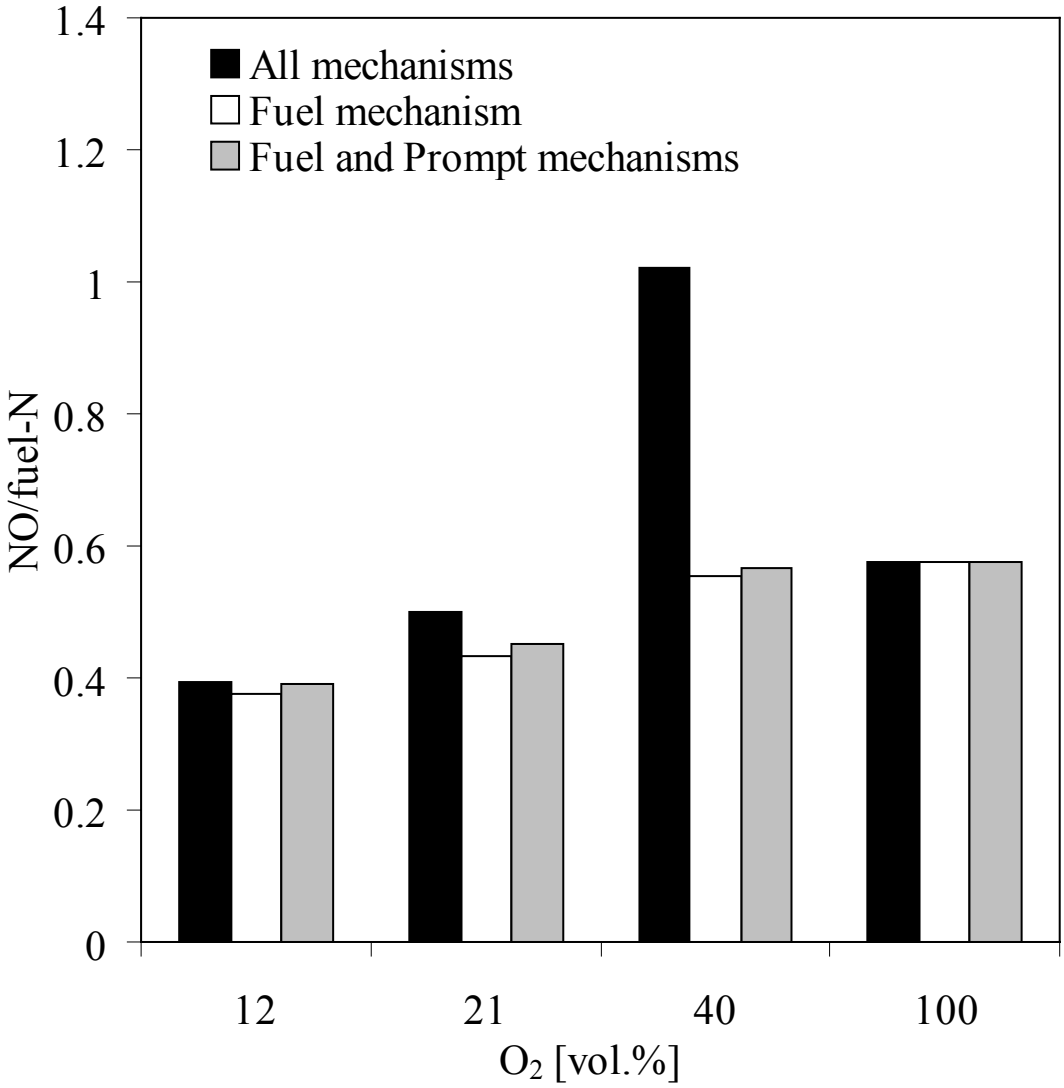

Figure 9. Contribution of fuel, prompt and thermal mechanisms to the conversion factor (conversion of HCN and NH_3 to NO) for simulations on pyrolysis gas from paper at different oxygen concentrations. Oxidiser temperature = 1123 K.

In order to investigate the effect of different concentrations and HCN/NH_3 ratios a sensitivity study was performed. Table 5 shows the concentrations of HCN and NH_3 and the calculated conversion factor for the different simulations on pyrolysis gas from paper. The oxygen concentration in the oxidiser nozzle was 21 vol.% and the temperature of the oxidiser was 1123 K. These results indicate that the total concentrations of NH_3 and HCN has a significant effect on the conversion factor, while the NH_3/HCN ratio is of minor importance. At a constant NH_3/HCN ratio, a decreasing conversion factor with increasing concentrations of HCN and NH_3 is

observed. This agrees with other work [21]. It is also interesting to observe that a larger fraction of NH_3 than HCN is converted to NO. A sensitivity study on the pyrolysis gas composition was also performed to investigate the effects of changing composition. Table 6 shows the variations in composition and conversion factors for the pyrolysis gas used in the sensitivity study. An oxidiser temperature of 1123 K and 21 vol.% of O_2 were used. The concentrations used in this sensitivity study reflect the range of compositions found in the literature [24]. The concentrations of HCN and NH_3 were held constant. Even with these fairly large variations in composition (each case adds 30% to the selected component, consequently adjusting the concentrations of the other components), the conversion factor varies very little: it deviated by a maximum of 12% from the base case.

Table 5. Sensitivity study on the effect of different NH_3 and HCN concentrations for simulations on paper.

Gas	Base case [vol%]	Comp. 1 [vol%]	Comp. 2 [vol%]	Comp. 3 [vol%]	Comp. 4 [vol%]	Comp. 5 [vol%]	Comp. 6 [vol%]
HCN	0.01	0.005	0.015	0.02	0.05	0.00	0.10
NH_3	0.09	0.045	0.135	0.18	0.05	0.10	0.00
NO/fuel-N	0.50	0.72	0.41	0.35	0.50	0.56	0.47

Table 6. Variations in pyrolysis gas composition and conversion factors for sensitivity study for simulations on paper.

Gas	Base case [vol%]	Comp. 1 [vol%]	Comp. 2 [vol%]	Comp. 3 [vol%]	Comp. 4 [vol%]	Comp. 5 [vol%]
H_2	0.40	0.52	0.32	0.30	0.39	0.40
CO	41.1	41.08	53.43	30.36	39.98	40.64
CO_2	46.5	46.40	36.74	60.45	45.24	45.97
CH_4	8.30	8.30	6.56	6.13	10.79	8.21
H_2O	3.60	3.60	2.85	2.66	3.50	4.68
HCN	0.01	0.01	0.01	0.01	0.01	0.01
NH_3	0.09	0.09	0.09	0.09	0.09	0.09
NO/fuel-N	0.50	0.50	0.56	0.47	0.56	0.50

Three cases with different velocities for the fuel and oxidiser were simulated for four different oxygen concentrations in the oxidiser and at three different temperatures. In addition, a comparison with the experimental results on NP was made. The results are shown in Figs. 10 and 11. The fuel/oxidiser velocity ratio was estimated from experiments. As can be seen from Figs. 10 and 11, a velocity of 40 cm/s for fuel and 80 cm/s (40/80 velocity ratio) for oxidiser provides the best agreement with the experimental trend observed for NP. The increase in conversion factor for the 20/40 velocity ratio as a function of oxygen concentration, observed in Fig. 10, is generally overestimated. However, the conversion factors for both the 40/80 and the 80/160 velocity ratio show a similar trend as the experimental data for

NP with regards to a change in oxygen concentration. However, comparing the conversion factor with experiments on NP as a function of temperature shows that the trend of increasing conversion factor with increasing temperature is not reflected for the 80/160 velocity ratio. Based on these results the 40/80 velocity ratio was chosen for further simulations.

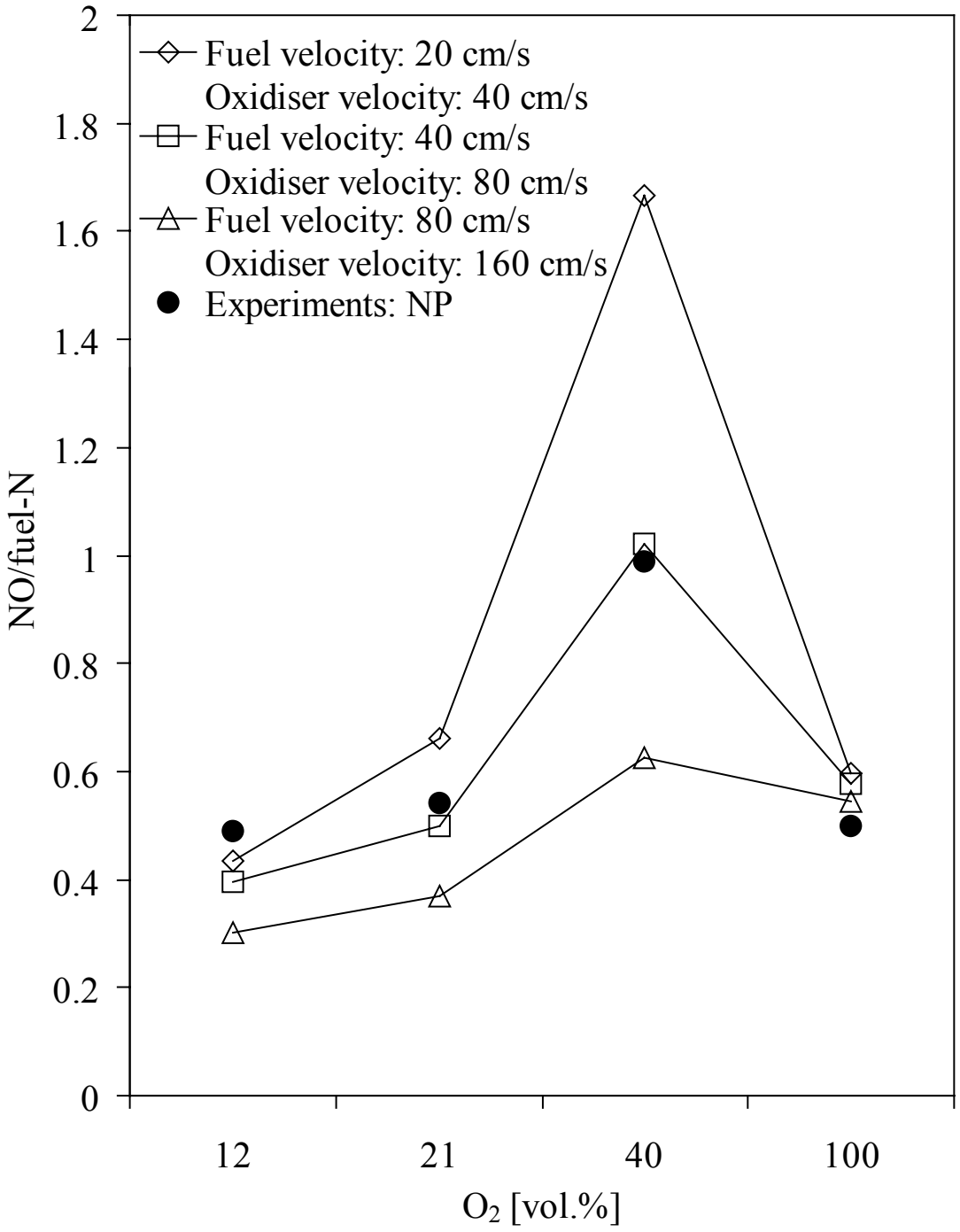

Figure 10. Comparison of conversion factor at different oxygen concentrations for simulations of pyrolysis gas from paper (conversion of HCN and NH_3 to NO) with different nozzle velocities and experiments on newspaper. Oxidiser temperature = 1123 K.

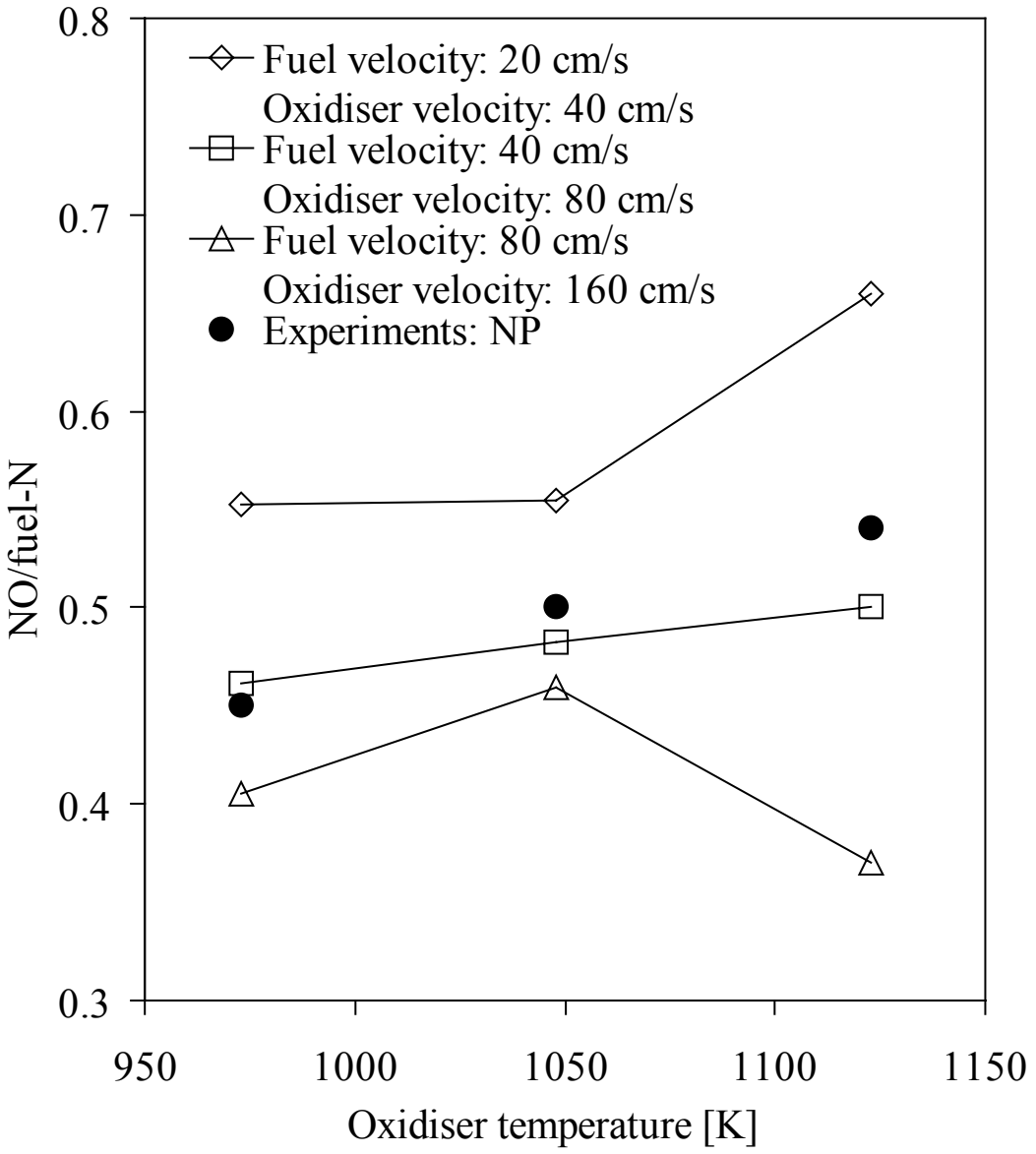

Figure 11. Comparison of conversion factor at different temperatures for simulations of pyrolysis gas from paper (conversion of HCN and NH_3 to NO) with different nozzle velocities and experiments on NP. Oxygen concentration is 21 vol%.

Figure 12 shows the influence of temperature and oxygen concentration in the oxidiser on the conversion factor for simulations on pyrolysis gas from paper. A minor increase is observed with increasing temperature at all oxygen concentrations. A major jump in conversion factor is observed when the oxygen concentration is increased from 21 to 40 vol.%, caused by the formation of thermal NO due to a higher flame temperature. It is also interesting to observe that the conversion factor for pure oxygen is similar to that for 21 vol.% oxygen. This is also consistent with the experimental results. The reason is that thermal NO cannot be formed at 100% oxygen, due to the absence of nitrogen, which again indicates that NO formed at 12

and 21 vol% oxygen is mainly fuel-NO. It can also be observed that NO formation at 40 vol% oxygen is more temperature-dependent, since a large portion of the NO formed is from the thermal mechanism.

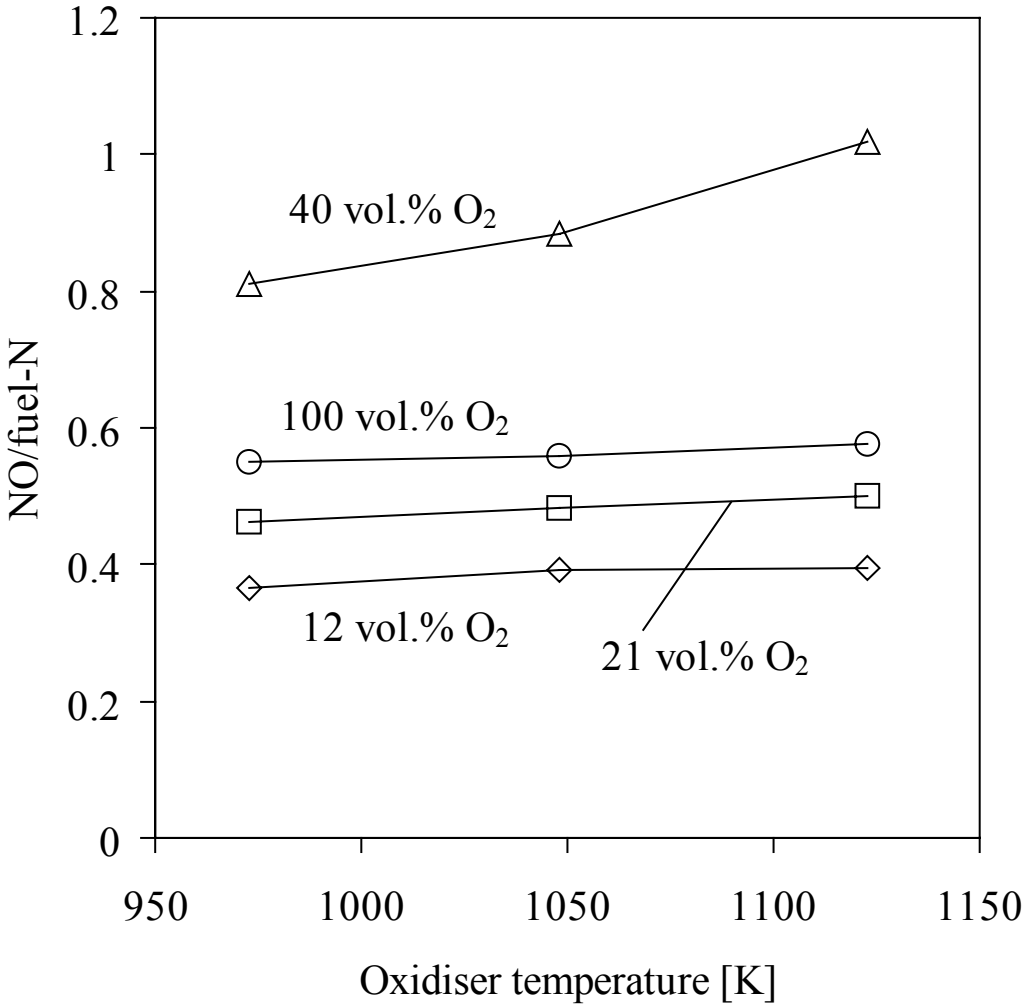

Figure 12. Influence of temperature and oxygen concentration on conversion factor (conversion of HCN and NH_3 to NO) for simulations of pyrolysis gas from paper.

Figure 13 compares conversion factors as a function of oxygen concentration in the oxidiser, for simulations on pyrolysis gas from paper and experiments on paper and cardboard. The experimental trends are well simulated, especially for NP and CB. The conversion factor for GP, however, is less influenced by an increase in oxygen concentration than observed in the simulations.

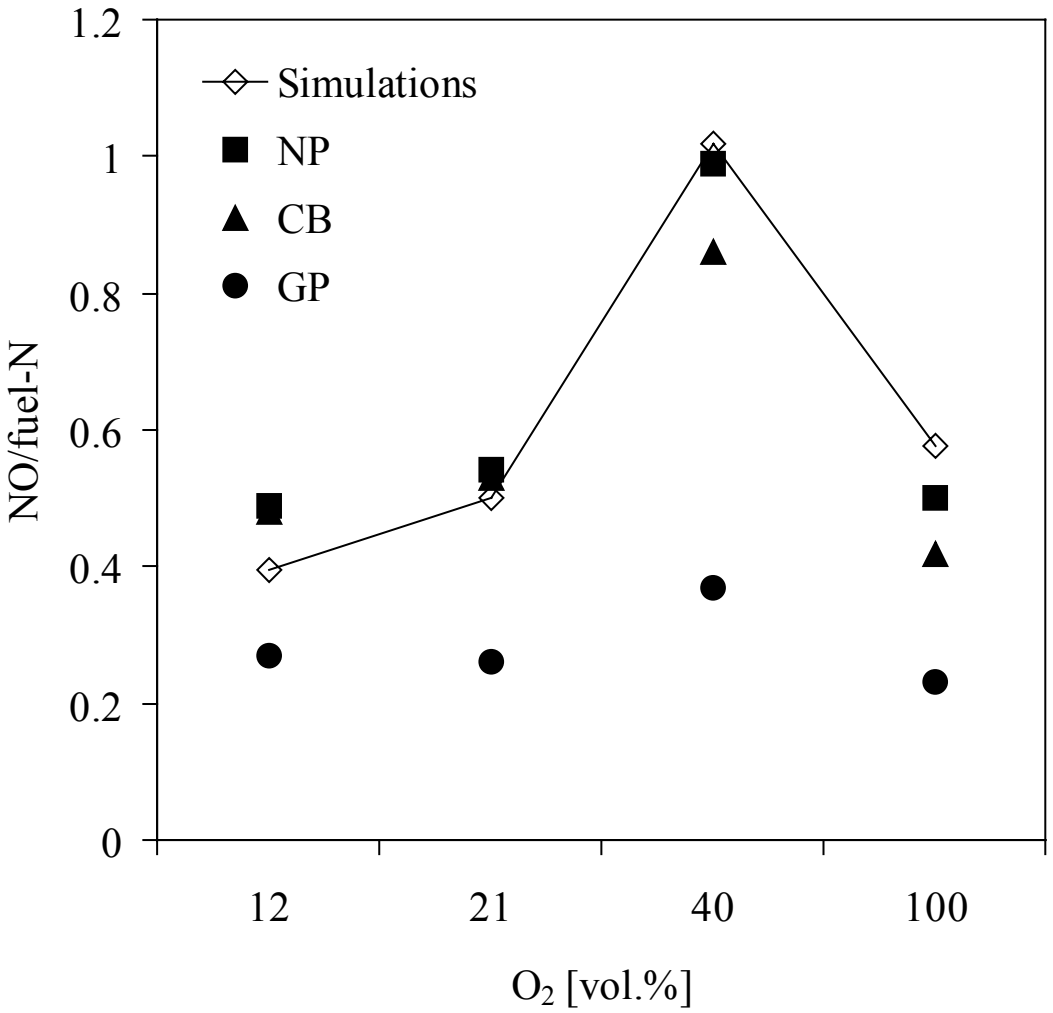

Figure 13. Comparison of conversion factors as a function of oxygen concentration in the oxidiser for simulations of pyrolysis gas from paper (conversion of HCN and NH_3 to NO) and experiments on NP, CB and GP. Oxidiser temperature = 1123 K.

4.5.3 Simulations on plastic

The simulations for plastic, taken as C_2H_4 in the case of LDPE, including NH_3 and HCN, are more difficult to interpret, since only the initial fuel consumption occurs in the opposed flow diffusion flame. Compared to the volatiles from paper with a lower hydrocarbon yield and higher levels of inert species, the volatiles from a plastic have a much higher stoichiometric oxygen requirement. The limited availability of oxygen in the opposed flow diffusion flame reduces the conversion of fuel to a small value. Therefore, performing simulations with HCN and NH_3 in the fuel gave no valuable results due to large *formation* of HCN and NH_3 rather than *consumption*. The HCN and NH_3 are formed from reactions in the prompt mechanism [44], which plays an important role in this flame due to the high level of hydrocarbons. Therefore simulations were performed with only C_2H_4 as fuel and hence including only thermal and prompt NO. Experiments on LDPE indicated that the major source of NO was

thermal and possibly prompt NO. Due to the high stoichiometric air requirement for C_2H_4, the simulations in OPPDIF were sensitive to the nozzle velocities for the oxidiser and fuel. This is the reason for not performing all simulations with the same velocities as for the simulations for paper.

Attempts were made to simulate the combustion of pyrolysis gas from PVC assuming the gas was HCl and C_2H_4. However, even a very small concentration of HCl caused the simulations to fail. Therefore simulations including chlorine were excluded from this study.

Figure 14 shows the emission index for various oxygen concentrations in the oxidiser and velocities in the fuel and oxidiser for simulations on C_2H_4 and experiments on LDPE. The emission index for the experiments is described by:

$$EI_{NO} = \left(\frac{M_{NO}}{M_N} \right) \cdot \left(\frac{V}{m_0 \cdot X_N / M_N} \right) \cdot \sum [NO] \cdot \Delta t \cdot Y_N \qquad (3)$$

In Eq. 3, M_{NO} [g/mol] is the atomic weight of nitric oxide and Y_N [gN/kg_{Fuel}] is the weight fraction of nitrogen in the fuel on a dry ash free basis. In Fig. 14 the contributions from fuel-NO have been subtracted from the experimental values for LDPE. The contribution from fuel-NO was estimated by subtracting the NO formed in pure oxygen, assuming that this is the contribution from fuel-nitrogen. This contribution of fuel-NO should be considered a maximum value, since the high oxygen concentration would result in a higher conversion of fuel-N to NO than for a lower oxygen concentration.

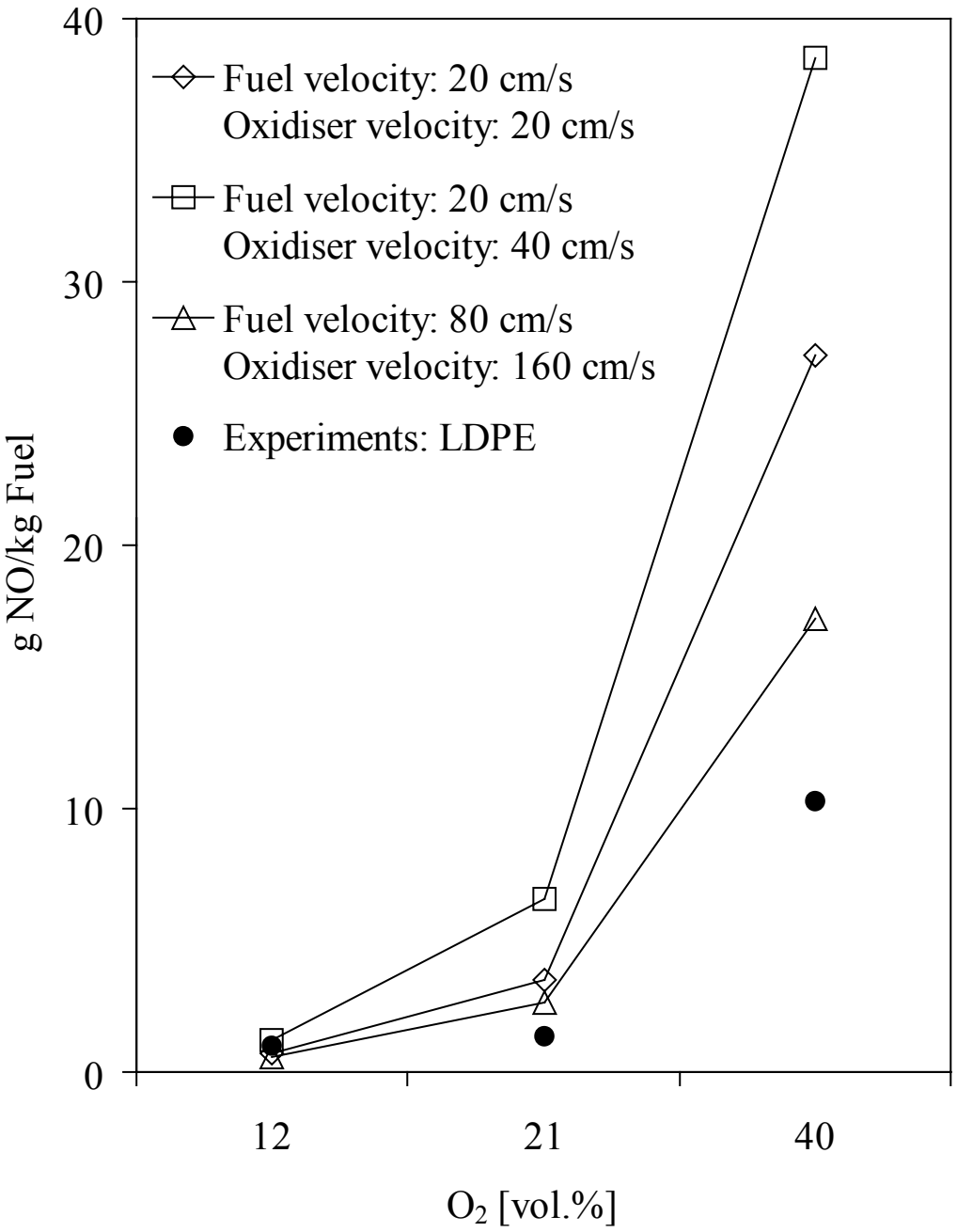

Figure 14. Emission index (g NO/kg Fuel) as a function of oxygen concentration of oxidiser and nozzle velocities. Comparison of simulations using C_2H_4 and experiments on LDPE. The experimental values are subtracted the contribution from fuel NO.

The emission index for simulations on plastic was calculated by integrating the production rate of NO multiplied with the molecular weight of NO over the control volume for the total distance from 0 to L (the distance between nozzles) and dividing this by the corresponding value for the actual fuel consumption. The emission index for the simulations can be described by:

$$EI_{NO} = \frac{\int_0^L W_{NO}\,\omega_{NO}\,dx}{-\int_0^L W_F\,\omega_F\,dx} \qquad (4)$$

In Eq. 4, W_{NO} and W_F are the molecular weights of NO and fuel, respectively; ω_{NO} and ω_F are the production rates of NO and the actual consumption rate of fuel. Further explanation of the emission index is given by Takeno [45]. As observed in Figure 14, the experimental trend of the emission index increasing with the oxygen concentration in oxidiser, is confirmed by the simulations. It is also observed that the influence of velocities and velocity ratio of fuel and oxidiser increases with increasing oxygen concentration. The calculated emission index for experiments on LDPE and simulations on C_2H_4 at 21 vol.% oxygen are of the same order of magnitude as found by Turns [38] for a C_2H_4 jet flame in air. Changes in emission index with velocity may be explained by changes in the flame structure causing parameters such as strain rate and residence time to change.

4.6 Conclusions

An experimental and theoretical study of NO formation from the combustion of volatiles from different components (paper, cardboard and plastics) of MSW and their mixtures has been performed. The experiments were performed in a laboratory furnace, while simulations were made with the CHEMKIN code OPPDIF for an opposed-flow diffusion flame.

Experiments and simulations on the combustion of volatiles from paper/cardboard show that NO is mainly formed from the fuel-nitrogen. For the plastics LDPE and PVC, however, the experiments show that NO mainly originates from the thermal and possibly the prompt NO mechanisms.

Increased formation of NO is observed for newspaper, cardboard, glossy paper, PVC and LDPE, when increasing the oxygen concentration in the oxidiser from 12 to 40 vol.%. Increasing the temperature of the oxidiser from 973 to 1123 K led to more NO from newspaper and LDPE. Simulations with OPPDIF confirmed these trends.

The measured conversion factor for fuel-N to NO for mixtures of paper and cardboard was compared to the conversion factor calculated from single components at 12, 21 and 40 vol.% oxygen. A significant difference between the measured and calculated conversion factor was only found at 40 vol.% oxygen, when the measured conversion factor for the mixture was 10-20% lower than the calculated value. This indicates that temperature differences and the contribution of thermal NO mainly cause the differences.

The comparison of the conversion factor for experiments on mixtures of paper/cardboard and plastics versus the weighted sum of single components showed a higher conversion factor for the sum of single components at all oxygen concentrations, but especially with 40 vol.% oxygen. The reason for this difference is

mainly that the conditions for forming thermal NO from LDPE as a single component are less favourable when LDPE is part of the mixture pellet, due to a lower flame temperature and a consequential decrease in thermal NO from LDPE in the mixture.

The Nordic Energy Research Programme is acknowledged for financial support, while CHEC (Combustion and Harmful Emission Control) group at the Technical University of Denmark are acknowledged for making their laboratory facilities available and for technical support and during this work.

4.7 References

1 Pickens, R.D., *Journal of Hazardous Materials*, 47:201 (1996).

2 Patel, N. M., Wheeler, P. and Ohlsson, O., *Fluidised Bed Combustion of Municipal Solid Waste*, Status Report for the International Energy Agency, 1994.

3 Farrow, R. L., Fisk, G. A., Hartwig, C. M., Hurt, R. H., Ringland, J.T., and Swansiger, W. A., *Technical Resource Document for Assured Thermal Processing of Wastes*, Report No. SAND94-8240 UC-1414, Sandia National Laboratory, USA, 1994, p. 117.

4 Sandgren, J., Heie, Aa. And Sverud, T., *Emissions from Waste Management of Municipal Solid Waste*, Report 96:16, Norwegian Pollution Control Authority, Norway, 1996, (in Norwegian).

5 Tillman, D. A., *The Combustion of Solid Fuels & Wastes*, Academic Press, USA, 1991.

6 Rydholm, S. A., *Pulping Processes*, Interscience Publishers, USA, 1965.

7 Aho, M.J., Hämäläinen, J.P., Tummavuori, J.L., *Combustion & Flame,* 95:22-30 (1993).

8 Bowman, C. T., *Proc. Comb. Inst.*, 24:859-878 (1992).

9 Abbas, T., Costen, P. and Lockwood, F. C., *A Review of Current NOx Control Methodologies for the Municipal Solid Waste Combustion Process*, 4th European Conference on Industrial Furnaces and Boilers, 1997.

10 Brydson, J.A., *in Plastics Materials*, Butterworth-Heinemann Ltd., Oxford, UK, 1995. p. 317.

11 Franklin, M. A., *Characterisation of Municipal Solid Waste in the United States 1960-2000 (Update 1988)*, Report No. PB88 – 232780, Franklin Associates Ltd., USA, 1988.

12 Kauffman, C.R., *Wastetech '91: Canadian Waste Management Conference*, Toronto, 1991, pp. 1-13.

13 Skreiberg, Ø., Glarborg, P., Jensen, A. and Dam-Johansen, K., *Fuel*, 76:671-682 (1997).

14 Rigo, H. G. and Chandler, A. J., *Proceedings of the National Waste Processing Conference*, ASME, 1994, pp. 49-63.

15 Mori, H., Asami, K. and Ohtsuka, Y., *Energy & Fuels*, 10:1022-1027 (1996).

16 Turns, S. R., *An Introduction to Combustion – Concepts and Applications,* McGraw-Hill, Singapore, 1996, p. 143.

17 Linak, W. P. and Wendt, J. O. L., *Combustion Science & Techology*, 115:69-82 (1996).

18 Yang, M. H., Hamins, A. and Puri, I. K., *Combustion & Flame*, 98:107-122 (1994).

19 Roesler, J. F, Yetter, R. A. and Dryer, F. L., *Combustion & Flame*, 100:495-504 (1995).

20 Roesler, J. F, Yetter, R. A. and Dryer, F. L., *Combustion Science & Technology*, 120:11-37 (1996).

21 Skreiberg, Ø., Hustad, J. E. and Karlsvik, E*., Developments in Thermochemical Biomass Conversion*, Blackie Academic & Professional, Ed. Bridgewater and Boocock, 1997.

22 Kee, R. J.,Rupley, F. M., Meeks, E. and Miller, J. A., *CHEMKIN III: A Fortran Chamical Kinetics Package for the Analysis of Gas-Phase Chemical and Plasma Kinetics*, Report No. SAND96-8216, Sandia National Laboratories, USA, 1996.

23 Westerhout, R. W. J, Waanders, J., Kuipers, J. A. M. and Swaaij, P. M., *Ind. Eng. Chem. Res.*, 37: 2293-2300 (1998).

24 Helt, J. E., Agrawal, R. K. and Myles, K. M., *Pyrolysis of Municipal Solid Waste*, Report no. ANL/CNSV--54 DE87 002352, Argonne National Laboratory, USA, 1985.

25 Necker, P., *Überblick über die NOx-Minderungsmassnamen in Europa*, Proceedings of NOx-Symposium Karlsruhe, Universität Karlsruhe, D1/D44, 1985.

26 Lutz, A. E., Kee, R. J, Grcar, J. F. and Rupley, F. M*., OPPDIF: A Fortran Program for Computing Opposed-Flow Diffusion Flames*, Report No. SAND96-8243, Sandia National Laboratories, 1997.

27 Hamins, A. and Seshadri, K*., Proc. Comb. Inst.*, 20:1905-1913 (1984).

28 Dixon-Lewis, G. and Missaghi, M*., Proc. Comb. Inst.*, 22:1461-1470 (1988).

29 Tanoff, M. A., Smooke, M. D., Osborne, R. J., Brown, T. M. and Pitz, R. W., *Proc. Comb. Inst.*, 26:1121-1128 (1996).

30 Bloor, M. I. G, David, T., Dixon-Lewis, G. and Gaskell, P. H*., Proc. Comb. Inst.*, 21:1501-1509 (1986).

31 Smooke, M. D., Puri, I. K. and Seshadri, K., *Proc. Comb. Inst.*, 21:1783-1792 (1986).

32 Dixon-Lewis, G., David, T., Gaskell, P. H., Fukutani, S., Jinno, H., Miller, J. A., Kee, R. J., Smooke, M. D., Peters, N., Effelsberg, E., Warnatz, J. and Behrendt, F., *Proc. Comb. Inst.*, 20: 1893-1904 (1984).

33 Papas, P., Glassman, I. And Law, C. K., *Proc. Comb. Inst.*, 25:1333-1339 (1994).

34 Brown, T. M., Tanoff, M. A., Osborne, R. J., Pitz, R. W. and Smooke, M. D., *Combustion Science & Technology*, 129:71-88 (1997).

35 Drake, M. C. and Blint, R. J., *Combustion & Flame*, 83:185-203 (1991).

36 Nishioka, M., Kondoh, Y. and Takeno, T., *Proc. Comb. Inst.*, 26:2139-2145 (1996).

37 Nishioka, M., Nakagawa, S., Ishikawa, Y. and Takeno, T., *Combustion & Flame*, 98:127-138 (1994).

38 Turns, S. R., *Progress in Energy & Combustion Science*, 21:361-385 (1995).

39 Glarborg, P., Alzueta, M. U., Miller, J. A. and Dam-Johansen, K., *Combustion & Flame*, 115:1-27 (1998).

40 Hämäläinen, J. P., Aho, M. J. and Tummavuori, J. L., *Fuel*, 73:1894-1898 (1994).

41 Aho, M. J., Hämäläinen, J. P. and Tummavuori, J. L., *Combustion & Flame*, 95:22-30 (1993).

42 Leppälahti, J., *Fuel*, 74:1363-1368 (1995).

43 Johnsson, J. E., *Fuel*, 73:1398-1415 (1994).

44 Miller, J. A. and Bowman, C. T., Progress in Energy & Combustion Science, 15:295 (1989).

45 Takeno, T. and Nishioka, M., *Combustion & Flame*, 92:465-468 (1993).

5 FURTHER WORK

MSW is a complex fuel consisting of various components with different properties and chemical composition at different mixture ratios. Knowing how to reduce harmful pollutant emissions and optimise operational conditions requires detailed knowledge regarding all aspects of MSW combustion. The complex fuel, varying compositions and stricter and stricter emission requirements makes design and operation of combustion plants a challenge. In general, some important subjects related to thermal conversion of MSW are:

- Modelling of MSW combustion. Development of models describing the devolatilisation of the solid fuel and the subsequent gas phase combustion.

- Further development of primary NO_x reduction methods applicable in MSW combustion.

- Environmental consequences of burning different waste fractions/components and mixtures thereof.